CLEAN Main TEXT on January 6, 2022

Microbiome and Metabolome Features of the Cardiometabolic Disease Spectrum

Authors:

Sebastien Fromentin[1,*], Sofia K. Forslund[2,3,4,5,6,*], Kanta Chechi[7,8,34*], Judith Aron-Wisnewsky[9,10,*], Rima Chakaroun[11,*], Trine Nielsen[12,*], Valentina Tremaroli[13], Boyang Ji[14], Edi Prifti[15,16], Antonis Myridakis[7], Julien Chilloux[7], Andrikopoulos Petros[7,34], Yong Fan[12], Michael T. Olanipekun[7], Renato Alves[2], Solia Adiouch[9], Noam Bar[18,19], Yeela Talmor-Barkan[18,19,20,21], Eugeni Belda[9,15,16], Robert Caesar[13], Luis Pedro Coelho[2], Gwen Falony[22,23], Soraya Fellahi[24], Pilar Galan[1], Nathalie Galleron[1], Gerard Helft[25], Lesley Hoyles[7,26], Richard Isnard[25], Emmanuelle Le Chatelier[1], Hanna Julienne[1], Lisa Olsson[13], Helle Krogh Pedersen[12], Nicolas Pons[1], Benoit Quinquis[1], Christine Rouault[9], Hugo Roume[1], Joe-Elie Salem[27], Thomas SB Schmidt[2], Sara Vieira-Silva[22,23], Peishun Li[14], Maria Zimmermann-Kogadeeva[2], Christian Lewinter[28], Nadja B Søndertoft[12], Tue H Hansen[12], Dominique Gauguier[29], Jens Peter Gøtze[30], Lars Køber[28], Ran Kornowski[20], Henrik Vestergaard[12,31], Torben Hansen[12], Jean-Daniel Zucker[15,17], Serge Hercberg[32], Ivica Letunic[33], Fredrik Bäckhed[12,13], Jean-Michel Oppert[10], Jens Nielsen[14], Jeroen Raes[22,23], Peer Bork[2], Michael Stumvoll[11], Eran Segal[18,19], Karine Clément[9,10,+], Marc-Emmanuel Dumas[7,34,35,+], S. Dusko Ehrlich[1,+], and Oluf Pedersen[12,+]

* Contributed equally

+ Corresponding authors

[1] MetaGenoPolis, INRAe, AgroParisTech, Université Paris-Saclay, Paris, France

[2] Structural and Computational Biology, European Molecular Biology Laboratory, Heidelberg, Germany

[3] Experimental and Clinical Research Center, a cooperation of Charité-Universitätsmedizin and the Max-Delbrück Center, Berlin, Germany

[4] Max Delbrück Center for Molecular Medicine (MDC), Berlin, Germany

[5] Charité University Hospital, Berlin, Germany

[6] DZHK (German Centre for Cardiovascular Research), partner site Berlin.

[7] Division of Systems Medicine, Department of Metabolism, Digestion and Reproduction, Faculty of Medicine, Imperial College London, Sir Alexander Fleming building, London SW7 2AZ, UK.

[8] School of Public Health, Faculty of Medicine, Imperial College London, Medical School Building, St Mary's Hospital, Norfolk Place, London W2 1PG, UK.

[9] Sorbonne Université, INSERM, Nutrition and obesities; systemic approaches (NutriOmics), Paris, France

[10] Assistance Publique Hôpitaux de Paris, Pitié-Salpêtrière Hospital, Nutrition department, Paris, France

[11] Medical Department III - Endocrinology, Nephrology, Rheumatology, University of Leipzig Medical Center, Leipzig, Germany

[12] Novo Nordisk Foundation Center for Basic Metabolic Research, Faculty of Health and Medical Sciences, University of Copenhagen, Copenhagen, Denmark

[13] The Wallenberg Laboratory, Department of Molecular and Clinical Medicine, Institute of Medicine, Sahlgrenska Academy, University of Gothenburg, Gothenburg, Sweden

[14] Department of Biology and Biological Engineering, Chalmers University of Technology, Gothenburg, Sweden

[15] Institute of Cardiometabolism and Nutrition, Integromics unit, Paris, Franc

[16] Integrative Phenomics, Paris, France

[17] Unité de modélisation mathématique et informatique des systèmes complexes, UMMISCO, F-93143, Bondy, France

[18] Department of Computer Science and Applied Mathematics, Weizmann Institute of Science, Rehovot 7610001, Israel

[19] Department of Molecular Cell Biology, Weizmann Institute of Science, Rehovot 7610001, Israel

[20] Department of Cardiology, Rabin Medical Center, Petah Tikva, Israel

[21] Sackler Faculty of Medicine, Tel-Aviv University, Tel-Aviv, Israel

[22] Laboratory of Molecular Bacteriology, Department of Microbiology and Immunology, Rega Institute, KU Leuven, Leuven, Belgium

[23] Center for Microbiology, VIB, Leuven, Belgium

[24] Assistance Publique-Hôpitaux de Paris, Hôpitaux Universitaires Henri Mondor, Département de biochimie-pharmacologie-biologie moléculaire-génétique médicale, Créteil, France

[25] Assistance Publique Hôpitaux de Paris, Pitié-Salpêtrière Hospital, Cardiology department, Paris France

[26] Nottingham Trent University, Department of Bioscience, School of Science and Technology, Clifton, Nottingham, UK

[27] AP-HP, Pitié-Salpêtrière Hospital, Department of Pharmacology, UNICO Cardio-oncology Program, CIC-1421; INSERM, Sorbonne Université, F-75013 Paris, France

[28] Department of Cardiology, Rigshospitalet, University of Copenhagen, Copenhagen, Denmark

[29] Université de Paris, INSERM UMR 1124, 75006 Paris, France.

[30] Department of Clinical Biochemetry, Rigshopitalet, University of Copenhagen, Copenhagen, Denmark

[31] Department of Medicine, Bornholms Hospital, Rønne, Denmark

[32] Sorbonne Paris Cité Epidemiology and Statistics Research Centre (CRESS), U1153 Inserm, U1125, Inra, Cnam, University of Paris 13, Nutritional Epidemiology Research Team (EREN), 93017, Bobigny, France

[33] Biobyte solutions GmbH, Bothestr 142, 69126 Heidelberg, Germany

[34] Genomic and Environmental Medicine, National Heart and Lung Institute, Faculty of Medicine, Imperial College London, Guy Scadding building, London SW3 6LY, UK

[35] European Genomics Institute for Diabetes, UMR1283/8199 INSERM, CNRS, Institut Pasteur de Lille, Lille University Hospital, University of Lille, 1 place de Verdun 59045, Lille, France

Corresponding authors

Oluf Pedersen, Novo Nordisk Foundation Center for Basic Metabolic Research, Faculty of Health and Medical Sciences, University of Copenhagen, Blegdamsvej 3B, 2200 Copenhagen, Denmark.

Email: oluf@sund.ku.dk

S. Dusko Ehrlich, Metagenopolis, INRAE, 78350 Jouy-en-Josas, France.

Email: stanislav.ehrlich@inrae.fr

Marc-Emmanuel Dumas, Imperial College London, Division of Systems Medicine, Department of Metabolism, Digestion and Reproduction, Faculty of Medicine, Sir Alexander Fleming building, London SW7 2AZ, UK; Genomic and Environmental Medicine, National Heart and Lung Institute, Faculty of Medicine, Guy Scadding building, London SW7 2AZ, UK; European Genomics Institute for Diabetes, UMR1283/8199 INSERM, CNRS, Institut Pasteur de Lille, Lille University Hospital, University of Lille, 1 place de Verdun 59045, Lille, France.

Email: m.dumas@imperial.ac.uk

Karine Clément, Sorbonne University, Inserm, NutriOmics, Faculty of Medicine Paris, 91 Boulevard de l'Hôpital, Paris, France.

Email: karine.clement@inserm.fr

Abstract

Previous microbiome and metabolome analyses exploring non-communicable diseases have paid scant attention to major confounders of study outcomes, such as common, pre-and co-morbid conditions or polypharmacy. Here in the context of ischemic heart disease (IHD), we used a study design that recapitulates disease initiation, escalation and response to treatment over time, mirroring a longitudinal study that would otherwise be difficult to perform given the protracted nature of IHD pathogenesis. We recruited 1,241 middle-aged Europeans including healthy individuals, individuals with dysmetabolic morbidities (obesity and type 2 diabetes) but lacking overt IHD diagnosis, and IHD cases at three distinct clinical stages; acute coronary syndrome, chronic IHD and IHD with heart failure, and characterized their phenome, gut metagenome and serum and urine metabolome. We found that about 75% of microbiome and metabolome features that distinguish IHD cases from healthy individuals after adjustment for effects of medication and lifestyle are present in individuals exhibiting dysmetabolism, suggesting that major alterations of the gut microbiome and metabolome may begin long before clinical onset of IHD. We further categorized microbiome and metabolome signatures related to prodromal dysmetabolism, specific to IHD in general or to each of its three subtypes, or related to escalation or de-escalation of IHD. Discriminant analysis based on specific IHD microbiome and metabolome features could better differentiate IHD cases from healthy individuals or metabolically-matched individuals as compared to the conventional risk markers, pointing to a pathophysiological relevance of these features.

Introduction

Epidemiological and genetic studies in humans and experimental studies in animals have shown that the pathogenesis of most common chronic non-communicable diseases involves a complex interplay between polygenic susceptibility, aging, sex and a multitude of environmental exposures[1]. Intriguingly, the environmental components like diet, physical activity and smoking may exert some of their pathogenic impact via modification of the intestinal microbiome[2]. Therefore, a first logical step in exploring a role of the intestinal microbiome as a putative chronic disease co-trigger appears to be conduction of studies integrating epidemiology and various –omics analyses. However, for the reliability of such study outcomes and for the planning of subsequent clinical interventions and mechanistic experiments, disease-specific microbiome and linked metabolome features need to be separated from confounders introduced by pre- and co-morbidities[3-5] and by multifactorial treatment[6]. Commonly prescribed drugs, for example, widely influence the gut microbiome and host metabolome[7], and can confuse for or even mask genuine disease signatures[7,8]. Accordingly, a recent report argues for extensive adjustments for confounders that influence human gut microbiome to avoid spurious associations and to identify genuine disease-specific variance[9].

The present microbiome and metabolome study is focused on ischemic heart disease (IHD), a leading cause of mortality worldwide[10]. Previous reports comparing microbiome and metabolome markers of IHD cases and controls usually failed to adjust for the massive confounding by polypharmacy[8] and the impact of metabolic abnormalities occurring during a long prodromal phase prior to diagnosis of IHD[11-13]. Such common metabolic dysfunctions include overweight and obesity[3,5], type 2 diabetes (T2D)[4], hypertension[14] and dyslipidaemia[15]

(collectively termed ―dysmetabolism" in the present study), all of which have been shown to exhibit both shared and disease-specific aberrations in microbiome and metabolome profiles. Individuals with the metabolic syndrome or overt T2D have vastly increased risk of IHD[16], and asymptomatic T2D is often coincidentally found at IHD diagnosis[17], highlighting these pre-morbidities to be a clinically relevant baseline for studying overt IHD. Most studies to date have overlooked this aspect by either comparing IHD cases with healthy lean individuals[11] or not focusing on IHD *per se* but on various forms of atherosclerotic organ damage[12,13,18]. Segregating IHD-specific changes in gut microbial and metabolomic features from such potential confounders, thus, remains an utmost priority.

In the MetaCardis consortium we designed the present cross-sectional study including healthy individuals, individuals with dysmetabolic morbidities and individuals with IHD at three distinct clinical stages capturing a wide spectrum of gut microbiome and plasma and urine metabolome signatures for cardiometabolic diseases (CMD). With our approach for integrative analysis of the –omics data we adjust for confounding by polypharmacy and the impact of metabolic abnormalities occurring during the prodromal phase prior to diagnosis of IHD. Further, we categorize microbiome and metabolome pathophysiological signatures related to dysmetabolism or to escalation, de-escalation or stabilization of IHD and its subtypes.

Results

Study design, in-depth phenotyping and multi-omics profiling. The study encompassed 372 IHD cases including 112 with acute coronary syndrome (ACS), 158 with chronic ischemic heart disease (CIHD) and 102 with ischemic heart disease and heart failure (HF). In addition, we

included 275 healthy controls (HC) matched on demographics, age and sex, and 222 untreated metabolically matched controls (UMMC); i.e. individuals with features of the metabolic syndrome and thus at increased risk of IHD but receiving no lipid-lowering or anti-diabetic or anti-hypertensive drugs. Finally, we included 372 controls matched with IHD cases on T2D status and body mass index (BMI), thereafter termed metabolically matched controls (MMC) (**Figure 1**). We profiled their serum and urine metabolome (1,558 metabolites and lipids), and examined their intestinal microbiome considering inter-individual variations in absolute fecal bacterial cell density, a factor potentially reflecting both the disease state and obscuring genuine microbiome involvement[19]. Inclusion of MMC and UMMC groups allowed for the differentiation of the gut microbial and metabolomic signatures of IHD from the often-accompanied metabolic dysfunctions and related drug intake.

As expected from inclusion criteria, we found increasing CMD phenotype severity and related drug intake along the implied progression from healthy controls (HC) through treated and untreated metabolically matched controls (MMC and UMMC, respectively) to overt IHD cases (**Extended Data Figure 1**, and **Supplementary Tables 1-3**). Despite matching for country, age, sex, body mass index (BMI) and T2D status, cases with IHD remained phenotypically distinct from MMC. They displayed increased visceral fat ($p = 0.048$), worse glycaemia (HbA1c; $p = 0.005$ and fasting plasma glucose; $p = 0.006$), higher plasma concentration of liver enzymes (ASAT, ALAT, GCT; $p < 0.001$) and increased prevalence and severity of hypertension ($p < 0.001$) (**Supplementary Tables 1-2**). Similarly, IHD cases had decreased heart contractility mirrored in reduced left ventricular ejection fraction (LVEF) and increased plasma pro-atrial natriuretic peptide (pro-ANP) levels relative to both HC and MMC ($p < 0.001$), which was

further altered in the HF subgroup relative to ACS and CIHD ($p < 0.001$) (**Extended Data Figure 1**, and **Supplementary Table 2)**.

Diet and physical activity variation across study groups. Diet affects microbiome composition and IHD risk[2]. We found that HC individuals reported healthier diets than the IHD and MMC groups with higher values of composite metrics such as alternative healthy eating index (aHEI[20]) (HC versus IHD; $p < 0.001$), diet diversity score (DDS[21]) (HC versus IHD; $p = 0.001$) and dietary approaches to stop hypertension (DASH[22]) score (HC versus IHD; $p = 0.013$), and lower overall daily energy intake (HC versus IHD; $p = 0.013$). HC consumed significantly less of fatty animal-based food and meat and more plant-based food rich in non-digestible polysaccharides (**Supplementary Table 4**). They further reported higher physical activity levels (**Extended Data Figure 1**), more often being in manual work and undertaking more frequent moderate to vigorous leisure time activities than IHD or MMC (**Supplementary Table 4**). Some of the microbiome differences between MMC and IHD as opposed to HC may also reflect a less healthy lifestyle.

Microbiome and metabolome changes related to dysmetabolism. Both the taxonomy and functional potential of the gut microbiome as well as the metabolome differed significantly between IHD and HC in accordance with previous reports[11-13]. Remarkably, comparing HC to MMC revealed even more differential features than comparing HC versus IHD (**Figure 2a**, and **Supplementary Tables 5-8)**. Moreover, the discriminatory potential of microbiome and metabolome features was significantly higher between IHD and HC than between IHD and MMC (**Figure 2b**). We recovered most previously published IHD-related gut microbiome findings (**Extended Data Figure 2**, and **Supplementary Tables 15-16**), primarily by contrasting

HC and IHD. However, most were already significant in MMC versus HC comparisons, suggesting that previous studies may have erroneously reported dysmetabolism features as *bona fide* IHD features. These might contribute to increased risk of IHD, but our analyses indicate that they are not specific for IHD.

At higher microbiome architecture levels, there was a significant shift from the *Bacteroides* 1 and *Ruminococcus* enterotypes towards the low bacterial cell count–associated *Bacteroides* 2 as disease worsened[23] (**Figure 2c**). These findings mirror significant loss of microbial gene richness (**Figure 2d**) and absolute gut bacterial cell load (i.e. microbial load) in both MMC and IHD relative to HC. In contrast, no differences were found when IHD were compared with MMC (**Supplementary Table 5**). Bacterial gene depletion and *Bacteroides* 2 prevalence were even more exacerbated in UMMC, possibly due to drugs not yet being prescribed and the presence of a more obese phenotype in this group[24]. Consistently, the total number of gut microbiome and metabolome features significantly differential in abundance was higher when HC was compared to UMMC relative to MMC (**Extended Data Figure 3).**

Microbiome and metabolome signatures of IHD. We consider the identification of genuine microbiome and metabolome signatures of IHD, i.e., disease features not better explained as indirect associations via drugs and demographics, a major contribution of our study. Additionally, we further differentiate IHD features from their metabolic morbidities by categorizing them according to their signatures among the various group comparisons across the CMD spectrum, focusing qualitatively on *condition specificity* and quantitatively on *effect size* (**Figure 3** and **Extended Data Figure 4).** We identify features as being specific to dysmetabolism (**Figure 3a, b**) or IHD (**Figure 3a, c**) by exhibiting a significant change only under the respective condition,

i.e. HC versus MMC/UMMC for dysmetabolic features (DMF) or MMC/UMMC versus IHD for IHD-specific features (IHDF). Additionally, we identify features based on whether they exhibit a typical shift in effect size in both dysmetabolism and IHD, either maintaining it in the same direction from dysmetabolism to IHD, i.e. escalation features (ESCF) or on the contrary in the opposite direction, i.e. de-escalation features (DSCF) (**Figure 3a, d**). Specifically, ESCF represents early markers of IHD that continue to increase/decrease during metabolic morbidity (i.e. HC versus MMC/UMMC) to overt IHD (i.e. MMC/UMMC versus IHD) (**Figure 4b**). In contrast, DSCF exhibit a reverse pattern of shift when considering the effects sizes between HC versus MMC/UMMC and MMC/UMMC versus IHD (**Figure 4c).** In brief, for features already aberrant in MMC, DSCF represents those being restored towards HC levels in diagnosed and treated IHD, plausibly associated to disease stabilization.

Most significant IHD-associated features were categorized as primarily indicators of general dysmetabolism rather than specific to IHD, whereas next in order of frequency were features specific to IHD, then de-escalation- and escalation features (**Figure 1**, **3**, **Supplementary Figure 1**, and **Supplementary Table 17**). This pattern remained largely valid also when the three IHD subtypes were considered separately (**Supplementary Figure 2**), in line with our observation of a major shift in gut microbiome and metabolome during the dysmetabolic stage prior to IHD diagnosis.

Of 121 species that were markers of dysmetabolism (i.e. DMFs) (**Supplementary Table 17**), an overwhelming majority (85 %) was depleted in IHD, paralleling observations for the ACS cases analyzed in the companion manuscript (Talmor-Barkan et al.). Twenty-three species were IHD specific markers (**Figures 4a, 5**), with a similar trend towards depletion in patients (65%). They

included three proteobacteria, *Acinetobacter, Turcimonas* and *Acetobacter,* previously reported depleted in IHD (**Extended Data Figure2**). Among eight species enriched in IHD, two were Betaproteobacteria of the Burkholderiales order. Interestingly, *Burkolderia pseudomallei* is reported as a possible cause of endocarditis[25]. A single species, an uncharacterized Ruminococcus depleted in IHD, was an IHD escalation marker (**Figure 4b**); ruminococci include butyrate producers and their depletion might contribute to the reduced production potential of short chain fatty acids (SCFAs) in IHD. Six species were de-escalation markers (**Figure 4c**); they belonged to Clostridiales order and all but one, *Eubacterium siraeum*, were unclassified at species or even genus taxonomic level. *Eubacterium* was previously reported to be depleted in atherosclerosis (**Figure 4, Supplementary Table 17**). In contrast, microbiome functions (GMM and KEGG modules) were mostly enriched in IHD **(Extended Data Figure 5).**

In parallel, the metabolome reporting most of IHD-specific markers, showed a marked enrichment with only 50 out of 203 IHD-specific markers (25%) being depleted in IHD relative to HC (**Figure 4, Supplementary Table 17**). We identified enrichment of a range of IHD-specific metabolites, including intermediaries of the choline and carnitine pathways quantified by UPLC-MS/MS, *i.e.* choline, betaine-aldehyde, 4-butyrobetaine, linoleylcarnitine, and trimethylamine (TMA), the precursor of trimethylamine *N*-oxide (TMAO) known to modulate IHD risk[26]. Other such carnitine metabolites included medium- and long-chain fatty acyl carnitines, suggesting an increase in transport into the mitochondria through the carnitine shuttle, typically for β-oxidation. In particular, microbial aromatic acids such as phenylacetate reported to be inversely associated with species-level genome bin (SGB) 4712 in the companion manuscript, Talmor-Barkan et al.) or benzoate follow a similar process producing

phenylacetatylcarnitine or benzoylcarnitine. They undergo conjugation with amino acids to form for instance phenylacetylglutamate or hippurate[27], of which both phenylacetylcarnitine and phenylacetylglutamate are IHD-specific markers in our study (**Figure 4a**).

Along the same lines, we observed an increase in proinflammatory lipids derived from arachidonic acid (C20:4) starting with arachidonoylcarnitine, 5-hydroxyeicosatetraenoic acid (5-HETE) as well as leukotriene B4 and 9- / 13- hydroxyoctadecadienoic acid (9-HODE/13-HODE) which are known mediators of inflammation and atherogenesis[28,29]. In contrast, fatty acid methyl esters including methyl hexadecanoate, methyl linolenate and methyl oleate along with alpha-tocopherol, known for vasoprotective[30] and antioxidant properties[31], respectively, were among the top metabolites whose depletion constitutes markers specific for IHD (**Figure 4a).** Importantly, similar patterns remained in IHD subtype-specific analyses (**Extended Data Figures 6-8, Supplementary Table 17**).

Most IHD-escalation features represented by the metabolome exhibited an initial depletion upon dysmetabolism, which continued following IHD diagnosis (**Figure 4b** and **Supplementary Table 17**). Besides a number of complex phospholipids including sphingomyelins and glycerophospholipids, several carotenoids (e.g. carotene diols and β-cryptoxanthin) and ergothioneine, which are known to improve cardiovascular health exhibited the above depletion pattern whereas glutathione metabolism and markers of oxidative stress (e.g. cystathionine, cys-gly oxidized) instead escalated. Ergothioneine, in particular, has been associated with reduced cardiovascular and overall mortality[32] and was also identified as a key metabolite exhibiting a positive correlation with SGB 4712 (*i.e.* both SGB 4712 and ergothioneine exhibiting depletion) in ACS cases relative to controls in the companion manuscript (Talmor-Barkan et al.).

Consistently, a reduction in circulating level of ergothioneine was also observed in ACS and HF cases relative to healthy controls in the present study **(Supplementary Table 17)**.

In contrast, 4-cresol exhibited an enrichment pattern from dysmetabolism to IHD (**Figure 4b**). 4-cresol is a bacterial product of colonic fermentation of phenylalanine and tyrosine and a precursor for uraemic toxin 4-cresylsulfate. Similarly, phenylacetylglutamine, another uraemic toxin derived from microbial phenylacetate and which acts through adrenergic receptors[33] showed an enrichment pattern from dysmetabolism to IHD. It was also shown to be inversely associated with SGB 4712 by Talmor-Barkan et al.). The findings implicate these metabolites as key targets for early intervention. 4-cresol, in particular, has been found in lower concentrations in the blood of vegetarians than of omnivores[34], and shown to inhibit colonocyte oxygen consumption[35] as well as to be reduced once fat intake is curbed[36]. In our study this compound appeared as a ACS and CIHD escalation feature and it was also one of the top markers specifically enriched in blood of HF cases, likely related to its role in uraemia[37] with dysregulation of fluid homeostasis being a key feature of HF (**Extended Data Figure 7**). Interestingly, we also observe in another MetaCardis study that 4-cresol plays a causal role in the gut microbiome–kidney–heart axis in HCs, culminating in increased pro-ANP levels (Chechi *et al*., in revision).

A majority of DSCF (89% and 100% for metabolites and predicted microbiome functions, respectively) exhibited the pattern of initial depletion at the stage of dysmetabolism but an apparent reversal at the stage of treated IHD (**Figure 4c)**. For instance, *O*-acetylsalicylate, the active component in aspirin, appeared as an archetypal DSCF putatively due to patient treatment compliance in IHD. Similarly, a number of catecholamine intermediates and end-products,

bilirubin products, bile acids and odd-chain lipids with bacterial origin were identified as DSCF. Moreover, TMA production (MC0022) and butyrate production II (MF0089) as gut microbial functional features exhibited a depletion at the dysmetabolism stage but an apparent restoration at the IHD stage (**Extended Data Figure 5**). Overall, these observations may point towards a responsiveness of both microbiome and metabolome features to long-term multifactorial treatment plausibly contributing to stabilization of IHD. In addition, achieving a stabilized IHD state appeared to involve restoring lost gut microbial cell density (**Figure 4c**) alongside a capacity to degrade BCAAs and galactose while restoring lost capacity for butyrate and acetate production (**Extended Data Figure 5**).

Microbiome and metabolome markers of IHD sub-phenotypes. Detailed analysis of ACS, CIHD and IHD-caused HF groups provided more granularity for relative shifts in microbiome and metabolome features (**Figure 5**, **Extended Data Figures 6-9**, and **Supplementary Table 17**).

The total number of features typical for each IHD subgroup compared with controls was highest for CIHD followed by HF and ACS. CIHD exhibited the most differential changes in the gut microbiome functional potentials (**Extended Data Figure 9**) whereas ACS exhibited predominantly differential changes in metabolome features (**Figure 5**, **Extended Data Figures 6-9**, and **Supplementary Table 17**).

Most (69%) of the dysmetabolism-linked species found by IHD versus HC comparisons were also present in comparisons of IHD subgroups versus HC, suggesting that the major disruption of the microbiome, which appears to be related to metabolic dysfunction, may persist throughout the various stages of IHD.

Strikingly, for the ACS subgroup, besides the 91 dysmetabolism-related species, no other species markers (ACS-specific, ESCF or DSCF- related) were found (**Supplementary Table 17**). In the same ACS group, the pattern was very different for serum metabolites where only 55% of markers were related to dysmetabolism while 25% were ACS-specific (**Supplementary Table 17**). We thus observed the acute disease phase being characterized by microbiome alterations almost exclusively related to dysmetabolism, presumably accumulating during the long prodromal stage, as well as host metabolome perturbations unrelated to dysmetabolism, presumably beginning only shortly before the ACS event. It is tempting to suggest that the conjunction of the two may be conducive to some of the decompensation observed in ACS.

When considering the metabolome markers specific to ACS, eight out of the top 10 metabolites were drug analytes or drug metabolites, related to aspirin, metroprolol and atorvastatin. There was also an increase in proinflammatory metabolites such as 5- and 12-hydroxyeicosatetraenoic acid (HETE), leukotriene B4 and B5, as well as products of microbial-host phenylalanine co-metabolism (phenylacetylcarnitine, phenylacetylglutamate, and 2-hydroxyphenylacetate), followed by indoxylsulfate and TMA, which is consistent with the identified overall IHD-specific signature. Likewise, some of the ACS-specific depleted metabolites were also less abundant in IHD, including health beneficial metabolites such as alpha-tocopherol, ergothioneine, methyl oleate and methyl hexadecanoate **(Extended Data Figure 6, Supplementary Table 17)**.

In contrast to the findings in ACS, 19 and 31 specific species markers were found, for CIHD and HF, respectively, indicating additional microbiome changes in the chronic phases of IHD. Noticeably, these changes affected genera represented by only a few species: 8/14 depleted and 11/17 enriched species in HF cases, respectively, belonged to genera represented by no more

than six species ($p=2.9 \times 10^{-5}$ as estimated by the number of species belonging to different genera found in our study (**Extended Data Figures 6-8**, and **Supplementary Table 17**).

The majority of the CIHD-specific features was enriched in cases over controls **(Extended Data Figures 7 & 9, supplementary Table 17)**. This was particularly the case for microbiome functional potentials for amino acid biosynthesis, including BCAA, (KEGG modules M00019, M00570, M00432), methionine (KEGG module M00017) and lysine (KEGG module M00030) (**Extended Data Figure 9**). Similarly, enhanced degradation of aromatic amino acids phenylalanine, tyrosine (GMM modules MF0027, MF0026) was reflected by increased abundance of phenylacetate metabolites (phenylacetylcarnitine and phenylacetylglutamate).We also observed increased abundance of methionine and two of its metabolites (*N*-acetylmethionine sulfoxide, and gamma-glutamylmethionine), which are known to be associated with cardiovascular phenotypes[38]. Of interest, the gut microbiome-derived L-methionine biosynthesis pathway was recently directly associated with atherosclerotic plaque burden and enhanced metabolic risk score for cardiovascular disease[18], whereas L-methionine sulfoxide as a product of protein methionine oxidation may influence thrombosis and vascular function[39] (**Extended Data Figures 7 & 9**, and **Supplementary Table 17**). In addition, the abundance of multiple UPLC-MS/MS quantified carnitines including decanoylcarnitine and oleoylcarnitine was elevated in CIHD.

Some metabolite features also exhibited HF-specificity with an enrichment of 4-cresol, 4-cresyl sulfate (also called p-cresol sulfate), 4-cresylglucuronide (also called p-cresol glucuronide), choline and TMA as well as several carnitines (3-methylglutarylcarnitine, suberoylcarnitine (C8), octadecanedioylcarnitine (C18), levulinoylcarnitine, including microbiome-derived carnitines

(benzoylcarnitine, phenylacetylcarnitine). In contrast, metabolites such as alpha-tocopherol, ergothioneine and 3-indoleglyoxylic acid exhibited HF-specific depletion (**Extended Data Figure 8, Supplementary Table 17**). These findings point towards altered fatty acid metabolism, which is known to play a crucial role in HF pathogenesis[40]**.**

Classification of participants into clinical subgroups. Robustness of our microbiome and metabolome signatures was evaluated by comparing the performance of orthogonal partial least squares discriminant analysis (O-PLS-DA) models for classifying ACS (n=112), CIHD (n=158) and HF (n=102) relative to HC (n=275) and MMC (n=372) (**Extended Data Figure 10**). Classification was based on (i) clinical markers routinely assessed during IHD diagnosis; (ii) deconfounded microbiome and metabolome markers specific for each IHD subtype identified in the current study and (iii) a combination of the two. Models were built by randomly splitting our MetaCardis study population into groups of 70% and 30%, respectively, and using the former for training and latter for testing; the process was iterated 1,000 times to minimize overfitting. The performance of the specific -omics markers on the testing sets yielded area under the curve (AUC) values superior to 0.7 in all cases and was systematically higher than that of clinical markers only, in particular for classification relative to the MMC group. Combination of the two marker types did not improve classification relative to MMC and only marginally improved classification relative to HC **(Extended Data Figure 10)**.

To validate our classification models further, we took advantage of the independent data set from the companion manuscript (Talmor-Barkan et al.), focusing on our ACS subgroup to match the pathology of the Israeli study sample. ACS-specific-metabolomics markers from the two studies were highly correlated (Cliff's Delta values computed relative to HC are shown in **Figure 6a,**

Supplementary Table 18), confirming that similar changes were observed in the two studies and validating a large fraction of our ACS-specific metabolome features. Importantly, our markers exhibited strong discriminatory potential when employed in O-PLS-DA models trained in our population and tested in the independent Israeli population (Talmor-Barkan et al.). Models based on our ACS-specific metabolome markers with (model 3, AUROC= 0.87) or without clinical variables (model 2, AUROC: 0.85) performed substantially better than a model based on clinical variables alone (AUROC; 0.764 **Figure 6c**). Altogether, this independent replication confirmed the robustness of the discriminatory potential of our deconfounded microbiome and metabolome markers in a clinical setting (**Figure 6** (metabolome markers) and **Extended Data Figure 10** (microbiome and metabolome marker**s**)).

Discussion

We show that a vast majority of the intestinal microbiome and circulating and urine metabolome signatures that were previously reported as characteristic of IHD and which do not reduce to drug treatment effects is in fact present already in individuals with common dysmetabolic phenotypes like obesity and T2D. Our observations further align with the presence of a reduced gut bacterial cell density and changes in the abundance of multiple species and microbial functional potentials. Accounting for bacterial cell density, we identify the low cell count *Bacteroides 2* enterotype[23] as a biomarker both in individuals with dysmetabolism and in individuals diagnosed with IHD. We particularly highlight low gut bacterial cell count as one of the microbiome features linked with IHD, which appears to reverse in treated IHD cases. Interestingly, both the present manuscript and another recent MetaCardis publication[41] suggest that statin drugs widely prescribed to CMD cases may help restore gut bacterial cell load. These

results are particularly relevant since several statins and their drug metabolites (mostly related to atorvastatin), and β-blockers (metroprolol and its metabolites) are reflected in the here identified specific signatures of IHD and its subtypes.

In cases with diagnosed IHD and treatment-induced improvement of vascular, inflammatory and lipid health markers, we found less aberrant microbiome and metabolome profiles when compared with healthy individuals. Still, we found bacterial species specifically altered in IHD cases and most of them were depleted in agreement with findings of the companion manuscript (Talmor-Barkan et al.). Similarly, we observed a depletion of IHD-specific metabolites including the fatty acid esters ergothioneine and alpha-tocopherol, known for vasoprotective[30] and antioxidant properties[31], whereas metabolites enriched in IHD cases included intermediates related to TMA and compounds derived from tryptophan and phenylalanine metabolism. Finally, 4-cresol and phenylacetylglutamine stood out as representatives of ESCF potentially mirroring disease severity.

In IHD subtype analyses, we identified multiple dysmetabolism-related gut microbiome changes in ACS cases, further strengthening our hypothesis that gut microbiome alterations take place in the prodromal stages prior the onset of IHD. In contrast, a substantial fraction of altered host metabolites (45%) in ACS cases was unrelated to dysmetabolism. In addition, we found alterations of the microbiome and metabolome that were specific for CIHD and HF, putatively conditioned by a conjunction of intervention and disease worsening.

Of relevance for actionable targets in future preclinical and clinical trials, we confirm reduced microbiome potentials for biosynthesis of SCFAs and increased production of BCAAs[42] in

individuals at increased risk of asymptomatic coronary atherosclerosis prior to IHD diagnosis. In the later phases of IHD pathogenesis, we show an overwhelming role for microbial-host metabolism of aromatic amino acids derived from phenylalanine and tyrosine, i.e. emerging from phenylacetate and cresol co-metabolism. Thus, our findings suggest that beyond diminishing microbial-host production of TMAO, future interventions aiming to delay or prevent IHD might be directed at increasing microbial SCFA biosynthesis but lowering microbial production of aromatic amino acids and BCCAs. Finally, the identified microbiome and metabolome features allowed us to stratify IHD cases from healthy individuals or metabolically matched individuals at levels above that achieved with conventional risk markers pointing to their pathophysiological relevance.

In conclusion, at prodromal dysmetabolic stages and at both early and late clinical manifestations of IHD, multiple deconfounded microbiome and metabolome alterations are present reflecting distinct metabolic pathways. Several of these are modifiable and might be targets for future mechanistic experiments and clinical trials aiming at IHD prevention.

Acknowledgements

We are indebted to the MetaCardis study participants and patient associations (Alliance du Coeur and CNAO) for their input and interface. Similarly, we are much indebted to the MetaCardis consortium (http://www.metacardis.net/) collaborators for contributions at multiple levels since consortium start in 2012. A full list of collaborators is given in Supplementary Information. We further thank Dr Dominique Bonnefont-Rousselot (Department of Metabolic Biochemistry, Pitié-Salpêtrière hospital) for the analysis of plasma lipid profiles. The assistance of nurses, dietitians,

laboratory technicians, clinical research assistants and data managers at Novo Nordisk Foundation Center for Basic Metabolic Research, Clinical Research Unit at Fredriksberg and Bispebjerg Hospitals, Copenhagen, Clinical Investigation Platform at the Institute of Cardiometabolism and Nutrition for patient investigations and the Clinical Investigation Center (CIC) from Pitié-Salpêtrière Hospital, Paris, and University of Leipzig Medical Center, Leipzig, is greatly appreciated. Quanta Medical provided regulatory oversight of the clinical study and contributed to the processing and management of electronic data.

Our study, Metagenomics in Cardiometabolic Diseases with the acronym METACARDIS was sponsored by the European Union's Seventh Framework Program for research, technological development and demonstration under grant agreement HEALTH-F4-2012-305312. Assistance Publique-Hôpitaux de Paris (AP-HP) is the promoter of the clinical investigation. Parts of the studies were also supported by the Metagenopolis grant ANR-11-DPBS-0001, the Leducq Foundation, the Novo Nordisk Foundation, the NIHR Imperial Biomedical Research Centre, and by grants from the French National Research Agency (ANR-10-LABX-46 [European Genomics Institute for Diabetes]), from the National Center for Precision Diabetic Medicine – PreciDIAB, which is jointly supported by the French National Agency for Research (ANR-18-IBHU-0001), by the European Union (FEDER), by the Hauts-de-France Regional Council (Agreement 20001891/NP0025517) and by the European Metropolis of Lille (MEL, Agreement 2019_ESR_11) and by Isite ULNE (R-002-20-TALENT-DUMAS), also jointly funded by ANR (ANR-16-IDEX-0004-ULNE), the Hauts-de-France Regional Council (20002845) and by the European Metropolis of Lille (MEL). The Novo Nordisk Foundation Center for Basic Metabolic Research is an independent research institution at the University of Copenhagen partially funded

by an unrestricted donation from the Novo Nordisk Foundation. KChe is supported by Medical Research Council (MRC) Skills Development Fellowship (grant number MR/S020039/1) and Wellcome Trust funded Institutional Strategic Support Fellowship [grant number 204834/Z/16/Z]. LH was in receipt of an MRC Intermediate Research Fellowship in Data Science (grant number MR/L01632X/1, UK Med-Bio). SKF was supported by DZHK (German Centre for Cardiovascular Research), by DFG (German Research Council - projects SFB1365, SFB1470 & KFO339) and by BMBF (German Ministry of Education and Research).

Author contributions

OP, SDE and ME-D developed the present project concept and protocol and supervised the project. KC (coordinator), OP, MS, SDE, PB, JR, M-ED, FB and JN conceived the overall objectives and study design of the MetaCardis initiative. MetaCardis cohort recruitment, phenotyping and lifestyle: JA-W, TN, RC, CL, LK, TH, THH, HV, KA and supervised by KC, MS and OP. Data curation: RC, KA, SKF, JA-W, TN. Faecal microbial DNA extraction and shotgun sequencing: NP, ELC, SF. Bacterial cell count measurement: GF, SVS. Serum and urine metabolome profiling: LH, JC, AM, MO. Biochemical analyses: J-PG. Bioinformatics and statistical analyses: SF, SKF, RA, LPC, SS, EP, EB, PA, BJ, KChe. Modelling of microbiome data: KChe, HJ, SKF, SF, GF, SVS. Drug-deconfounding: SKF and MZ-K. The manuscript was drafted by J-AW, RC, SKF, KChe, M.-E.D., S.D.E. and OP. All authors participated in the project development, discussion of results, and revision of article and approved the final version for publication.

Competing Interests Statement

519 F.B. is shareholder in Implexion Pharma AB. K.C. is a consultant for Danone Research, LNC
520 therapeutics and CONFO therapeutics for work that is unassociated with the present study. K.C.
521 has held a collaborative research contract with Danone Research in the context of MetaCardis
522 project. The other authors declare no competing interests.

Figure Legends

Figure 1. Overview of the study design. Top, the individuals studied are a subset of 1,241 individuals from the European MetaCardis cohort, in which participants underwent deep bioclinical phenotyping combined with gut microbiome and serum and urine metabolome profiling. Participants were classified as being healthy controls (HC, n = 275, healthy by self-report and no intake of lipid-lowering, anti-diabetic or anti-hypertensive drugs) and a combined group of patients diagnosed with ischemic heart disease (IHD, n = 372, on various drugs). The IHD group included cases with acute coronary syndrome (ACS, n = 112), chronic ischemic heart disease (CIHD, n = 158) and heart failure (HF, n = 102) due to CIHD. Two additional control groups were included: metabolically matched controls without diagnosed IHD (MMC, n = 372, matched on age, body mass index and T2D status of the IHD cases, some of whom were prescribed lipid-lowering, antidiabetic and anti-hypertensive medication but no IHD related drugs) and untreated (non-medicated) metabolically matched non-IHD controls (UMMC, n = 222, no intake of lipid-lowering, anti-diabetic, anti-hypertensive or IHD drugs). Bottom, microbiome and metabolome features were segregated into four categories, as indicated. The human icons were adapted from **smart.servier.com.**

Figure 2. Alterations of gut microbiome and metabolome features along the natural history of ischaemic heart disease. a, Violin plots representing the distribution of significant gut microbiome and metabolome features among various group comparisons before and after data being subjected to the drug-deconfounding pipeline (lower line, lower quartile; medium line, median; upper line, upper quartile). Numbers below each subplot represent total features in the respective group comparison (shown as x-axis) that retained significance (FDR $\leq$ 0.1)

plotted against the Cliff's Delta (y-axis) for each set of features before (uncorrected) or after drug deconfounding (corrected) **b**, Boxplots showing classifier performance comparison using HC or MMC as controls relative to IHD cases, based either on all microbial features (left) or quantified metabolome features (right) as input (center line, median; box limits, upper and lower quartiles; whiskers, 1.5× interquartile range; points, outliers). Two-sided MWU *P* are included for each comparison. **c**, Pie chart (right) comparing the percent (shown as numbers) distribution of four enterotypes among various study groups. Table (left) shows the Chi^2 *P* for each study group relative to the three control groups i.e., HC, MMC, and UMMC. **d**, Boxplots (upper) comparing gut bacterial gene richness among the indicated study groups (violin, distribution; center line, median; box limits, upper and lower quartiles; whiskers, 1.5× interquartile range; points, outliers). Table (below) shows the two-sided MWU *P* for each study group relative to the three control groups i.e., HC, MMC, and UMMC. Two-sided MWU and Chi^2 tests were used for assessing the significance of group-wise comparisons in a, b, d and c, respectively, using HC (n = 275), MMC (n = 372), UMMC (n = 222), IHD (n = 372), ACS (n = 112), CIHD (n = 158), HF (n = 102) groups. Multiple testing corrections were done using Benjamini-Hochberg method and FDR <= 0.1 was considered significant. HC: healthy controls, MMC: metabolically matched controls, UMMC unmedicated metabolically matched controls, IHD: ischemic heart disease, ACS: acute coronary syndrome, CIHD: chronic IHD, HF: heart failure due to IHD, MGS: metagenomic species, GMM: gut microbial modules, KEGG, Kyoto Encyclopedia of Genes and Genomes, MWU: Mann-Whitney U, FDR: false-discovery rate.

Figure 3. Approach used for categorization of microbiome and metabolome features in the cross-sectional study. Gut microbiome and plasma and urine metabolome features that exhibited a statistically significant shift uniquely when either metabolically matched controls

(MMC), untreated metabolically matched controls (UMMC) or cases with ischemic heart disease (IHD) were compared to healthy controls (HC) were categorized as dysmetabolism features (DMF; a, b) as these features exhibited significant alterations in association with metabolic syndrome (i.e. obesity, type 2 diabetes) and not IHD *per se*. In contrast, gut microbiome and plasma and urine metabolome features that exhibited a significant change when either MMC or UMMC subjects were compared with IHD cases were categorized as IHD-specific features (IHDF; a, c). In addition, features exhibiting a significant change in IHD cases relative to HC subjects were categorized as IHDF when they exhibited a simultaneous significant shift in IHD cases relative to MMC or UMMC subjects. Next, we considered the natural trajectory of IHD in two stages i.e., HC vs MMC or UMMC (representing the dysmetabolism stage) and MMC or UMMC vs IHD (representing the IHD stage). Features exhibiting a significant change under both dysmetabolic and IHD stages, and in the same direction (representing disease progression), were thus labelled as escalation features (ESCF; a, d), whereas those exhibiting a significant change in the reverse direction (representing disease stabilization) were labelled as de-escalation features (DSCF; a, d). Our approach evaluated every feature across all group comparisons using the criteria of 1) non-confounded status (i.e., feature cannot be confounded by any tested host variables including drug treatment). 2) significance status i.e., feature has to exhibit FDR < 0.1 for respective group comparison, and 3) a directional alignment status (i.e., direction of change when disease stages are considered) for categorization as either as DMF (b), IHDF (c), ESCF or DSCF (d). Please see Extended Data Figure 4 and the Methods for more details. The arrow size further reflects the number of features identified by each route for respective categorization: 767 DMFs, 283 IHDFs and 98 each of ESCFs and DSCFs were identified. Two-sided MWU tests were used for assessing the significance of group-wise comparisons using HC (n = 275), MMC

(n = 372), UMMC (n = 222) and IHD (n = 372) groups. Multiple testing corrections were done using Benjamini-Hochberg method and FDR <= 0.1 was considered significant. MWU: Mann-Whitney U, FDR: false-discovery rate. The human icons were adapted from **smart.servier.com**.

Figure 4. Microbiome and metabolome features linked with ischaemic heart disease and its dysmetabolic pre-morbidities. Using the categorization scheme described in **Figure 3** and **Extended Data Figure 4**, gut microbiome and metabolome markers were categorized as dysmetabolic features (DMF), IHD-specific features (IHDF), IHD-escalation features (ESCF) or IHD de-escalation features (DSCF), of which IHDF (a), ESCFs (b) and DSCFs (c) are displayed here. In each panel, arrow length show effect sizes (Cliff's Delta) for respective group comparisons. Cliff's Delta for HC vs IHD comparison are displayed for IHDFs (a), whereas Cliff's Delta for both HC vs MMC and MMC vs IHD are displayed for ESCFs (b) and DSCFs (c), with arrow head pointing to the direction of change. Only features exhibiting an absolute effect size > 0.1 are displayed; inclusive of serum metabolites, metagenomic species and microbial density indices (see **Supplementary Table 17** for a description of effect sizes and confounding status). Two-sided MWU tests were used for assessing the significance of group-wise comparisons using HC (n = 275), MMC (n = 372), UMMC (n = 222) and IHD (n = 372) groups. Multiple testing corrections were done using Benjamini-Hochberg method and FDR <= 0.1 was considered significant. IHD: ischemic heart disease, HC: healthy controls, MMC: metabolically matched controls, UMMC: unmedicated metabolically matched controls, MWU: Mann-Whitney U, FDR: false-discovery rate.

Figure 5. Metabolome and microbiome features altered uniquely in ischaemic heart disease (IHD) and its subtypes. Circle plot shows gut microbial species and serum metabolites that were categorized as being specific to IHD or to its subtypes; ACS, CIHD and HF due to CIHD as

per our categorization scheme shown in **Figure 3** and **Extended Data Figure 4**. Each layer shows effect sizes (Cliff's Delta) for individual features that were either enriched or depleted in cases (IHD or its subtypes) versus healthy controls (see also **Supplementary Table 17** for all features listed as being specific to IHD and its subtypes. Only features exhibiting absolute effect sizes > 0.1 for HC vs IHD are displayed. HC: healthy controls, IHD: ischemic heart disease, ACS: acute coronary syndrome, CIHD: chronic IHD, HF: heart failure due to IHD.

Figure 6. Validation of markers for acute coronary syndrome (ACS). For the gut microbial and plasma metabolome features common to both MetaCardis and Israeli cohorts, a Spearman correlation analysis (a) was conducted between the effect sizes (Cliff's Delta) for HC vs ACS comparison in each study after recalculating Cliff's Delta's in the Israeli population. Next, ROC curves depicting the classifier performance (AUROC) of five-fold cross-validated O-PLS-DA models based on the overlapped set of ACS biomarkers in three settings are shown for MetaCardis as the training population (b) and Israeli cohort as the test population (c). Model 1 included nine clinical ACS risk variables (*i.e.* age, sex, body mass index, systolic blood pressure, diastolic blood pressure, glycated haemoglobin (factored as > 5.7, 5.7-6.4 and < 6.4 mmol/l) and smoking status), fasting total-cholesterol and HDL-cholesterol (mmol/l). Model 2 included ACS-specific biomarkers identified in our study that were also found in Talmor-Barkan et al (118 variables) whereas model 3 involved all variables considered for model 1 and 2 (i.e., 127 variables). Two-sided MWU tests were used for assessing the significance of group-wise comparisons using HC (n = 275) and ACS (n = 112) in MetaCardis population and HC (n = 473) vs ACS (n =156) in the Israeli population. Multiple testing corrections were done using Benjamini-Hochberg method and FDR <= 0.1 was considered significant. HC: healthy controls, ACS: acute coronary syndrome, O-PLS-DA: orthogonal partial least squares-discriminant

637 analysis, ROC: Receiver-operating characteristics, AUROC: Area under the ROC curve, MWU:
638 Mann-Whitney U, FDR: false-discovery rate.
639
640 **Reference:**

641 1 Heymsfield, S. B. & Wadden, T. A. Mechanisms, pathophysiology, and management of
642 obesity. *N. Engl. J. Med.* **376**, 254-266 (2017).
643 2 Rothschild, D. *et al.* Environment dominates over host genetics in shaping human gut
644 microbiota. *Nature* **555**, 210-215 (2018).
645 3 Cotillard, A. *et al.* Dietary intervention impact on gut microbial gene richness. *Nature*
646 **500**, 585-588 (2013).
647 4 Karlsson, F. H. *et al.* Gut metagenome in European women with normal, impaired and
648 diabetic glucose control. *Nature* **498**, 99-103 (2013).
649 5 Le Chatelier, E. *et al.* Richness of human gut microbiome correlates with metabolic
650 markers. *Nature* **500**, 541-546 (2013).
651 6 Forslund, K. *et al.* Disentangling type 2 diabetes and metformin treatment signatures in
652 the human gut microbiota. *Nature* **528**, 262-266 (2015).
653 7 Maier, L. *et al.* Extensive impact of non-antibiotic drugs on human gut bacteria. *Nature*
654 **555**, 623-628 (2018).
655 8 Forslund, S. K. *et al.* Combinatorial, additive and dose-dependent drug–microbiome
656 associations. *Nature*, 1-6 (2021).
657 9 Vujkovic-Cvijin, I. *et al.* Host variables confound gut microbiota studies of human
658 disease. *Nature*, 1-7 (2020).

10 Mozaffarian, D. *et al.* American Heart Association Statistics C, Stroke Statistics S: Heart disease and stroke statistics--2015 update: a report from the American Heart Association. *Circulation* **131**, e29-322 (2015).

11 Jie, Z. *et al.* The gut microbiome in atherosclerotic cardiovascular disease. *Nat. Commun.* **8**, 1-12 (2017).

12 Pasini, E. *et al.* Pathogenic gut flora in patients with chronic heart failure. *JACC: Heart Failure* **4**, 220-227 (2016).

13 Karlsson, F. H. *et al.* Symptomatic atherosclerosis is associated with an altered gut metagenome. *Nat. Commun.* **3**, 1-8 (2012).

14 Li, J. *et al.* Gut microbiota dysbiosis contributes to the development of hypertension. *Microbiome* **5**, 1-19 (2017).

15 Matey-Hernandez, M. L. *et al.* Genetic and microbiome influence on lipid metabolism and dyslipidemia. *Physiol. Genomics* **50**, 117-126 (2018).

16 Einarson, T. R., Acs, A., Ludwig, C. & Panton, U. H. Prevalence of cardiovascular disease in type 2 diabetes: a systematic literature review of scientific evidence from across the world in 2007–2017. *Cardiovasc. Diabetol.* **17**, 83 (2018).

17 Association, A. D. Classification and diagnosis of diabetes: standards of medical care in diabetes—2019. *Diabetes Care* **42**, S13-S28 (2019).

18 Kurilshikov, A. *et al.* Gut microbial associations to plasma metabolites linked to cardiovascular phenotypes and risk: a cross-sectional study. *Circ. Res.* **124**, 1808-1820 (2019).

19 Vieira-Silva, S. *et al.* Quantitative microbiome profiling disentangles inflammation-and bile duct obstruction-associated microbiota alterations across PSC/IBD diagnoses. *Nat. Microbiol.* **4**, 1826-1831 (2019).

20 Consortium, I. Adherence to predefined dietary patterns and incident type 2 diabetes in European populations: EPIC-InterAct Study. *Diabetologia* **57**, 321-333 (2014).

21 Jeurnink, S. *et al.* Variety in vegetable and fruit consumption and the risk of gastric and esophageal cancer in the European prospective investigation into cancer and nutrition. *Int. J. Cancer* **131**, E963-E973 (2012).

22 Sacks, F. M. *et al.* Rationale and design of the Dietary Approaches to Stop Hypertension trial (DASH): a multicenter controlled-feeding study of dietary patterns to lower blood pressure. *Ann. Epidemiol.* **5**, 108-118 (1995).

23 Vandeputte, D. *et al.* Quantitative microbiome profiling links gut community variation to microbial load. *Nature* **551**, 507-511 (2017).

24 Aron-Wisnewsky, J. *et al.* Major microbiota dysbiosis in severe obesity: fate after bariatric surgery. *Gut* **68**, 70-82 (2019).

25 Velusamy, R. & Muhi, S. Melioidosis and the heart: A systematic review. *Trop. Med. Infect. Dis.* **5**, 121 (2020).

26 Tang, W. W., Bäckhed, F., Landmesser, U. & Hazen, S. L. Intestinal microbiota in cardiovascular health and disease: JACC state-of-the-art review. *J. Am. Coll. Cardiol.* **73**, 2089-2105 (2019).

27 Pallister, T. *et al.* Hippurate as a metabolomic marker of gut microbiome diversity: Modulation by diet and relationship to metabolic syndrome. *Sci. Rep.* **7**, 1-9 (2017).

28 Kaduce, T. L., Figard, P. H., Leifur, R. & Spector, A. A. Formation of 9-hydroxyoctadecadienoic acid from linoleic acid in endothelial cells. *J. Biol. Chem.* **264**, 6823-6830 (1989).

29 Jang, M. K. *et al.* Oxidized low-density lipoproteins may induce expression of monocyte chemotactic protein-3 in atherosclerotic plaques. *Biochem. Biophys. Res. Commun.* **323**, 898-905 (2004).

30 Lee, Y.-C. *et al.* Role of perivascular adipose tissue–derived methyl palmitate in vascular tone regulation and pathogenesis of hypertension. *Circulation* **124**, 1160-1171 (2011).

31 Ziegler, M., Wallert, M., Lorkowski, S. & Peter, K. Cardiovascular and Metabolic Protection by Vitamin E: A Matter of Treatment Strategy? *Antioxidants* **9**, 935 (2020).

32 Smith, E. *et al.* Ergothioneine is associated with reduced mortality and decreased risk of cardiovascular disease. *Heart* **106**, 691-697 (2020).

33 Nemet, I. *et al.* A cardiovascular disease-linked gut microbial metabolite acts via adrenergic receptors. *Cell* **180**, 862-877. e822 (2020).

34 Patel, K. P., Luo, F. J.-G., Plummer, N. S., Hostetter, T. H. & Meyer, T. W. The production of p-cresol sulfate and indoxyl sulfate in vegetarians versus omnivores. *Clin. J. Am. Soc. Nephrol.* **7**, 982-988 (2012).

35 Andriamihaja, M. *et al.* The deleterious metabolic and genotoxic effects of the bacterial metabolite p-cresol on colonic epithelial cells. *Free Radic. Biol. Med.* **85**, 219-227 (2015).

36 Wan, Y. *et al.* Effects of dietary fat on gut microbiota and faecal metabolites, and their relationship with cardiometabolic risk factors: a 6-month randomised controlled-feeding trial. *Gut* **68**, 1417-1429 (2019).

37 Poesen, R. *et al.* Cardiovascular disease relates to intestinal uptake of p-cresol in patients with chronic kidney disease. *BMC Nephrol.* **15**, 87 (2014).

38 Razavi, A. C. *et al.* Pseudouridine and N-formylmethionine associate with left ventricular mass index: metabolome-wide association analysis of cardiac remodeling. *J. Mol. Cell. Cardiol.* **140**, 22-29 (2020).

39 Gu, S. X., Stevens, J. W. & Lentz, S. R. Regulation of thrombosis and vascular function by protein methionine oxidation. *Blood* **125**, 3851-3859 (2015).

40 Lopaschuk, G. D., Ussher, J. R., Folmes, C. D., Jaswal, J. S. & Stanley, W. C. Myocardial fatty acid metabolism in health and disease. *Physiol. Rev.* **90**, 207-258 (2010).

41 Vieira-Silva, S. *et al.* Statin therapy is associated with lower prevalence of gut microbiota dysbiosis. *Nature* **581**, 310-315 (2020).

42 Pedersen, H. K. *et al.* Human gut microbes impact host serum metabolome and insulin sensitivity. *Nature* **535**, 376-381 (2016).

Online Methods

Study design and participants

The MetaCardis project included healthy control individuals and individuals at increasing stages of dysmetabolism and ischaemic heart disease (IHD) severity, aged 18–75 years old, and recruited from Denmark, France and Germany between 2013 and 2015. IHD cases were classified into: patients with first case of acute coronary syndrome (<15 days) (ACS), patients with chronic IHD (CIHD) with normal heart function and patients with documented heart failure (HF) and IHD as demonstrated by echocardiography-evaluated left ventricular ejection fraction (LVEF)<45%. Our study encompassed 372 IHD cases (112 ACS, 158 with CIHD and 102 with HF caused by CIHD). In addition, 275 healthy controls (HC) matched on demographics, age and sex, and 222 untreated metabolically matched controls (UMMC); i.e. individuals with features of the metabolic syndrome but receiving no lipid-lowering,anti-diabetic or anti-hypertensive drugs. Finally, we included 372 controls matched with IHD cases on type 2 diabetes (T2D) status and body mass index (BMI), metabolically matched controls (MMC) thereafter.

Exclusion criteria were known confounders of the gut microbiome; i.e., antibiotic use in the 3months prior to inclusion, past history of abdominal cancer+/- radiation therapy, intestinal resection except for appendectomy, inflammatory or infectious diseases including, Hepatitis B and C or human immunodeficiency virus.

Additionally,, patients with a history of organ transplantation,receiving immunosuppressants, estimated Glomerular Filtration Rate (eGFR) < 50 ml/min.1.73/m^2), drug or alcohol addiction

were excluded. Ethical approval was obtained from the Ethics Committee CPP Ile-de France, the Ethical Committees of the Capital Region of Denmark (H-3-2013-145) and Ethics Committee at the Medical Faculty at the University of Leipzig (047-13-28012013). All study participants provided written informed consent and all clinical investigations were undertaken according to Helsinki Declaration II.

Bioclinical variables

Clinical measurements were made using standardized operating procedures concludedprior patient recruitment. Bioclinical variables include age, sex, BMI, smoking status, dietary intake, physical activity, and drug intake. We obtained habitual dietary information using food-frequency questionnaires (FFQ) adapted to cultural habits of each of country of recruitment. Smoking status was obtained from a standardized questionnaire while information on physical activity was assessed using the Recent Physical Activity Questionnaire (RPAQ). Drug intake was assessed by either recall or from medication list, and a medical specialist interviewed study participants about adherence to prescribed medication.

T2D was defined as fasting plasma glucose ≥ 7 mmol/l and/or Hba1c ≥ 6.5% and/or individuals taking any glucose lowering agents; hypertension was defined as systolic blood pressure>140 mmHg and/or diastolic blood pressure>90 mmHg and/or subjects taking anti-hypertensive drugs. Echocardiography enabled the measure of left ventricular ejection fraction (LVEF) for diagnosis of HF (LVEF <45%). Renal function was assessed via eGFR calculated using the Modification of Diet in Renal Disease (MDRD) equation[43].

Blood was collected in the morning after an overnight fast. Plasma and serum samples were stored at the clinical centres at -80°C until shipment to a central laboratory facility. Fasting plasma glucose, total and HDL cholesterol, triglycerides, creatinine and HbA1c levels were measured using standard enzymatic methods. LDL-cholesterol concentrations were measured enzymatically for German participants or by the Friedwald equation for French and Danish participants. Alanine aminotransferase (ALAT), aspartate aminotransferase (ASAT), and γ-glutamyltransferase (GGT) were measured by enzyme-coupled kinetic assays. Ultrasensitive C-reactive protein (usCRP) was measured using an Image Automatic Immunoassay System (Beckman Coulter). High-sensitivity IL-6 was measured using the Human IL-6 Quantikine HSELISA Kit (R&D Systems). IFN-γ–induced protein 10 (IP-10) and C-X-C motif chemokine ligand 5 (CXCL5), CCL2, Eotaxin, IL7, MIF, MIP1b, SDF1 and VEGFa were measured using a Luminex assay (ProcartaPlex Mix&Match Human 13-plex; eBioscience, San Diego, CA, USA). Plasma pro-ANP was measured using a processing-independent assay[44].

Stool sample collection

Stool samples were processed according to International Human Microbiome Standards (IHMS) guidelines (SOP03V1). Samples were collected by study subjects at home and immediately stored at -20°C until they were transported on dry ice and frozen 4-24h later at -80°C in plastic tubes at the biobanks of corresponding recruitment centers.

Microbial load measurement by flow cytometry

Microbial loads of fecal samples were processed and analyzed as described[23]. Briefly, 0.2g frozen (-80°C) aliquots were suspended in physiological solution to a total volume of 100mL

(8.5g/L NaCl; VWR), the slurry was diluted 1,000 times andsamples were filtered using a sterile syringe filter (pore-size 5µm; Sartorius). Next, 1mL of the microbial cell suspension was stained with 1µL SYBR Green I (1:100 dilution in DMSO; shaded 15min incubation at 37°C; 10,000 concentrate, Thermo Fisher Scientific). The flow cytometry analysis was performed using a C6 Accuri flow cytometer (BD Biosciences) based on Prest *et al.*[45]. Events were monitored using the FL1 533/30nm and FL3 >670nm detectors. Instrument and gating settings were kept identical for all samples (fixed staining/gating strategy[45]) and cell counts were converted to microbial loads per gram of faecal material (microbial load index).

Stool sample processing and metagenomic analyses

Total faecal DNA was extracted following the International Human Microbiome Standards (IHMS) guidelines (SOP-07V2 H). Samples were sequenced in a non-randomized order using ion-proton technology (ThermoFisher Scientific) resulting in 23.3 ± 4.0 million (mean ± SD) single-end short reads with an on average length of 150 bases. Sequencing was carried out with standardized protocols at a single site (Metagenopolis, Paris) over a period of 18 months. There was no significant bias of the sequencing date for different Metacardis groups (Kruskal Wallis p value of 0.4 for HC, MMC, UMMS & IHD groups). Reads were cleaned using Alien Trimmer (v0.4.0)[46] in order (i) to remove resilient sequencing adapters and (ii) to trim low-quality nucleotides at the 3' side using a quality and length cut-off of 20 and 45bp, respectively. Cleaned reads were subsequently filtered from human and other possible food contaminant DNA using human genome RCh37-p10, *Bos taurus* and *Arabidopsis thaliana* with an identity score threshold of 97%. Gene abundance profiling was performed using the 9.9 million gene integrated reference catalogue of the human microbiome[47]. Filtered high-quality reads were

mapped with an identity threshold of 95% to the 9.9million-gene catalogue using Bowtie2 (v2.3.4)[48] included in METEOR v3.2 (https://forgemia.inra.fr/metagenopolis/meteor) software[49]. Gene abundance profiling table was generated by means of a two-step procedure using METEORv3.2. First, reads mapped to a unique gene in the catalogue were attributed to their corresponding genes. Second, reads that mapped with the same alignment score to multiple genes in the catalogue were attributed according to the ratio of their unique mapping counts. Gene abundance table was processed for rarefaction and normalization and further analysis using the MetaOMineR (momr, v1.31) R package[5]. To decrease technical bias due to different sequencing depth and avoid any artifacts of sample size on low abundance genes, read counts were rarefied. The gene abundance table was rarefied to 10million reads per sample by random sampling of 10million mapped reads without replacement. The resulting rarefied gene abundance table was normalized according to the fragments per kilo base per million mapped reads (FPKM) approach to give the gene abundance profile table.

Metagenomic species (MGS) are co-abundant gene groups with more than 500 genes corresponding to microbial species. 1436 MGS were clustered from 1267 human gut microbiome samples used to construct the 9.9 million-gene catalogue[47]. MGS abundances were estimated as the mean abundance of the 50 genes defining a robust centroid of the cluster (if more than 10% these genes gave positive signals). Abundances were corrected for bacterial cell count by multiplying by an index factor calculated as the bacterial cell count of the sample divided by the mean value of this bacterial cell count over the dataset as a whole. MGS taxonomical annotation was performed using all genes by sequence similarity using NCBI blast N; a species-level assignment was given if >50% of the genes matched the same reference genome of the NCBI database (November 2016 version) at a threshold of 95% of identity and

90% of gene length coverage. Remaining MGS were assigned to a given taxonomical level from genus to super-kingdom level, if more than 50% of their genes had the same level of assignment. MGS richness (MGS count) was calculated directly from the rarefied MGS abundance matrix. Bacterial gene richness (gene count) was calculated by counting the number of genes detected at least once in a given sample, using the average number of genes counted in 10 independent rarefaction experiments. MGS richness (MGS count) was calculated directly from the rarefied MGS abundance matrix.

Customized microbial module analysis

Customized module sets included previously described gut metabolic modules (GMM)[50] covering bacterial and archaeal metabolism specific to the human gut environment with a focus on anaerobic fermentation processes, expanded with a specific set of six modules zooming in on bacterial TMA metabolism[51]. Additionally, following a previously published strategy to build manually curated gutspecific metabolic modules[50,52], we constructed a novel set of 20 modules describing microbial phenylpropanoid metabolism (phenylpropanoid metabolism modules, PPM) from shotgun metagenomic data. Abundances of customized modules were derived from the ortholog abundance tables using Omixer-RPMv1.0 (https://github.com/raeslab/omixer-rpm)[50,53]. The coverage of each metabolic variant encoded in a module was calculated as the number of steps for which at least one of the orthologous groups was found in a metagenome, divided by the total number of steps constituting the variant. The coverage of the GMM was defined as equal to the one of the variants with maximum coverage. Module presence/absence was identified with a detection-threshold of more than 66% coverage to provide tolerance to miss-annotations and missing data in

metagenomes. Module abundance was calculated as the median of KEGG orthology (KO) abundance in the pathway with maximum coverage. Abundances were corrected for bacterial cell count similarly to MGSs.

Metabolic profiling

We deployed a comprehensive metabolic phenotyping strategy combining in-house analysis by proton nuclear magnetic resonance (^{1}H-NMR) spectroscopy, gas chromatography coupled to mass spectrometry (GC-MS) and targeted ultra-performance liquid chromatography coupled to tandem mass spectrometry (UPLC-MS/MS) with untargeted UPLC-MS data generated by Metabolon as described in detail below:

^{1}H Nuclear Magnetic Resonance spectroscopy (^{1}H-NMR): ^{1}H-NMR experiments were carried out using a Bruker Avance spectrometer (Bruker GmbH) operating at 600MHz as reported[54-56]. Structural assignment was performed using data from literature, HMDB (http://www.hmdb.ca/), S-Base (Bruker GmbH) and in-house databases[54]. ^{1}H-NMR spectra were pre-processed and exported to Matlab for multivariate statistical analyses using orthogonal partial least square discriminant analysis (O-PLS-DA) as previously reported[57]. Absolute metabolite quantifications were also derived using Bruker's ~~"~~In Vitro Diagnostics for research" (IVDr) quantification algorithms.

Gas Chromatography coupled Mass Spectrometry (GC-MS) semi-targeted profiling: Serum samples were prepared, analyzed and processed using standard protocols. Briefly, serum samples (100µL) were cleaned up with methanol protein precipitation, evaporated to dryness, derivatized and injected to an Agilent 7890B-5977B Inert Plus GC-MS system. The

chromatographic column was an Agilent ZORBAX DB5- MS (30 m X 250µm X 0.25µm + 10m Duragard). The temperature gradient was 37.5min long and the mass analyzer was operated in full scan mode between 50-600m/z. Peaks were annotated with the use of the Fiehn library (Agilent G1676AA Fiehn GC/MS Metabolomics RTL Library, User Guide, Agilent Technologies, https://www.agilent.com/cs/library/usermanuals/Public/G1676-90001_Fiehn.pdf). Metabolic features with high reproducibility (CV <30%) and linearity (i.e. dilution signal rho > 0.9 FDR corrected $p < 0.05$ (1-tailed-Spearman)) were kept in the final dataset resulting in one hundred and two annotated metabolic features.

UPLC-MS/MS isotopic quantification of methylamines and carnitines. Ultra-Performance Liquid Chromatography-Tandem Mass Spectrometry (UPLC-MS/MS) was employed for the determination of absolute concentrations for trimethylamine (TMA), trimethylamine-*N*-oxide (TMAO), choline, betaine, γ-butyrobetaine, betaine-aldehyde, butyryl-carnitine, isovaleryl-carnitine, OH-isovaleryl-carnitine, stearoyl-carnitine, oleoyl-carnitine, linoleoyl-carnitine, myristoyl-carnitine, lauroyl-carnitine and decanoyl-carnitine.

Serum samples (50µL) were prepared as follows: I) samples were spiked with 10µL Internal Standard (IS) solution ($^{13}C_3/^{15}N$-TMA, d_9-TMAO, d_4-choline, d_9-isovaleryl carnitine and d_9-betaine in water; 1mg/L, Sigma-Aldrich), II) 30µL of ethyl-2-bromoacetate solution (22.5g/L ethyl-2-bromoacetate, 1.4% NH_4OH in acetonitrile) were added and derivatisation of trimethylamines (TMA and $^{13}C_3/^{15}N$-TMA) to their ethoxy- analogues was completed after 30minutes at room T^o, III) 910µL of protein/lipid precipitation solution (94% acetonitrile/5%water/1% formic acid) was added, samples were centrifuged for 20minutes (4^{o}C,

20,000g) and 400µL the supernatants were transferred to UPLC-autosampler 500µL well-plates. Sample injections (5µL, full loop) were performed to a Waters Acquity UPLC-Xevo TQ-S UPLCMS/MS system equipped with an Acquity BEH HILIC (2.1×100mm, 1.7µm) chromatographic column. An isocratic elution was applied with 10mM ammonium formate in 95:5 (v/v) acetronitrile:water for 11.5minutes at 500µL/min and 50^{o}C. Positive electrospray (ESI+) was used as ionisation source and mass spectrometer parameters were set as follows: capillary, cone and sources voltages at -700, -18 and 50V, respectively, desolvation temperature at 600^{o}C, desolvation/cone/nebuliser gases were high purity nitrogen at 1000L/hr, 150L/hr and 7bar, respectively. Collision gas was high purity argon. Mass spectrometer was operated in a multiple reaction monitoring (MRM) mode. The monitored transitions were the following: for derivatised-TMA, +146à+118/59 m/z (23/27V); for derivatised-$^{13}C_3$/^{15}N-TMA, +150à+63/122 m/z (27/22V); for TMAO, +76à+59/58 m/z (12/13V); for d_9-TMAO, +85à+68/66 m/z (18/20 V); for choline, +104à+60/45 m/z (20/22V); for d_4-choline, +108à+60/45 m/z (20/22V); for isovaleryl-carnitine, +246à+85/145 m/z (19/19V); for d_9-isovaleryl-carnitine, +255à+85 m/z (19V); for betaine, +118à+59/73 m/z (18/19V); for d_9-betaine, +127à+68 m/z (19V); for γ-butyrobetaine, +146à+87/60 m/z (17/19V); for betaine aldehyde, +103à+60.5/74 m/z (12/12V); for butyryl-carnitine, +232à+85/173 m/z (14/12V); for OH-isovaleryl-carnitine, +262à+86/61 m/z (20/20V); for stearoyl-carnitine, +428à+86/371 m/z (21/17V); for oleoyl-carnitine, +426à+86/61 m/z (22/22V); for linoleoyl-carnitine, +424à+86/69 m/z (24/24V); for myristoyl-carnitine, +372.5à+86/61 m/z (24/24V); for lauroyl-carnitine, +344.5à+86/61 m/z (21/21V); for decanoyl-carnitine, +316.5à+86/145 m/z (21/21V). The system was controlled by the MassLynx^{TM} (Waters corporation; Version 4.2) software, also used for the data acquisition and analysis.

Ultra-Performance Liquid Chromatography coupled to Mass Spectrometry (UPLC-MS)

untargeted profiling. Serum samples were extracted and profiled by Metabolon (Durham, NC) using a UPLC-MS based methodology[58]. Annotated metabolites and unknown features (denoted X-00000) were identified by comparing sample features with ion features in a reference database of pure chemical standards and previously detected unknowns, followed by detailed visual inspection and quality control as reported[59].

For all metabolomic assays, we randomized the sample preparation order across the whole study so that each sample preparation batch included samples from all study groups. For MS untargeted assays, median batch-correction was performed by adjusting batch-wise study sample variable medians according to a scalar derived from adjusting pooled reference sample medians, so that pooled reference sample medians are identical across all batches.

The randomized sample-preparation batches were also tested for association with study groups using univariate statistics (Fisher's Exact or Kruskal-Wallis) and $P > 0.05$ was observed across all methods (GCMS, Fisher's Exact $P = 0.23$; UPLCMS targeted, Fisher's exact $P = 0.12$ and UPLCMS untargeted (Metabolon) Fisher's Exact $P = 0.65$). In addition, NMR run order exhibited a Kruskal Wallis $P = 0.49$. To choose a single measurement for the duplicate metabolites observed across platforms, we prioritized measurements based on the analytical quality of the data as following:

1) Targeted quantification using isotopic standards (e.g. UPLC-MS/MS for acylcarnitines and TMA).

2) Relative abundance with structural ID confirmed by native standards (e.g. Metabolon UPLC-MS).

3) Relative/absolute or quantification by NMR calibrated against a database/reference dataset (e.g. > NMR quantifications and manually assigned peaks)

4) Relative or quantification with metabolite ID check against a standards database (e.g. GC-MS)

Drug deconfounding analysis

The pipeline was used to assess to what extent observed differences between groups of study participants in microbiome, metabolome and bioclinical feature abundance are confounded, in the sense of, being consequences of other (treatment or risk factor) variables different between the groups more so than characteristic of the specific phenotype itself. We employed the *post-hoc* filtering approach implemented in the R package metadeconfoundR (v0.1.8 - see https://github.com/TillBirkner/metadeconfoundR or https://doi.org/10.5281/zenodo.4721078) that was devised within the MetaCardis consortium[8].

The pipeline has two steps. In the first, all associations between -omics features and the set of independent variables (disease status, drug treatment status, and risk markers including age, and smoking status) are determined under nonparametric statistics (Mann-Whitney U test or Spearman tests, adjusted for multiple testing using the Benjamini-Hochberg method). For each feature significantly (FDR < 0.1) associated with defined phenotype status, it is checked whether it has significant associations with any potential confounder. If not, it is considered

trivially unconfounded (NC - Not Confounded). If at least one covariate also has significant association with the feature, then for each such covariate a *post-hoc* test for confounding is applied. This test takes the form of a nested linear model comparisons (likelihood ratio test for P-values), where the dependent variable is the feature (X), and the independent variables are the disease status (A) and the tested covariate (B) versus a model containing only the covariate (B), thus testing whether disease status (A) adds explanatory statistical power beyond the covariate (B). If this holds (likelihood ratio test (LRT) $p < 0.05$) for all covariates (B), then disease status is confidentially deconfounded (CD) concerning its effect on feature X; it cannot be reduced to any confounding factor. For each covariate (B) where significance is lost, a complementary modelling test is performed of the complementary model pairs - predicting X as a function of (A) and (B) versus a model containing (A) alone, thus testing whether the covariate (B) in turn is equally reducible to (A). If for at least one such covariate (B), (B) has independent effect (LRT $p < 0.05$) on top of (A), then the feature X is considered confounded by (B). However, if in none of the pairwise tests, the original significance holds, then (A) and (B) are considered so correlated that their relative influence cannot be disentangled. We consider these cases laxly deconfounded (LD), in the sense that for these cases clear confounding influence can neither be concluded nor ruled out. The R package was applied to the present dataset considering medication status either as binary variables or as normalized dosages.

Our deconfounding pipeline takes into account linear effects related to drug categories. Still, we were not able to control for every possibly lifestyle confounding factor making a lack of full confounding adjustment a limitation of our study.

Statistical analyses

Down-sampled microbiome functional profile and taxonomic composition data, metabolite and quantitative clinical phenotype measurements were assessed between and within groups using nonparametric tests (Mann-Whitney U test, Spearman test) corrected for multiple testing using the Benjamini-Hochberg approach. All tests undertaken as part of the univariate biomarker analyses involved comparing only two groups. The main exception was the comparison between the three study centers where we applied a Kruskal-Wallis test. Nonparametric directional standardized effect sizes were likewise taken as the Cliff's Delta and Spearman Rho, respectively. Classification models were built using multivariate orthogonal partial least squares- discriminant analysis (O-PLS-DA) using ropls r package. ROC analysis was performed using ROCR package. To control for influence of covariates associated with disease severity including sex, smoking, dietary indices and drug treatment a *post-hoc* test approach was adopted as outlined above. R packages including lmtest, orddom, ropls, ROCR, circlize, ggplot2, PCMCR using R versions 4.0.2 and R studio versions 1.4.1717 and 1.2.5033 were used for various analyses.

Data Availability

Supplementary Information on data availability is linked to the online version of the paper at www.nature.com/nature. Raw shotgun sequencing data that support the findings of this study have been deposited in European Nucleotide Archive with accession codes PRJEB37249, PRJEB38742, PRJEB41311, and PRJEB46098 with public access. Metabolome data have been uploaded to Metabolights and MassIVE with respective accession numbers i.e., serum UPLCMS, serum NMR and urine NMR with accession number MTBLS3429, serum GCMS with accession

number MassIVE MSV000088042, and additional isotopically quantified serum metabolites using UPLC-MS/MS with accession number MassIVE MSV000088043. Processed pseudonymized per-subject -omics and metadata are provided in Supplementary Tables 9-13, and medication profiles are given in Supplementary Table 14.

Code availability

The novel drug-aware univariate biomarker testing pipeline, described in full elsewhere[8] , is available as an R package (metadeconfoundR; Birkner et al., manuscript in preparation) on Github (https://github.com/TillBirkner/metadeconfoundR) and also under https://doi.org/10.5281/zenodo.4721078. The latest version (0.1.8) of this package was used to generate the data shown in this publication. In addition, the scripts using this package to perform the analysis here presented available under https://doi.org/10.5281/zenodo.5516219.

Extended Data Figure 1. Overview of selected bio-clinical variables of the various groups. Box plots (above) representing the distribution of key bio-clinical variables in various study groups (lower line, lower quartile; medium line, median; upper line, upper quartile). Table (below) shows the two-sided MWU *P* for respective group comparisons using HC (n = 275), MMC (n = 372), UMMC (n = 222), IHD (n = 372), ACS (n = 112), CIHD (n = 158), HF (n = 102). IHD: ischemic heart disease patients, HC: healthy controls, MMC: metabolically matched controls, UMMC unmedicated metabolically matched controls, ACS: acute coronary syndrome, CIHD: chronic IHD, HF: heart failure due to CIHD, BMI: body mass index; HbA1c: glycated haemoglobin, pro-ANP: pro-atrial natriuretic peptide, MWU: Mann-Whitney U.

Extended Data Figure 2. Microbiome findings from the literature. Cuneiform plot shows literature review of gut microbial taxonomic and predicted functional features reported to be associated with IHD, while highlighting their individual replication in the present MetaCardis study group either as a general dysmetabolism biomarker (seen only in case of HC versus MMC), or as an IHD biomarker (seen also in case of MMC versus IHD) (**Supplementary Table 15**). The literature review was performed as a keyword search in PubMed (Medline) using combinations of the words "microbiota" and "microbiome" with the word "atherosclerosis", "cardiovascular disease", "coronary artery disease", "ischemic heart disease", "myocardial infarction", "acute coronary syndrome", "angina pectoris" and "heart failure". Studies[11,13,60-71] were identified that met the following criteria: 1) published during the recent 15 years, 2) reporting data from human studies with at least 15 participants, 3) using culture-independent methods for microbiota profiling and 4) evaluating the link between human microbiota and manifestations of impaired heart disease (**Supplementary Table 16**). Results on functional features were derived from four studies using whole-genome shotgun sequencing[11,13,69,70] Results imputed from 16S rRNA gene analyses were not included. Point marker color and size reflect MetaCardis findings (Cliff's delta), with arrows displaying direction of effects. Literature findings are shown at a uniform effect size. Markers are shown only for features significantly different in abundance (FDR < 0.1) and have a bold border if they cannot be reduced to the confounding influence of any drug or drug combination prescribed to treat dysmetabolism. While the majority of literature findings are recaptured in our study when comparing HC and IHD, relatively fewer were found in MMC and IHD comparisons, implying them to be general markers of dysmetabolism rather than being IHD-only microbiome markers. Two-sided MWU tests were used for assessing the significance of group-wise comparisons using HC (n = 275),

MMC (n = 372), UMMC (n = 222) and IHD (n = 372) groups. Multiple testing corrections were done using Benjamini-Hochberg method and FDR <= 0.1 was considered significant. IHD: ischemic heart disease patients, HC: healthy controls, MMC: metabolically matched controls, MWU: Mann-Whitney-U tests, FDR: false-discovery rate.

Extended Data Figure 3: Distribution of differential features among various group comparisons pre- and post- deconfounding. (a) Venn diagrams showing the comparative shift in the number of gut microbiome and metabolome features that remain differentially abundant (FDR <0.1) in various group comparisons when healthy individuals (HC) and drug-treated IHD cases are compared to untreated metabolically matched controls (UMMC) or (b) drug-treated metabolically matched controls (MMC) without any adjustments for potential confounders followed by (c) drug-deconfounding. Two-sided MWU tests were used for assessing the significance of group-wise comparisons using HC (n = 275), MMC (n = 372), UMMC (n = 222) and IHD (n = 372) groups. Multiple testing corrections were done using Benjamini-Hochberg method and FDR <= 0.1 was considered significant. IHD: ischemic heart disease patients, MWU: Mann-Whitney-U tests, FDR: false-discovery rate.

Extended Data Figure 4: Operational classification of microbiome and metabolome features from the perspective of IHD pathology (Further details covered in supplementary methods section).

A classification tree was constructed based on significance and alignment of effect size and directionality of microbiome and metabolome features in the various group comparisons leading to the identification of:

1) Features that reflect metabolic dysregulation in the individual but are not associated with diagnosed IHD: **dysmetabolism features (DMF).**

2) Features that are significantly associated with IHD but are also significantly altered in metabolically dysregulated individuals in the same direction; we suggest that these features are early markers of IHD pathogenesis in individuals with metabolic dysregulation: **IHD escalation features (ESCF).**
3) Features that are significantly associated with IHD but are also significantly altered in metabolically dysregulated individuals in the reverse direction; we suggest that these features are early markers of IHD seen in metabolically dysregulated individuals. However, they exhibit reversibility. This may plausibly be due to 1) long-term drug-treatment and improvement in overall lifestyle of the IHD individuals, 2) a compensatory response to the initiation of disease or 3) a trajectory-associated differential response to disease development. We propose that some of these features contribute to the stabilization of IHD and dysmetabolism and we coin those **IHD de-escalation features (DSCF)**.
4) **IHD-specific features (IHDF)** that achieve a significant shift only under IHD diagnoses.

Two-sided MWU tests were used for assessing the significance of group-wise comparisons using HC (n = 275), MMC (n = 372), UMMC (n = 222), IHD (n = 372), ACS (n = 112), CIHD (n = 158), HF (n = 102) groups. Multiple testing corrections were done using Benjamini-Hochberg method and FDR <= 0.1 was considered significant. HC: healthy controls, MMC: metabolically matched controls, UMMC unmedicated metabolically matched controls, IHD: ischemic heart disease, ACS: acute coronary syndrome, CIHD: chronic IHD, HF: heart failure due to IHD, MWU: Mann-Whitney U, FDR: false-discovery rate.

Extended Data Figure 5: Gut microbial functional features categorization. Gut microbial functional features (GMM and KEGG modules) categorized as escalation-, de-escalation-, and IHD-specific biomarkers when features classification scheme (as shown in Figure 3, Extended Data Figure 4 and described in supplementary methods) was applied to various group comparisons involving HC, MMC and IHD subjects. HC: healthy controls, MMC: metabolically matched controls, IHD: ischemic heart disease.

Extended Data Figure 6: Features categorization for ACS subgroup. Microbiome and metabolome features categorized as escalation-, de-escalation-, and ACS-specific biomarkers when features classification scheme (as shown in Figure 3, Extended Data Figure 4 and described in supplementary methods) was applied to various group comparisons involving HC, MMC and ACS groups. HC: healthy controls, MMC: metabolically matched controls, ACS: acute coronary syndrome, ESCF: escalation features, DSCF: De-escalation features. Gut microbiome features included taxonomic (prefix: Taxon) and microbiome density indices, whereas metabolome features included serum and urinary metabolites. Only features exhibiting absolute effect size > 0.1 are displayed whereas the full list is given in **Supplementary Table 17**).

Extended Data Figure 7: Features categorization for CIHD subgroup. Microbiome and metabolome features categorized as escalation-, de-escalation- and CIHD-specific biomarkers when features classification scheme (as shown in Figure 3, Extended Data Figure 4 and described in supplementary methods) was applied to various group comparisons involving HC, MMC and CIHD groups. HC: healthy controls, MMC: metabolically matched controls, CIHD: chronic IHD. ESCF: escalation features, DSCF: De-escalation features. Gut microbiome features

included both taxonomic (prefix: Taxon) and microbiome density indices, whereas metabolome features included serum and urinary metabolites. Only features exhibiting absolute effect size > 0.1 are displayed whereas the full list is given in **Supplementary Table 17**).

Extended Data Figure 8: Features categorization for HF subgroup. Microbiome and metabolome features categorized as escalation-, de-escalation- and HF-specific biomarkers when features classification scheme (as shown in Figure 3, Extended Data Figure 4 and described in supplementary methods) was applied to various group comparisons involving HC, MMC and HF groups. HC: healthy controls, MMC: metabolically matched controls, HF: heart failure due to CIHD. ESCF: escalation features, DSCF: De-escalation features. Gut microbiome features included both taxonomic (prefix: Taxon) and microbiome density indices, whereas metabolome features included serum and urinary metabolites. Only features exhibiting absolute effect size > 0.1 are displayed whereas the full list is given in **Supplementary Table 17).**

Extended Data Figure 9: Gut microbial functional features categorization for IHD subgroups. Microbial functional features (GMM and KEG modules) categorized as escalation-, de-escalation- and subtype-specific biomarkers when features classification scheme (as shown in Figure 3, Extended Data Figure 4 and described in supplementary methods) was applied to various group comparisons involving HC, MMC and IHD subgroups (i.e., ACS, CIHD and HF). HC: healthy controls, MMC: metabolically matched controls, ACS: acute coronary syndrome, CIHD: chronic IHD, HF: heart failure due to CIHD. Only features exhibiting absolute effect size > 0.1 are displayed whereas the full list is given in **Supplementary Table 17**).

Extended Data Figure 10. Discriminatory potential IHD subtype-specific features. Here, we compared clinical variables assessed for risk prediction in the companion manuscript (Model 1)

(Talmor-Barkan et al.) with our IHD subgroup-specific gut microbiome and metabolomic features (Model 2) and a combination of the two (Model 3) for their discriminatory potentials using orthogonal partial least squares- discriminant analysis (O-PLS-DA; ropls r package). Model 1 included ten variables (*i.e.* age, sex, body mass index, waist circumference, hip circumference, waist to hip ratio, systolic blood pressure, diastolic blood pressure, glycated haemoglobin (factored as > 5.7, 5.7-6.4 and < 6.4 mmol/l) and smoking status). Model 2 included each IHD subgroup-specific metagenomic species and fasting serum metabolites. Model 3 involved a combination of model 1 and 2 variables. OPLS-DA models were trained on 70% of the subgroup specific population and then tested in 30% of the remaining subgroup population using 1000 iterations of random sampling (bootstrapping). Boxplots represent the distribution (center line, median; box limits, upper and lower quartiles; whiskers, 1.5× interquartile range; points, outliers) of area under the receiver operating characteristic (ROC) curves derived from 1000 bootstraps based on these models in the training set (A) and test set (B) using both healthy controls (HC, n = 275) and metabolically matched controls (MMC, n = 372) relative to the IHD subtype cases (ACS, n = 112, CIHD n = 158 and HF n = 102). Models were compared using Kruskal-Wallis test and Dunn's pairwise multiple comparisons post hoc testing with Bonferroni correction. Dunn's test *P* are shown for each comparison HC: healthy controls, MMC: metabolically matched controls, IHD: ischemic heart disease. ACS: acute coronary syndrome, CIHD: chronic IHD, HF: heart failure due to CIHD.

Reference:

43 Levey, A. S. *et al.* A more accurate method to estimate glomerular filtration rate from serum creatinine: a new prediction equation. *Ann. Intern. Med.* **130**, 461-470 (1999).

44 Hunter, I., Rehfeld, J. F. & Goetze, J. P. Measurement of the total proANP product in mammals by processing independent analysis. *J. Immunol. Methods* **370**, 104-110 (2011).

45 Prest, E., Hammes, F., Kötzsch, S., van Loosdrecht, M. C. & Vrouwenvelder, J. S. Monitoring microbiological changes in drinking water systems using a fast and reproducible flow cytometric method. *Water Res.* **47**, 7131-7142 (2013).

46 Criscuolo, A. & Brisse, S. AlienTrimmer: a tool to quickly and accurately trim off multiple short contaminant sequences from high-throughput sequencing reads. *Genomics* **102**, 500-506 (2013).

47 Li, J. *et al.* An integrated catalog of reference genes in the human gut microbiome. *Nat. Biotechnol.* **32**, 834-841 (2014).

48 Langmead, B. & Salzberg, S. L. Fast gapped-read alignment with Bowtie 2. *Nat. Methods* **9**, 357 (2012).

49 Pons, N. *et al.* METEOR, a platform for quantitative metagenomic profiling of complex ecosystems. *Journées Ouvertes en Biologie, Informatique et Mathématiques http://www. jobim2010. fr/sites/default/files/presentations/27Pons. pdf* (2010).

50 Vieira-Silva, S. *et al.* Species–function relationships shape ecological properties of the human gut microbiome. *Nat. Microbiol.* **1**, 1-8 (2016).

51 Falony, G., Vieira-Silva, S. & Raes, J. Microbiology meets Big Data: the case of gut microbiota–derived trimethylamine. *Annu. Rev. Microbiol.* **69**, 305-321 (2015).

52 Valles-Colomer, M. *et al.* The neuroactive potential of the human gut microbiota in quality of life and depression. *Nat. Microbiol.* **4**, 623-632 (2019).

53 Darzi, Y., Falony, G., Vieira-Silva, S. & Raes, J. Towards biome-specific analysis of meta-omics data. *ISME J.* **10**, 1025-1028 (2016).

54 Dona, A. C. *et al.* A guide to the identification of metabolites in NMR-based metabonomics/metabolomics experiments. *Comput. Struct. Biotechnol. J.* **14**, 135-153 (2016).

55 Rodriguez-Martinez, A. *et al.* J-resolved 1H NMR 1D-projections for large-scale metabolic phenotyping studies: application to blood plasma analysis. *Anal. Chem.* **89**, 11405-11412 (2017).

56 Dona, A. C. *et al.* Precision high-throughput proton NMR spectroscopy of human urine, serum, and plasma for large-scale metabolic phenotyping. *Anal. Chem.* **86**, 9887-9894 (2014).

57 Würtz, P. *et al.* Metabolite profiling and cardiovascular event risk: a prospective study of 3 population-based cohorts. *Circulation* **131**, 774-785 (2015).

58 Long, T. *et al.* Whole-genome sequencing identifies common-to-rare variants associated with human blood metabolites. *Nat. Genet.* **49**, 568-578 (2017).

59 DeHaven, C. D., Evans, A. M., Dai, H. & Lawton, K. A. Organization of GC/MS and LC/MS metabolomics data into chemical libraries. *J. Cheminformatics* **2**, 1-12 (2010).

60 Liu, H. *et al.* Alterations in the gut microbiome and metabolism with coronary artery disease severity. *Microbiome* **7**, 68 (2019).

61 Lanter, B. B., Sauer, K. & Davies, D. G. Bacteria present in carotid arterial plaques are found as biofilm deposits which may contribute to enhanced risk of plaque rupture. *MBio* **5** (2014).

62 Emoto, T. *et al.* Characterization of gut microbiota profiles in coronary artery disease patients using data mining analysis of terminal restriction fragment length polymorphism: gut microbiota could be a diagnostic marker of coronary artery disease. *Heart Vessels* **32**, 39-46 (2017).

63 Ott, S. J. *et al.* Detection of diverse bacterial signatures in atherosclerotic lesions of patients with coronary heart disease. *Circulation* **113**, 929-937 (2006).

64 Yin, J. *et al.* Dysbiosis of gut microbiota with reduced trimethylamine- N- oxide level in patients with large- artery atherosclerotic stroke or transient ischemic attack. *J. AM. Heart Assoc.* **4**, e002699 (2015).

65 Zhu, Q. *et al.* Dysbiosis signatures of gut microbiota in coronary artery disease. *Physiol. Genomics* **50**, 893-903 (2018).

66 Kelly, T. N. *et al.* Gut microbiome associates with lifetime cardiovascular disease risk profile among bogalusa heart study participants. *Circ. Res.* **119**, 956-964 (2016).

67 Zheng, Y.-Y. *et al.* Gut Microbiome-Based Diagnostic Model to Predict Coronary Artery Disease. *J. Agric. Food Chem.* **68**, 3548-3557 (2020).

68 Koren, O. *et al.* Human oral, gut, and plaque microbiota in patients with atherosclerosis. *Proc. Natl. Acad. Sci. USA* **108**, 4592-4598 (2011).

69 Feng, Q. *et al.* Integrated metabolomics and metagenomics analysis of plasma and urine identified microbial metabolites associated with coronary heart disease. *Sci. Rep.* **6**, 1-14 (2016).

70 Cui, X. *et al.* Metagenomic and metabolomic analyses unveil dysbiosis of gut microbiota in chronic heart failure patients. *Sci. Rep.* **8**, 1-15 (2018).

71 Sanchez-Alcoholado, L. *et al.* Role of gut microbiota on cardio-metabolic parameters and immunity in coronary artery disease patients with and without type-2 diabetes mellitus. *Front. Microbiol.* **8**, 1936 (2017).

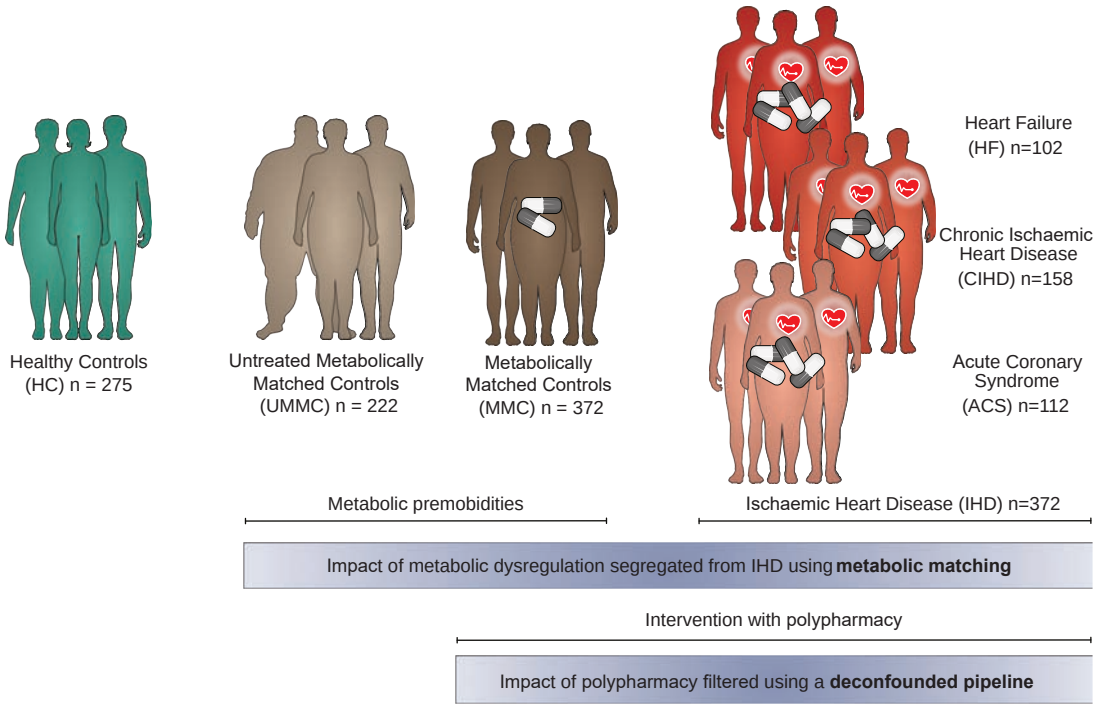

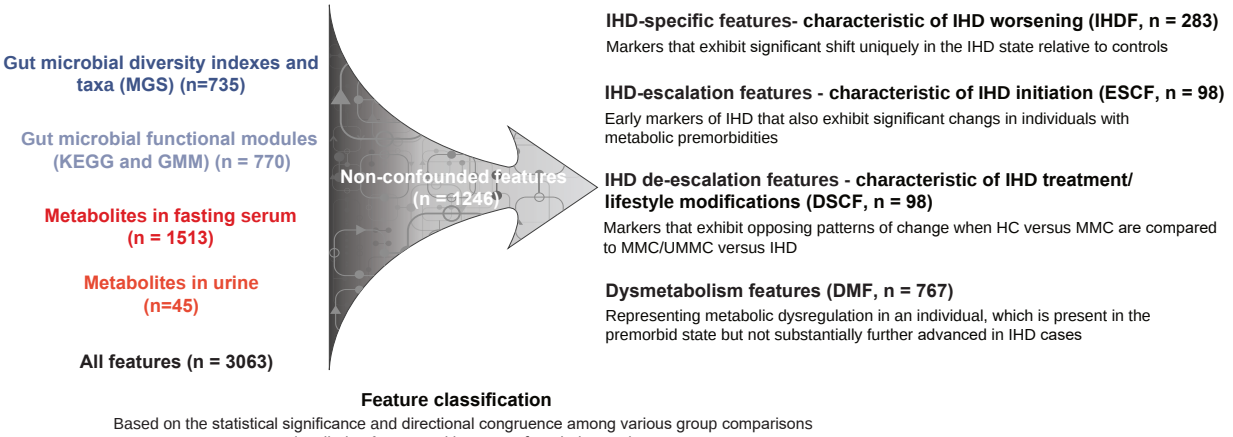

Feature classification

Based on the statistical significance and directional congruence among various group comparisons (applied to features with non-confounded status)

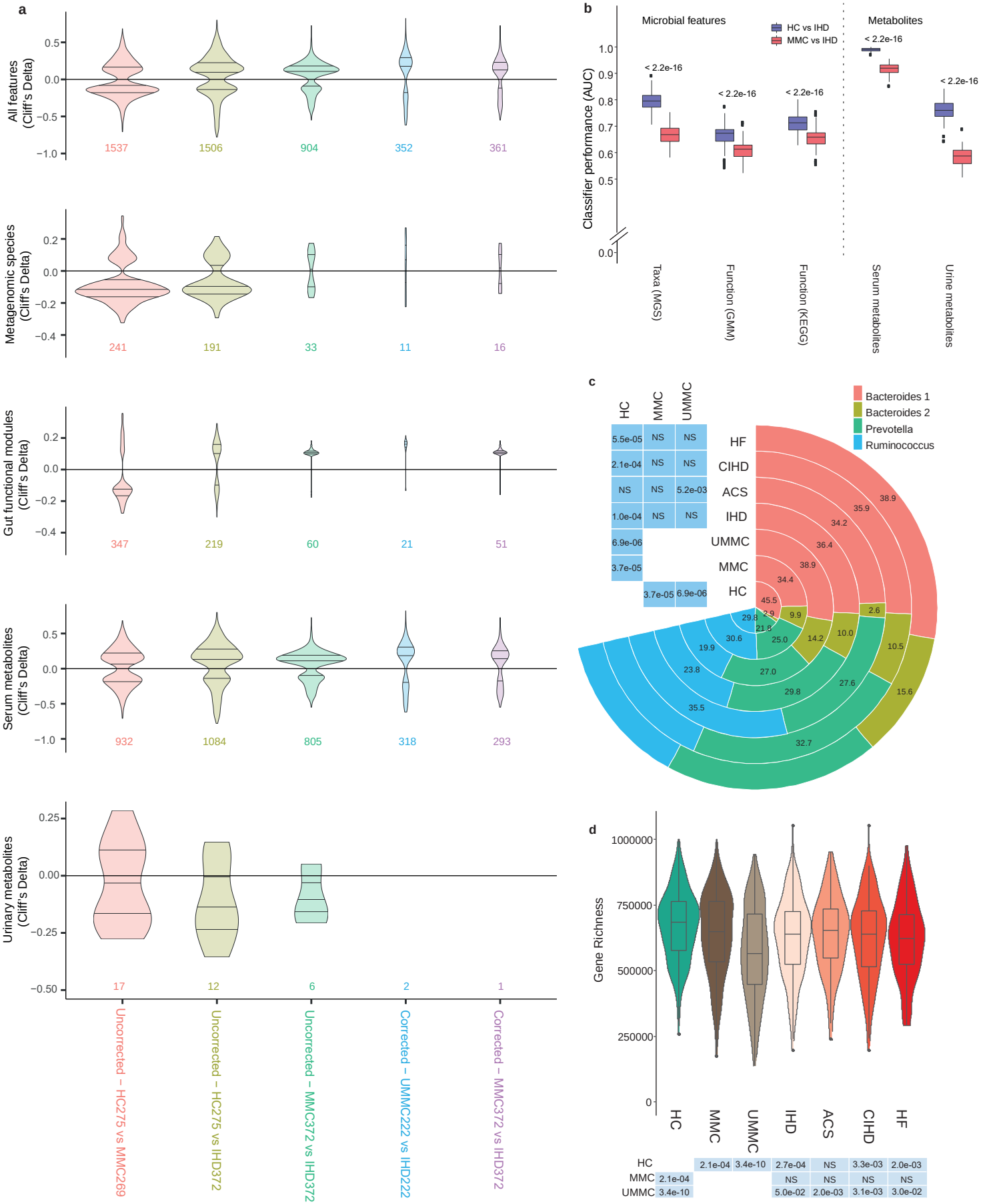
a
All features (Cliff's Delta)
1537
1506
904
352
361
Metagenomic species (Cliff's Delta)
241
191
33
11
16
Gut functional modules (Cliff's Delta)
347
219
60
21
51
Serum metabolites (Cliff's Delta)
932
1084
805
318
293
Urinary metabolites (Cliff's Delta)
17
12
6
2
1
Uncorrected – HC275 vs MMC269
Uncorrected – HC275 vs IHD372
Uncorrected – MMC372 vs IHD372
Corrected – UMMC222 vs IHD222
Corrected – MMC372 vs IHD372
b
Microbial features
Metabolites
HC vs IHD
MMC vs IHD
Classifier performance (AUC)
< 2.2e-16
Taxa (MGS)
Function (GMM)
Function (KEGG)
Serum metabolites
Urine metabolites
c
HC
MMC
UMMC
HF
CIHD
ACS
IHD
UMMC
MMC
HC
Bacteroides 1
Bacteroides 2
Prevotella
Ruminococcus
d
Gene Richness
HC
MMC
UMMC
IHD
ACS
CIHD
HF

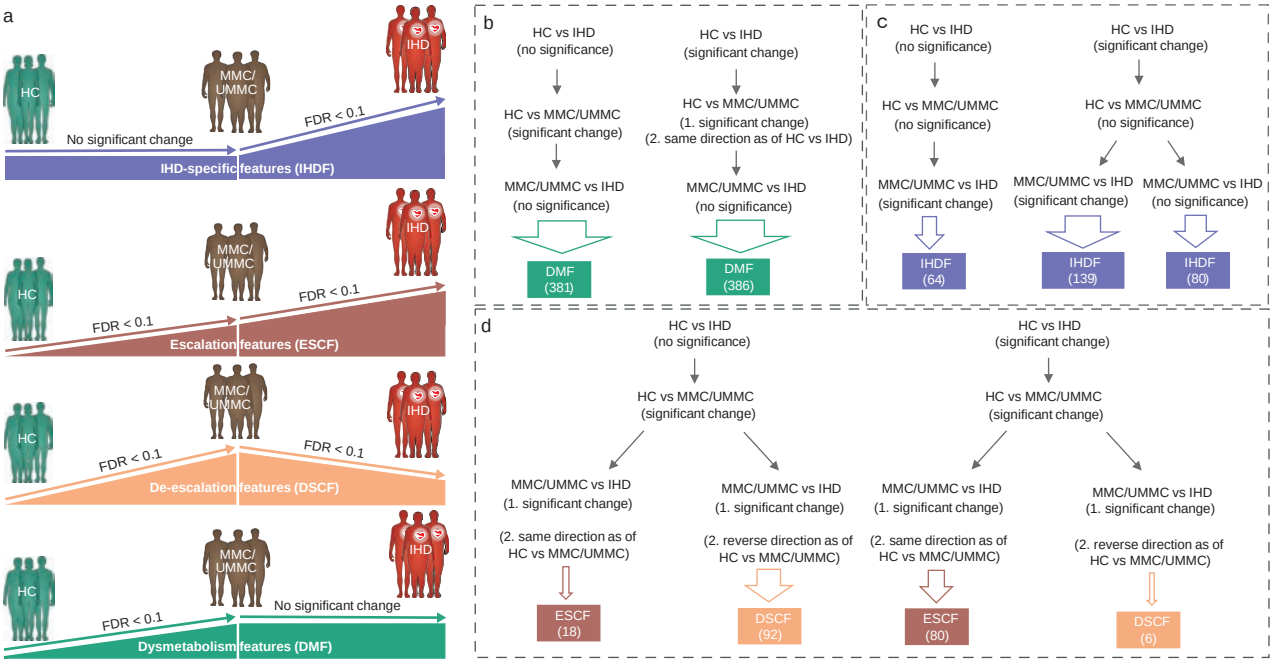
a
HC
MMC/ UMMC
IHD
No significant change
FDR < 0.1
IHD-specific features (IHDF)
FDR < 0.1
FDR < 0.1
Escalation features (ESCF)
FDR < 0.1
FDR < 0.1
De-escalation features (DSCF)
FDR < 0.1
No significant change
Dysmetabolism features (DMF)
b
HC vs IHD (no significance)
HC vs MMC/UMMC (significant change)
MMC/UMMC vs IHD (no significance)
DMF (381)
HC vs IHD (significant change)
HC vs MMC/UMMC (1. significant change) (2. same direction as of HC vs IHD)
MMC/UMMC vs IHD (no significance)
DMF (386)
c
HC vs IHD (no significance)
HC vs MMC/UMMC (no significance)
MMC/UMMC vs IHD (significant change)
IHDF (64)
HC vs IHD (significant change)
HC vs MMC/UMMC (no significance)
MMC/UMMC vs IHD (significant change)
IHDF (139)
MMC/UMMC vs IHD (no significance)
IHDF (80)
d
HC vs IHD (no significance)
HC vs MMC/UMMC (significant change)
MMC/UMMC vs IHD (1. significant change)
(2. same direction as of HC vs MMC/UMMC)
ESCF (18)
MMC/UMMC vs IHD (1. significant change)
(2. reverse direction as of HC vs MMC/UMMC)
DSCF (92)
HC vs IHD (significant change)
HC vs MMC/UMMC (significant change)
MMC/UMMC vs IHD (1. significant change)
(2. same direction as of HC vs MMC/UMMC)
ESCF (80)
MMC/UMMC vs IHD (1. significant change)
(2. reverse direction as of HC vs MMC/UMMC)
DSCF (6)

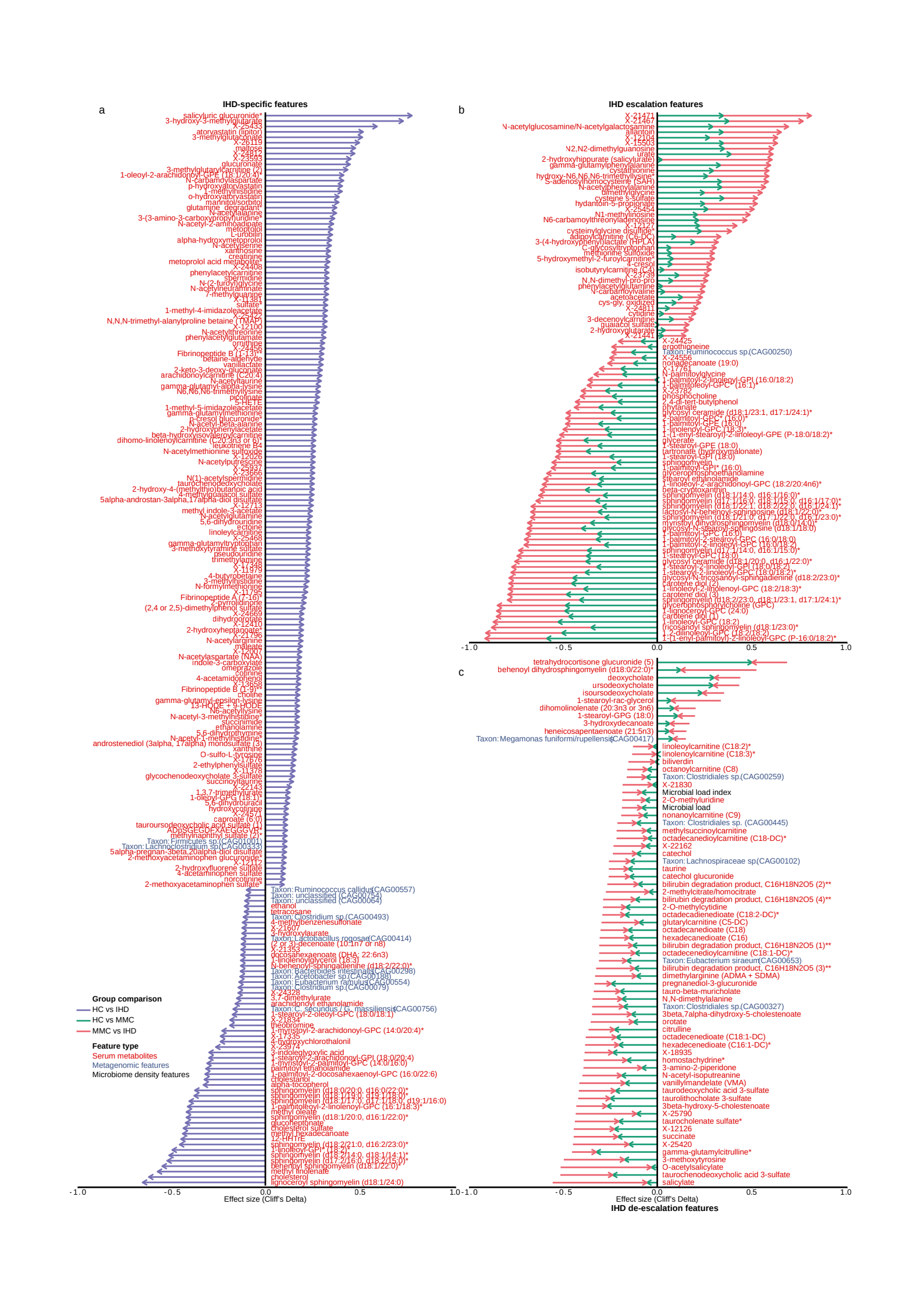
a
IHD-specific features
salicyluric glucuronide*
3-hydroxy-3-methylglutarate
X-25433
atorvastatin (lipitor)
3-methylglutaconate
X-26119
maltose
X-24812
X-23393
glucuronate
3-methylglutarylcarnitine (2)
1-oleoyl-2-arachidonoyl-GPE (18:1/20:4)
N-carbamoylaspartate
p-hydroxyatorvastatin
1-methylhistidine
o-hydroxyatorvastatin
mannitol/sorbitol
glutamine degradant*
N-acetylalanine
3-(3-amino-3-carboxypropyl)uridine*
N-acetyl-2-aminoadipate
metoprolol
L-urobilin
alpha-hydroxymetoprolol
N-acetylserine
xanthosine
creatinine
metoprolol acid metabolite*
X-24408
phenylacetylcarnitine
spermidine
N-(2-furoyl)glycine
N-acetylneuraminate
7-methylguanine
X-11381
sulfate*
1-methyl-4-imidazoleacetate
X-24542
N,N,N-trimethyl-alanylproline betaine (TMAP)
X-12100
N-acetylthreonine
phenylacetylglutamate
ornithine
X-24456
Fibrinopeptide B (1-13)**
betaine aldehyde
vanillactate
2-keto-3-deoxy-gluconate
arachidonoylcarnitine (C20:4)
N-acetyltaurine
gamma-glutamyl-alpha-lysine
N6,N6,N6-trimethyllysine
picolinate
5-HETE
1-methyl-5-imidazoleacetate
gamma-glutamylmethionine
p-cresol glucuronide*
N-acetyl-beta-alanine
2-hydroxyphenylacetate
beta-hydroxyisovalerylcarnitine
dihomo-linolenoylcarnitine (C20:3n3 or 6)*
leukotriene B4
N-acetylmethionine sulfoxide
X-12026
N-acetylputrescine
X-25937
X-23666
N(1)-acetylspermidine*
taurochenodeoxycholate
2-hydroxy-4-(methylthio)butanoic acid
4-methylguaiacol sulfate
5alpha-androstan-3alpha,17alpha-diol disulfate
X-12713
methyl indole-3-acetate
N-acetylglutamine
5,6-dihydrouridine
ectoine
linoleylcarnitine
X-25468
gamma-glutamyltryptophan
3-methoxytyramine sulfate
pseudouridine
trimethylamine N-oxide
X-17448
X-11878
4-butyrobetaine
3-methylhistidine
N-formylmethionine
X-11795
Fibrinopeptide A (7-16)*
2-pyrrolidinone
(2,4 or 2,5)-dimethylphenol sulfate
X-24669
dihydroorotate
X-12410
2-hydroxyheptanoate*
X-21796
N-acetylarginine
maleate
X-17401
N-acetylaspartate (NAA)
indole-3-carboxylate
omeprazole
cotinine
4-acetamidophenol
X-13659
Fibrinopeptide B (1-9)*
choline
gamma-glutamyl-epsilon-lysine
13-HODE + 9-HODE
N6-acetyllysine
N-acetyl-3-methylhistidine*
succinimide
ethanolamine
5,6-dihydrothymine
N-acetyl-1-methylhistidine*
androstenediol (3alpha, 17alpha) monosulfate (3)
xanthine
O-sulfo-L-tyrosine
X-17676
2-ethylphenylsulfate
X-11378
glycochenodeoxycholate 3-sulfate
succinoyltaurine
X-22143
1,3,7-trimethylurate
1-oleoyl-GPG (18:1)*
5,6-dihydrouracil
hydroxycotinine
X-24571
caproate (6:0)
tauroursodeoxycholic acid sulfate (1)
ADPGGEGDFXAEGGGVR*
methylnaphthyl sulfate (2)*
Taxon: Firmicutes sp.(CAG01001)
Taxon: Lachnoclostridium sp.(CAG00339)
5alpha-pregnan-3beta,20alpha-diol disulfate
2-methoxyacetaminophen glucuronide*
X-12112
2-hydroxyfluorene sulfate
4-acetaminophen sulfate
norcotinine
2-methoxyacetaminophen sulfate*
Taxon: Ruminococcus callidus (CAG00557)
Taxon: unclassified (CAG00754)
Taxon: unclassified (CAG00064)
ethanol
tetracosane
Taxon: Clostridium sp.(CAG00493)
4-methylbenzenesulfonate
X-21607
3-hydroxylaurate
Taxon: Lactobacillus rogosae (CAG00414)
(2 or 3)-decenoate (10:1n7 or n8)
X-21353
docosahexaenoate (DHA; 22:6n3)
1-linolenoylglycerol (18:3)
N-behenoyl-sphingadienine (d18:2/22:0)*
Taxon: Bacteroides intestinalis (CAG00298)
Taxon: Acetobacter sp.(CAG00188)
Taxon: Eubacterium ramulus (CAG00554)
Taxon: Clostridium sp.(CAG00079)
X-24328
3,7-dimethylurate
arachidonoyl ethanolamide
Taxon: C. secundus / C. massiliensis (CAG00756)
1-stearoyl-2-oleoyl-GPC (18:0/18:1)
X-21834
theobromine
1-myristoyl-2-arachidonoyl-GPC (14:0/20:4)*
X-17335
4-hydroxychlorothalonil
X-23974
3-indoleglyoxylic acid
1-stearoyl-2-arachidonoyl-GPI (18:0/20:4)
1-myristoyl-2-palmitoyl-GPC (14:0/16:0)
palmitoyl ethanolamide
1-palmitoyl-2-docosahexaenoyl-GPC (16:0/22:6)
cholestanol
alpha-tocopherol
sphingomyelin (d18:0/20:0, d16:0/22:0)*
sphingomyelin (d18:1/19:0, d19:1/18:0)*
sphingomyelin (d18:1/17:0, d17:1/18:0, d19:1/16:0)
1-palmitoleoyl-2-linolenoyl-GPC (16:1/18:3)*
methyl oleate
sphingomyelin (d18:1/20:0, d16:1/22:0)*
glucoheptonate
cholesterol sulfate
methyl hexadecanoate
12-HHTrE
sphingomyelin (d18:2/21:0, d16:2/23:0)*
1-linoleoyl-GPI* (18:2)*
sphingomyelin (d18:2/14:0, d18:1/14:1)*
sphingomyelin (d17:2/16:0, d18:2/15:0)*
behenyl sphingomyelin (d18:1/22:0)*
methyl linolenate
cholesterol
lignoceroyl sphingomyelin (d18:1/24:0)
-1.0
-0.5
0.0
0.5
1.0
Effect size (Cliff's Delta)
Group comparison
HC vs IHD
HC vs MMC
MMC vs IHD
Feature type
Serum metabolites
Metagenomic features
Microbiome density features
b
IHD escalation features
X-21471
X-21467
N-acetylglucosamine/N-acetylgalactosamine
allantoin
X-12104
X-15503
N2,N2-dimethylguanosine
urate
2-hydroxyhippurate (salicylurate)
gamma-glutamylphenylalanine
cystathionine
hydroxy-N6,N6,N6-trimethyllysine*
S-adenosylhomocysteine (SAH)
N-acetylphenylalanine
dimethylglycine
cysteine s-sulfate
hydantoin-5-propionate
X-25454
N1-methylinosine
N6-carbamoylthreonyladenosine
X-11427
cysteinylglycine disulfide*
adipoylcarnitine (C6-DC)
3-(4-hydroxyphenyl)lactate (HPLA)
C-glycosyltryptophan
methionine sulfoxide
5-hydroxymethyl-2-furoylcarnitine*
4-cresol
isobutyrylcarnitine (C4)
X-23739
N,N-dimethyl-pro-pro
phenylacetylglutamine
N-carbamoylvaline
acetoacetate
cys-gly, oxidized
X-24811
cytidine
3-decenoylcarnitine
guaiacol sulfate
2-hydroxyglutarate
X-21441
X-24425
ergothioneine
Taxon: Ruminococcus sp.(CAG00250)
X-24556
nonadecanoate (19:0)
X-17761
N-palmitoylglycine
1-palmitoyl-2-linoleoyl-GPI (16:0/18:2)
1-palmitoleoyl-GPC* (16:1)*
X-21792
phosphocholine
2,4-di-tert-butylphenol
phytanate
glycosyl ceramide (d18:1/23:1, d17:1/24:1)*
2-palmitoyl-GPC* (16:0)*
1-palmitoyl-GPE (16:0)*
1-linolenoyl-GPC (18:3)*
1-(1-enyl-stearoyl)-2-linoleoyl-GPE (P-18:0/18:2)*
glycerate
1-stearoyl-GPE (18:0)
tartronate (hydroxymalonate)
1-stearoyl-GPI (18:0)
sphingomyelin
1-palmitoyl-GPI* (16:0)
glycerophosphoethanolamine
stearoyl ethanolamide
1-linoleoyl-2-arachidonoyl-GPC (18:2/20:4n6)*
beta-cryptoxanthin
sphingomyelin (d18:1/14:0, d16:1/16:0)*
sphingomyelin (d17:1/16:0, d18:1/15:0, d16:1/17:0)*
sphingomyelin (d18:1/22:1, d18:2/22:0, d16:1/24:1)*
lactosyl-N-behenoyl-sphingosine (d18:1/22:0)*
sphingomyelin (d18:1/21:0, d17:1/22:0, d16:1/23:0)*
myristoyl dihydrosphingomyelin (d18:0/14:0)*
glycosyl-N-stearoyl-sphingosine (d18:1/18:0)
1-palmitoyl-GPC (16:0)
1-palmitoyl-2-stearoyl-GPC (16:0/18:0)
1-palmitoyl-2-linoleoyl-GPC (16:0/18:2)
sphingomyelin (d17:1/14:0, d16:1/15:0)*
1-stearoyl-GPC (18:0)
glycosyl ceramide (d18:1/20:0, d16:1/22:0)*
1-stearoyl-2-linoleoyl-GPI (18:0/18:2)*
1-stearoyl-2-linoleoyl-GPC (18:0/18:2)*
glycosyl-N-tricosanoyl-sphingadienine (d18:2/23:0)*
carotene diol (2)
1-linoleoyl-2-linolenoyl-GPC (18:2/18:3)*
carotene diol (3)
sphingomyelin (d18:2/23:0, d18:1/23:1, d17:1/24:1)*
glycerophosphorylcholine (GPC)
1-lignoceroyl-GPC (24:0)
carotene diol (1)
1-linoleoyl-GPC (18:2)
tricosanoyl sphingomyelin (d18:1/23:0)*
1,2-dilinoleoyl-GPC (18:2/18:2)
1-(1-enyl-palmitoyl)-2-linoleoyl-GPC (P-16:0/18:2)*
-1.0
-0.5
0.0
0.5
1.0
c
tetrahydrocortisone glucuronide (5)
behenoyl dihydrosphingomyelin (d18:0/22:0)*
deoxycholate
ursodeoxycholate
isoursodeoxycholate
1-stearoyl-rac-glycerol
dihomolinolenate (20:3n3 or 3n6)
1-stearoyl-GPG (18:0)
3-hydroxydecanoate
heneicosapentaenoate (21:5n3)
Taxon: Megamonas funiformi/rupellensis (CAG00417)
linoleoylcarnitine (C18:2)*
linolenoylcarnitine (C18:3)*
biliverdin
octanoylcarnitine (C8)
Taxon: Clostridiales sp.(CAG00259)
X-21830
Microbial load index
2-O-methyluridine
Microbial load
nonanoylcarnitine (C9)
Taxon: Clostridiales sp. (CAG00445)
methylsuccinoylcarnitine
octadecanedioylcarnitine (C18-DC)*
X-22162
catechol
Taxon: Lachnospiraceae sp(CAG00102)
taurine
catechol glucuronide
bilirubin degradation product, C16H18N2O5 (2)**
2-methylcitrate/homocitrate
bilirubin degradation product, C16H18N2O5 (4)**
2-O-methylcytidine
octadecadienedioate (C18:2-DC)*
glutarylcarnitine (C5-DC)
octadecanedioate (C18)
hexadecanedioate (C16)
bilirubin degradation product, C16H18N2O5 (1)**
octadecenedioylcarnitine (C18:1-DC)*
Taxon: Eubacterium siraeum (CAG00653)
bilirubin degradation product, C16H18N2O5 (3)**
dimethylarginine (ADMA + SDMA)
pregnanediol-3-glucuronide
tauro-beta-muricholate
N,N-dimethylalanine
Taxon: Clostridiales sp.(CAG00327)
3beta,7alpha-dihydroxy-5-cholestenoate
orotate
citrulline
octadecenedioate (C18:1-DC)
hexadecenedioate (C16:1-DC)*
X-18935
homostachydrine*
3-amino-2-piperidone
N-acetyl-isoputreanine
vanillylmandelate (VMA)
taurodeoxycholic acid 3-sulfate
taurolithocholate 3-sulfate
3beta-hydroxy-5-cholestenoate
X-25790
taurocholenate sulfate*
X-12126
succinate
X-25420
gamma-glutamylcitrulline*
3-methoxytyrosine
O-acetylsalicylate
taurochenodeoxycholic acid 3-sulfate
salicylate
-1.0
-0.5
0.0
0.5
1.0
Effect size (Cliff's Delta)
IHD de-escalation features

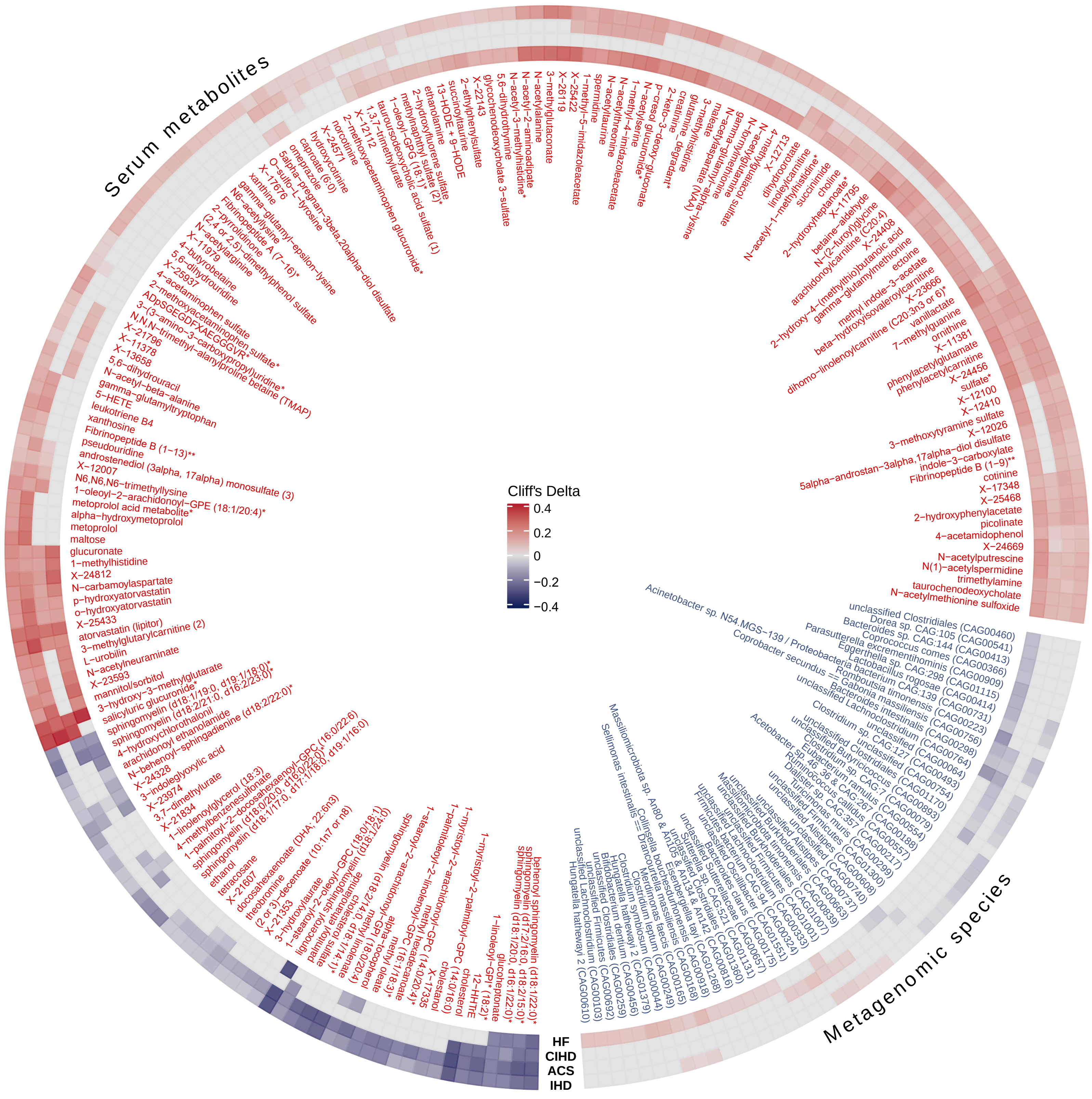
Serum metabolites
Metagenomic species
Cliff's Delta
0.4
0.2
0
−0.2
−0.4
HF
CIHD
ACS
IHD

a

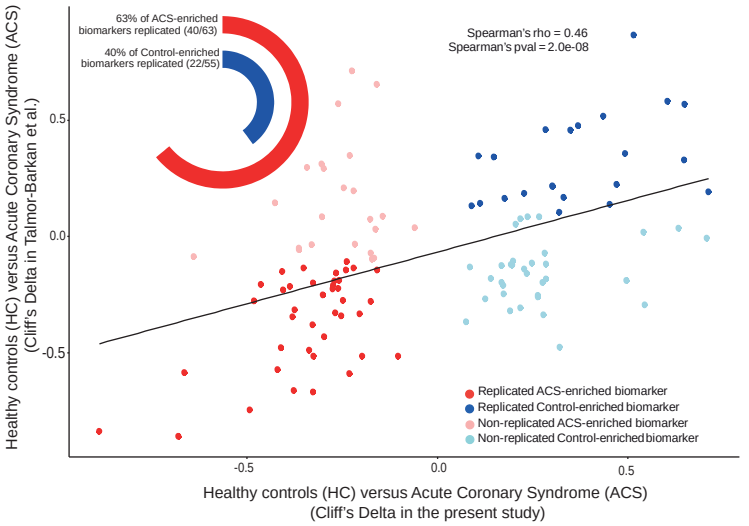

b

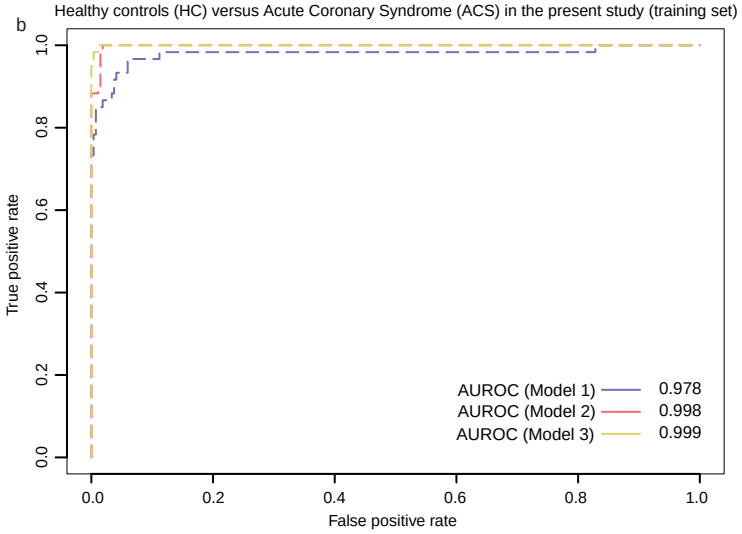

c

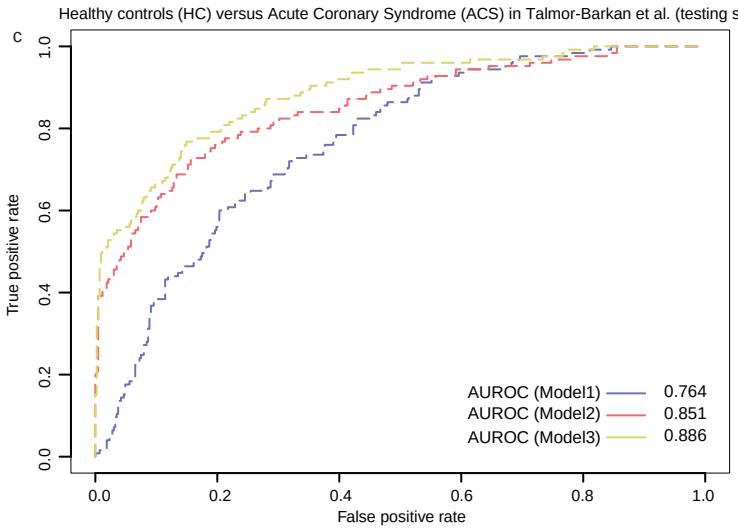

Model 1: Clinical variables alone
Model 2: ACS-specific biomarkers
Model 3: Clinical variables with ACS-specific biomarkers

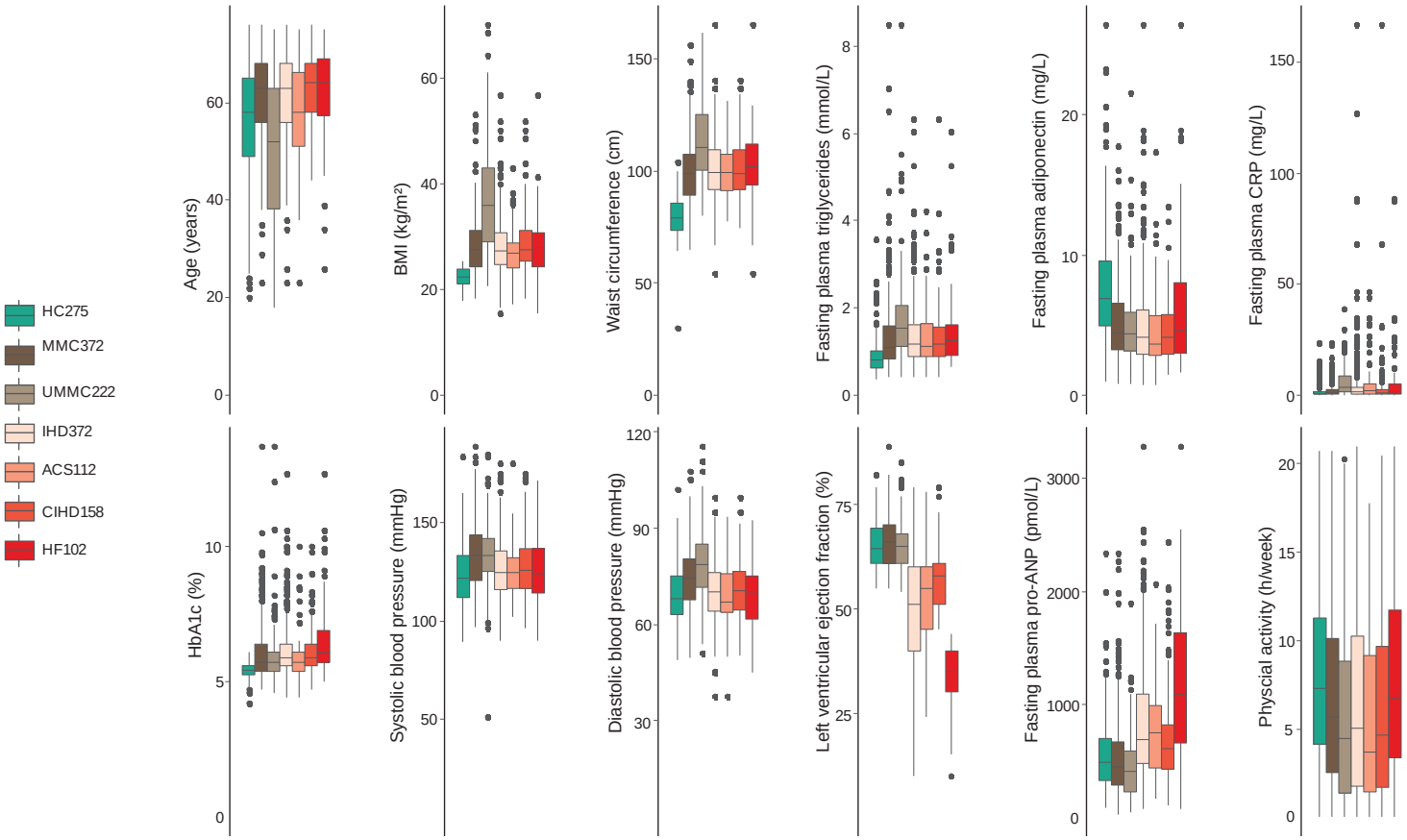

	HC vs MMC	HC vs UMMC	HC vs IHD	HC vs ACS	HC vs CIHD	HC vs HF	MMC vs IHD	MMC vs ACS	MMC vs CIHD	MMC vs HF	UMMC vs IHD	UMMC vs ACS	UMMC vs CIHD	UMMC vs HF
Age (years)	2.8e-10	1.2e-05	2.2e-09	NS	3.1e-10	3.6e-07	NS	3.0e-03	NS	NS	1.0e-06	6.5e-07	< 2.2e-16	3.1e-14
BMI (kg/m²)	< 2.2e-16	< 2.2e-16	< 2.2e-16	< 2.2e-16	< 2.2e-16	< 2.2e-16	NS	NS	NS	NS	< 2.2e-16	< 2.2e-16	< 2.2e-16	< 2.2e-16
Wasit circumference (cm)	< 2.2e-16	< 2.2e-16	< 2.2e-16	< 2.2e-16	< 2.2e-16	< 2.2e-16	NS	NS	NS	NS	2.0e-08	1.3e-08	5.6e-11	8.8e-07
Fasting plasma triglycerides (mmol/L)	< 2.2e-16	< 2.2e-16	< 2.2e-16	7.2e-12	< 2.2e-16	< 2.2e-16	NS	NS	NS	NS	3.5e-05	1.0e-04	7.5e-07	7.0e-04
Fasting plasma adiponectin (mg/L)	< 2.2e-16	< 2.2e-16	< 2.2e-16	9.5e-13	< 2.2e-16	1.2e-06	NS	2.0e-02	2.1e-02	NS	6.3e-03	NS	NS	NS
Fasting plasma CRP (mg/L)	2.3e-11	< 2.2e-16	2.2e-09	2.8e-07	1.2e-13	2.0e-07	NS	1.7e-02	NS	3.7e-02	1.2e-04	4.2e-03	4.2e-13	3.3e-04
HbA1c	< 2.2e-16	< 2.2e-16	< 2.2e-16	< 2.2e-16	< 2.2e-16	< 2.2e-16	5.1e-03	NS	1.4e-02	1.2e-04	5.1e-04	NS	1.0e-04	2.1e-07
Systolic blood pressure (mmHg)	2.3e-16	9.6e-14	1.4e-02	NS	8.9e-03	NS	1.5e-07	1.4e-04	2.1e-04	2.8e-04	6.9e-10	3.5e-06	1.3e-05	3.4e-05
Diastolic blood pressure (mmHg)	8.7e-15	< 2.2e-16	NS	NS	NS	NS	3.0e-08	2.0e-04	1.2e-04	3.7e-05	2.1e-13	3.0e-09	1.4e-12	7.7e-11
Left ventricular ejection fraction (%)	NS	NS	< 2.2e-16	2.5e-15	2.5e-13	< 2.2e-16	< 2.2e-16	< 2.2e-16	< 2.2e-16	< 2.2e-16	< 2.2e-16	< 2.2e-16	2.0e-15	< 2.2e-16
Fasting plasma pro-ANP (pmol/L)	NS	1.1e-04	7.8e-13	3.8e-05	4.2e-04	< 2.2e-16	< 2.2e-16	1.0e-06	1.3e-06	< 2.2e-16	7.2e-12	2.8e-09	3.4e-10	< 2.2e-16
Physical activity (h/week)	2.9e-05	2.2e-07	8.4e-05	5.8e-04	5.4e-04	NS	NS	NS	NS	NS	NS	NS	NS	NS

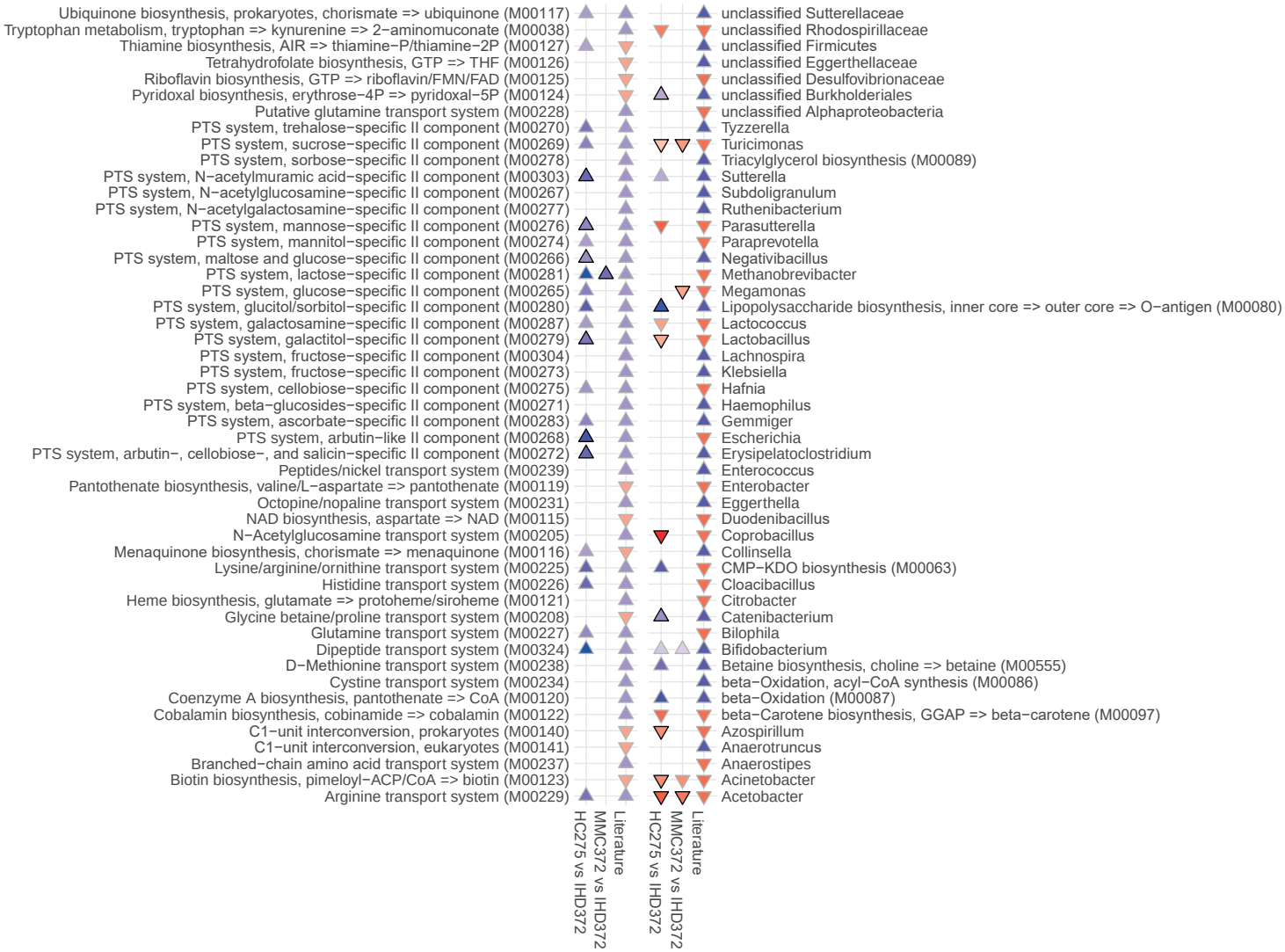
Ubiquinone biosynthesis, prokaryotes, chorismate => ubiquinone (M00117)
Tryptophan metabolism, tryptophan => kynurenine => 2−aminomuconate (M00038)
Thiamine biosynthesis, AIR => thiamine−P/thiamine−2P (M00127)
Tetrahydrofolate biosynthesis, GTP => THF (M00126)
Riboflavin biosynthesis, GTP => riboflavin/FMN/FAD (M00125)
Pyridoxal biosynthesis, erythrose−4P => pyridoxal−5P (M00124)
Putative glutamine transport system (M00228)
PTS system, trehalose−specific II component (M00270)
PTS system, sucrose−specific II component (M00269)
PTS system, sorbose−specific II component (M00278)
PTS system, N−acetylmuramic acid−specific II component (M00303)
PTS system, N−acetylglucosamine−specific II component (M00267)
PTS system, N−acetylgalactosamine−specific II component (M00277)
PTS system, mannose−specific II component (M00276)
PTS system, mannitol−specific II component (M00274)
PTS system, maltose and glucose−specific II component (M00266)
PTS system, lactose−specific II component (M00281)
PTS system, glucose−specific II component (M00265)
PTS system, glucitol/sorbitol−specific II component (M00280)
PTS system, galactosamine−specific II component (M00287)
PTS system, galactitol−specific II component (M00279)
PTS system, fructose−specific II component (M00304)
PTS system, fructose−specific II component (M00273)
PTS system, cellobiose−specific II component (M00275)
PTS system, beta−glucosides−specific II component (M00271)
PTS system, ascorbate−specific II component (M00283)
PTS system, arbutin−like II component (M00268)
PTS system, arbutin−, cellobiose−, and salicin−specific II component (M00272)
Peptides/nickel transport system (M00239)
Pantothenate biosynthesis, valine/L−aspartate => pantothenate (M00119)
Octopine/nopaline transport system (M00231)
NAD biosynthesis, aspartate => NAD (M00115)
N−Acetylglucosamine transport system (M00205)
Menaquinone biosynthesis, chorismate => menaquinone (M00116)
Lysine/arginine/ornithine transport system (M00225)
Histidine transport system (M00226)
Heme biosynthesis, glutamate => protoheme/siroheme (M00121)
Glycine betaine/proline transport system (M00208)
Glutamine transport system (M00227)
Dipeptide transport system (M00324)
D−Methionine transport system (M00238)
Cystine transport system (M00234)
Coenzyme A biosynthesis, pantothenate => CoA (M00120)
Cobalamin biosynthesis, cobinamide => cobalamin (M00122)
C1−unit interconversion, prokaryotes (M00140)
C1−unit interconversion, eukaryotes (M00141)
Branched−chain amino acid transport system (M00237)
Biotin biosynthesis, pimeloyl−ACP/CoA => biotin (M00123)
Arginine transport system (M00229)
unclassified Sutterellaceae
unclassified Rhodospirillaceae
unclassified Firmicutes
unclassified Eggerthellaceae
unclassified Desulfovibrionaceae
unclassified Burkholderiales
unclassified Alphaproteobacteria
Tyzzerella
Turicimonas
Triacylglycerol biosynthesis (M00089)
Sutterella
Subdoligranulum
Ruthenibacterium
Parasutterella
Paraprevotella
Negativibacillus
Methanobrevibacter
Megamonas
Lipopolysaccharide biosynthesis, inner core => outer core => O−antigen (M00080)
Lactococcus
Lactobacillus
Lachnospira
Klebsiella
Hafnia
Haemophilus
Gemmiger
Escherichia
Erysipelatoclostridium
Enterococcus
Enterobacter
Eggerthella
Duodenibacillus
Coprobacillus
Collinsella
CMP−KDO biosynthesis (M00063)
Cloacibacillus
Citrobacter
Catenibacterium
Bilophila
Bifidobacterium
Betaine biosynthesis, choline => betaine (M00555)
beta−Oxidation, acyl−CoA synthesis (M00086)
beta−Oxidation (M00087)
beta−Carotene biosynthesis, GGAP => beta−carotene (M00097)
Azospirillum
Anaerotruncus
Anaerostipes
Acinetobacter
Acetobacter
HC275 vs IHD372
MMC372 vs IHD372
Literature
HC275 vs IHD372
MMC372 vs IHD372
Literature

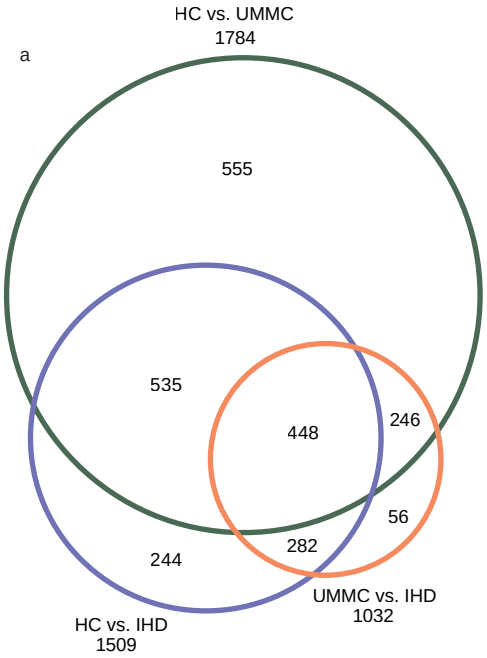

Group comparisons using healthy controls, drug-naive metabolically-matched controls and drug-treated IHD cases (no deconfounding)

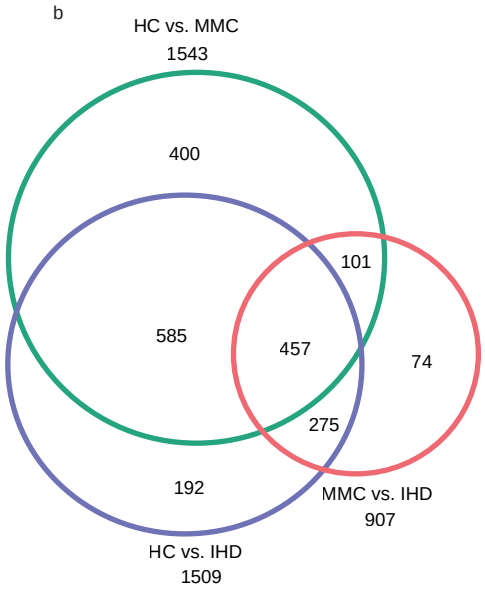

Group comparisons using healthy controls, drug-treated metabolically-matched controls and IHD cases (no deconfounding)

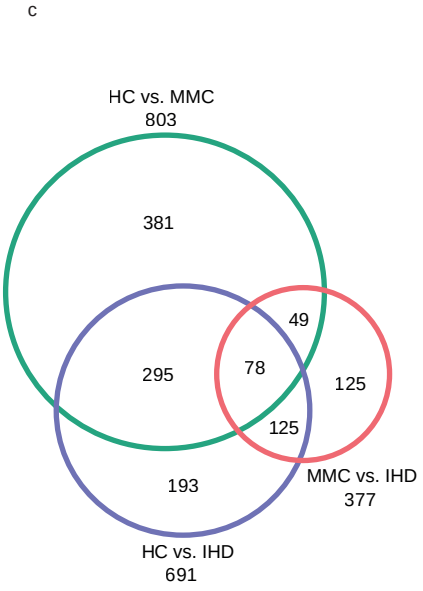

Group comparisons using healthy controls, drug-treated metabolically-matched controls and IHD cases (with deconfounding)

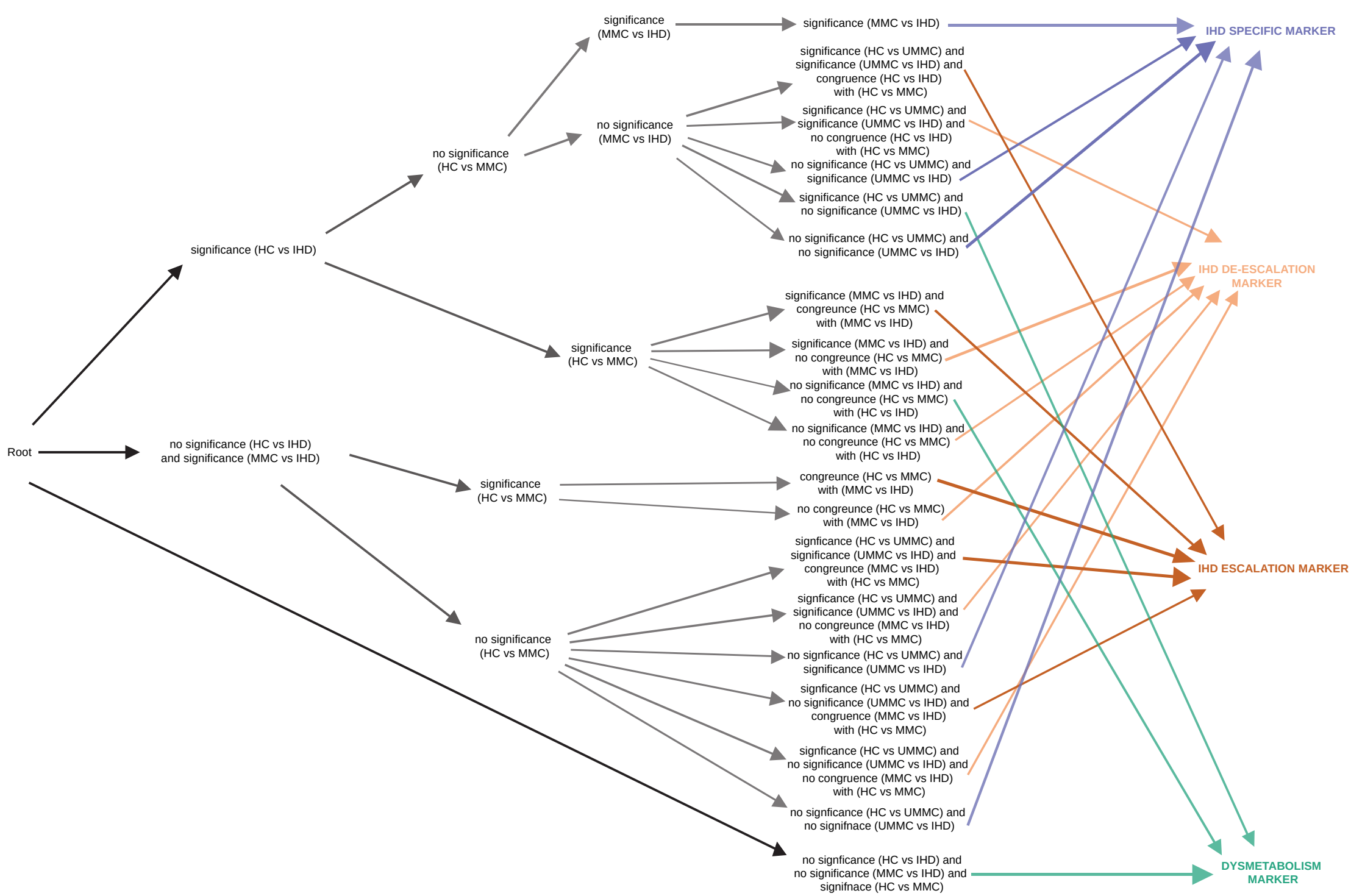

* in all cases, directional alignment has been reported using HC vs MMC and MMC vs IHD/HC vs IHD in order to be consistent with Figure 3.
HC vs UMMC, UMMC vs IHD always exhibited directional alignment with HC vs MMC and MMC vs IHD, respectively, for our escalation and de-escalation markers.


IHD specific features
Function: Multidrug resistance, efflux pump MdtABC (M00648)
Function: D-Allose transport system (M00217)
Function: Multidrug resistance, PatAB transporter (M00708)
Function: PTS system, arbutin-, cellobiose-, and salicin-specific II component (M00272)
Function: PTS system, N-acetylmuramic acid-specific II component (M00303)
Function: Multidrug resistance, efflux pump SmeABC (M00645)
Function: BaeS-BaeR (envelope stress response) regulator (M00450)
Function: AI-2 transport system (M00219)
Function: Putative amino-acid transport system (M00586)
Function: CitA-CitB (citrate fermentation) regulator (M00486)
Function: Nitrate assimilation (M00615)
Function: PTS system, galactitol-specific II component (M00279)
Function: Cationic antimicrobial peptide (CAMP) resistance (M00721)
Function: Spliceosome, U4/U6.U5 tri-snRNP (M00354)
Function: CAM (Crassulacean acid metabolism), dark (M00168)
Function: Cytochrome d ubiquinol oxidase (M00153)
Function: Lactosylceramide biosynthesis (M00066)
Function: Lipopolysaccharide biosynthesis (M00080)
Function: aspartate degradation II (MF0029)
Function: lactose and galactose degradation (MF0007)
Function: PTS system, sucrose-specific II component (M00269)
Function: Molybdate transport system (M00189)
Function: PTS system, mannose-specific II component (M00276)
Function: succinate production (MF0096)
Function: PTS system, maltose and glucose-specific II component (M00266)
Function: Lysine degradation, lysine => acetoacetyl-CoA (M00032)
Function: Cytochrome b6f complex (M00162)
Function: Spliceosome, 35S U5-snRNP (M00355)
Function: CMP-KDO biosynthesis (M00063)
Function: SsrA-SsrB regulator (M00663)
Function: Lincosamide resistance, efflux pump LmrB (M00715)
Function: BRCA1-associated genome surveillance complex (BASC) (M00295)
Function: BasS-BasR (antimicrobial peptide resistance) regulator (M00451)
Function: alanine degradation II (MF0034)
Function: cysteine degradation II (MF0045)
Function: Nitrogen fixation, nitrogen => ammonia (M00175)
Function: arabinose degradation (MF0014)
Function: DevS-DevR (redox response) regulator (M00482)
Function: glycerol degradation I (MF0060)
Function: aspartate degradation I (MF0028)
Function: acetate to acetyl-CoA (MF0075)
Function: cagA pathogenicity island (M00564)
Function: Multidrug resistance, efflux pump YkkCD
-1.0
-0.5
0.0
0.5
1.0
Effect size (Cliff's Delta)

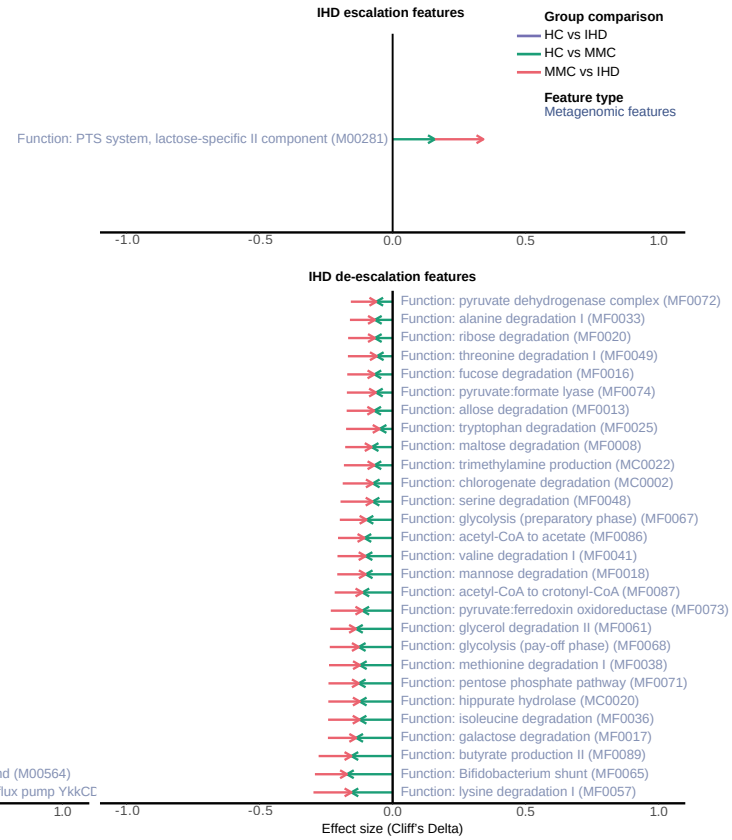
IHD escalation features
Group comparison
HC vs IHD
HC vs MMC
MMC vs IHD
Feature type
Metagenomic features
Function: PTS system, lactose-specific II component (M00281)
-1.0
-0.5
0.0
0.5
1.0
IHD de-escalation features
Function: pyruvate dehydrogenase complex (MF0072)
Function: alanine degradation I (MF0033)
Function: ribose degradation (MF0020)
Function: threonine degradation I (MF0049)
Function: fucose degradation (MF0016)
Function: pyruvate:formate lyase (MF0074)
Function: allose degradation (MF0013)
Function: tryptophan degradation (MF0025)
Function: maltose degradation (MF0008)
Function: trimethylamine production (MC0022)
Function: chlorogenate degradation (MC0002)
Function: serine degradation (MF0048)
Function: glycolysis (preparatory phase) (MF0067)
Function: acetyl-CoA to acetate (MF0086)
Function: valine degradation I (MF0041)
Function: mannose degradation (MF0018)
Function: acetyl-CoA to crotonyl-CoA (MF0087)
Function: pyruvate:ferredoxin oxidoreductase (MF0073)
Function: glycerol degradation II (MF0061)
Function: glycolysis (pay-off phase) (MF0068)
Function: methionine degradation I (MF0038)
Function: pentose phosphate pathway (MF0071)
Function: hippurate hydrolase (MC0020)
Function: isoleucine degradation (MF0036)
Function: galactose degradation (MF0017)
Function: butyrate production II (MF0089)
Function: Bifidobacterium shunt (MF0065)
Function: lysine degradation I (MF0057)
-1.0
-0.5
0.0
0.5
1.0
Effect size (Cliff's Delta)

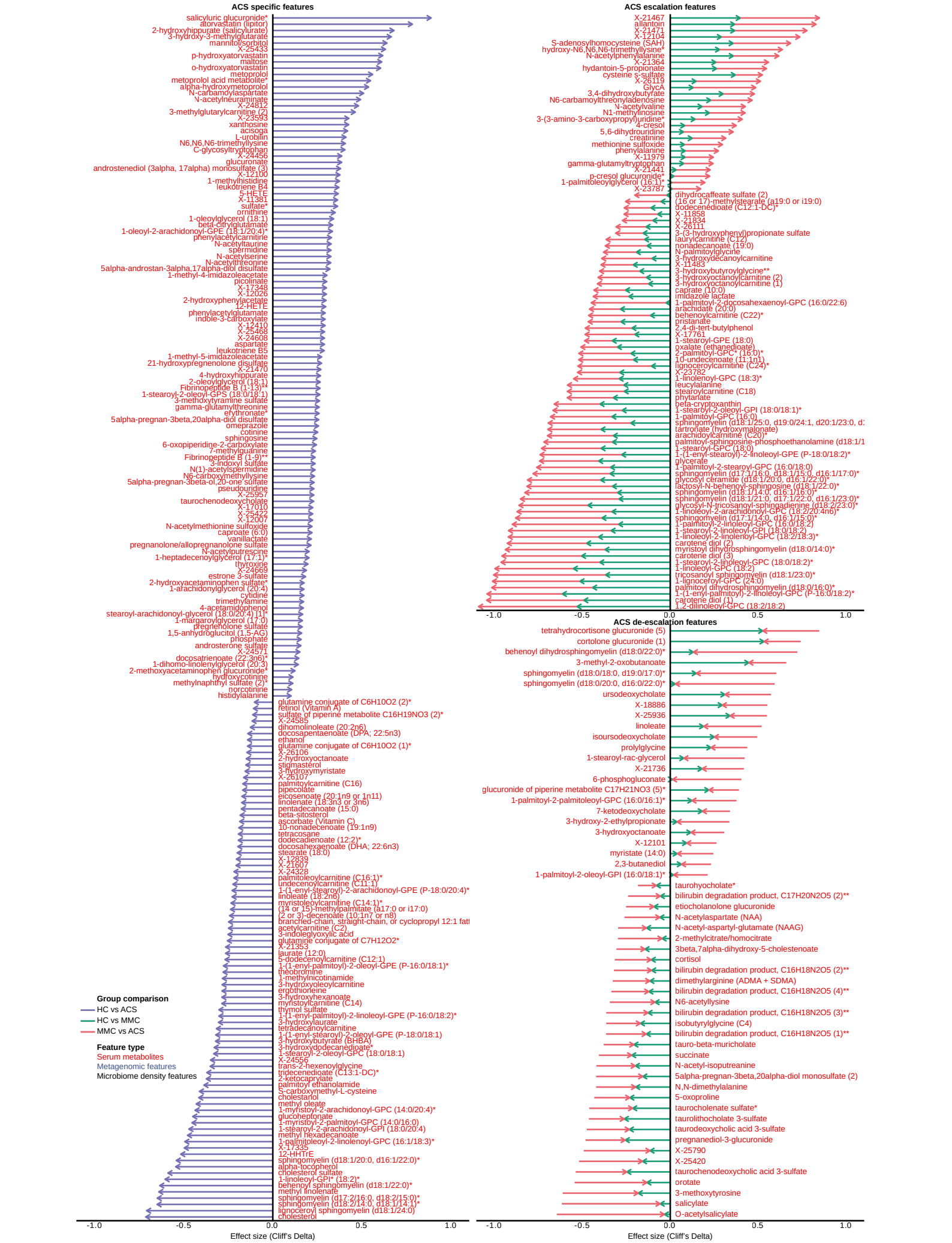
ACS specific features
salicyluric glucuronide*
atorvastatin (lipitor)
2-hydroxyhippurate (salicylurate)
3-hydroxy-3-methylglutarate
mannitol/sorbitol
X-25433
p-hydroxyatorvastatin
maltose
o-hydroxyatorvastatin
metoprolol
metoprolol acid metabolite*
alpha-hydroxymetoprolol
N-carbamoylaspartate
N-acetylneuraminate
X-24812
3-methylglutarylcarnitine (2)
X-23593
xanthosine
acisoga
L-urobilin
N6,N6,N6-trimethyllysine
C-glycosyltryptophan
X-24456
glucuronate
androstenediol (3alpha, 17alpha) monosulfate (3)
X-12100
1-methylhistidine
leukotriene B4
5-HETE
X-11381
sulfate*
ornithine
1-oleoylglycerol (18:1)
beta-citrylglutamate
1-oleoyl-2-arachidonoyl-GPE (18:1/20:4)*
phenylacetylcarnitine
N-acetyltaurine
spermidine
N-acetylserine
N-acetylthreonine
5alpha-androstan-3alpha,17alpha-diol disulfate
1-methyl-4-imidazoleacetate
picolinate
X-17348
X-12026
2-hydroxyphenylacetate
12-HETE
phenylacetylglutamate
indole-3-carboxylate
X-12410
X-25468
X-24608
aspartate
leukotriene B5
1-methyl-5-imidazoleacetate
21-hydroxypregnenolone disulfate
X-21470
4-hydroxyhippurate
2-oleoylglycerol (18:1)
Fibrinopeptide B (1-13)**
1-stearoyl-2-oleoyl-GPS (18:0/18:1)
3-methoxytyramine sulfate
gamma-glutamylthreonine
erythronate*
5alpha-pregnan-3beta,20alpha-diol disulfate
omeprazole
cotinine
sphingosine
6-oxopiperidine-2-carboxylate
7-methylguanine
Fibrinopeptide B (1-9)**
3-indoxyl sulfate
N(1)-acetylspermidine
N6-carboxymethyllysine
5alpha-pregnan-3beta-ol,20-one sulfate
pseudouridine
X-25957
taurochenodeoxycholate
X-17010
X-25422
X-12007
N-acetylmethionine sulfoxide
caproate (6:0)
vanillactate
pregnanolone/allopregnanolone sulfate
N-acetylputrescine
1-heptadecenoylglycerol (17:1)*
thyroxine
X-24669
estrone 3-sulfate
2-hydroxyacetaminophen sulfate*
1-arachidonylglycerol (20:4)
cytidine
trimethylamine
4-acetamidophenol
stearoyl-arachidonoyl-glycerol (18:0/20:4) [1]*
1-margaroylglycerol (17:0)
pregnenolone sulfate
1,5-anhydroglucitol (1,5-AG)
phosphate
androsterone sulfate
X-24571
docosatrienoate (22:3n6)*
1-dihomo-linolenylglycerol (20:3)
2-methoxyacetaminophen glucuronide*
hydroxycotinine
methylnaphthyl sulfate (2)*
norcotinine
histidylalanine
glutamine conjugate of C6H10O2 (2)*
retinol (Vitamin A)
sulfate of piperine metabolite C16H19NO3 (2)*
X-24585
dihomolinoleate (20:2n6)
docosapentaenoate (DPA; 22:5n3)
ethanol
glutamine conjugate of C6H10O2 (1)*
X-26106
2-hydroxyoctanoate
stigmasterol
3-hydroxymyristate
X-26107
palmitoylcarnitine (C16)
pipecolate
eicosenoate (20:1n9 or 1n11)
linolenate (18:3n3 or 3n6)
pentadecanoate (15:0)
beta-sitosterol
ascorbate (Vitamin C)
10-nonadecenoate (19:1n9)
tetracosane
dodecadienoate (12:2)*
docosahexaenoate (DHA; 22:6n3)
stearate (18:0)
X-12839
X-21607
X-24328
palmitoleoylcarnitine (C16:1)*
undecenoylcarnitine (C11:1)
1-(1-enyl-stearoyl)-2-arachidonoyl-GPE (P-18:0/20:4)*
linoleate (18:2n6)
myristoleoylcarnitine (C14:1)*
(14 or 15)-methylpalmitate (a17:0 or i17:0)
(2 or 3)-decenoate (10:1n7 or n8)
branched-chain, straight-chain, or cyclopropyl 12:1 fatt
acetylcarnitine (C2)
3-indoleglyoxylic acid
glutamine conjugate of C7H12O2*
X-21353
laurate (12:0)
5-dodecenoylcarnitine (C12:1)
1-(1-enyl-palmitoyl)-2-oleoyl-GPE (P-16:0/18:1)*
theobromine
1-methylnicotinamide
3-hydroxyoleoylcarnitine
ergothioneine
3-hydroxyhexanoate
myristoylcarnitine (C14)
thymol sulfate
1-(1-enyl-palmitoyl)-2-linoleoyl-GPE (P-16:0/18:2)*
3-hydroxylaurate
tetradecanoylcarnitine
1-(1-enyl-stearoyl)-2-oleoyl-GPE (P-18:0/18:1)
3-hydroxybutyrate (BHBA)
3-hydroxydodecanedioate*
1-stearoyl-2-oleoyl-GPC (18:0/18:1)
X-24556
trans-2-hexenoylglycine
tridecenedioate (C13:1-DC)*
2-ketocaprylate
palmitoyl ethanolamide
S-carboxymethyl-L-cysteine
cholestanol
methyl oleate
1-myristoyl-2-arachidonoyl-GPC (14:0/20:4)*
glucoheptonate
1-myristoyl-2-palmitoyl-GPC (14:0/16:0)
1-stearoyl-2-arachidonoyl-GPI (18:0/20:4)
methyl hexadecanoate
1-palmitoleoyl-2-linolenoyl-GPC (16:1/18:3)*
X-17335
12-HHTrE
sphingomyelin (d18:1/20:0, d16:1/22:0)*
alpha-tocopherol
cholesterol sulfate
1-linoleoyl-GPI* (18:2)*
behenoyl sphingomyelin (d18:1/22:0)*
methyl linolenate
sphingomyelin (d17:2/16:0, d18:2/15:0)*
sphingomyelin (d18:2/14:0, d18:1/14:1)*
lignoceroyl sphingomyelin (d18:1/24:0)
cholesterol
-1.0
-0.5
0.0
0.5
1.0
Effect size (Cliff's Delta)
Group comparison
HC vs ACS
HC vs MMC
MMC vs ACS
Feature type
Serum metabolites
Metagenomic features
Microbiome density features
ACS escalation features
X-21467
allantoin
X-21471
X-12104
S-adenosylhomocysteine (SAH)
hydroxy-N6,N6,N6-trimethyllysine*
N-acetylphenylalanine
X-21364
hydantoin-5-propionate
cysteine s-sulfate
X-26119
GlycA
3,4-dihydroxybutyrate
N6-carbamoylthreonyladenosine
N-acetylvaline
N1-methylinosine
3-(3-amino-3-carboxypropyl)uridine*
4-cresol
5,6-dihydrouridine
creatinine
methionine sulfoxide
phenylalanine
X-11979
gamma-glutamyltryptophan
X-21441
p-cresol glucuronide*
1-palmitoleoylglycerol (16:1)*
X-23787
dihydrocaffeate sulfate (2)
(16 or 17)-methylstearate (a19:0 or i19:0)
dodecenedioate (C12:1-DC)*
X-11859
X-21834
X-26111
3-(3-hydroxyphenyl)propionate sulfate
laurylcarnitine (C12)
nonadecanoate (19:0)
N-palmitoylglycine
3-hydroxydecanoylcarnitine
X-11483
3-hydroxybutyroylglycine**
3-hydroxyoctanoylcarnitine (2)
3-hydroxyoctanoylcarnitine (1)
caprate (10:0)
imidazole lactate
1-palmitoyl-2-docosahexaenoyl-GPC (16:0/22:6)
arachidate (20:0)
behenoylcarnitine (C22)*
pristanate
2,4-di-tert-butylphenol
X-17761
1-stearoyl-GPE (18:0)
oxalate (ethanedioate)
2-palmitoyl-GPC* (16:0)*
10-undecenoate (11:1n1)
lignoceroylcarnitine (C24)*
X-23782
1-linolenoyl-GPC (18:3)*
leucylalanine
stearoylcarnitine (C18)
phytanate
beta-cryptoxanthin
1-stearoyl-2-oleoyl-GPI (18:0/18:1)*
1-palmitoyl-GPC (16:0)
sphingomyelin (d18:1/25:0, d19:0/24:1, d20:1/23:0, d
tartronate (hydroxymalonate)
arachidoylcarnitine (C20)*
palmitoyl-sphingosine-phosphoethanolamine (d18:1/1
1-stearoyl-GPC (18:0)
1-(1-enyl-stearoyl)-2-linoleoyl-GPE (P-18:0/18:2)*
glycerate
1-palmitoyl-2-stearoyl-GPC (16:0/18:0)
sphingomyelin (d17:1/16:0, d18:1/15:0, d16:1/17:0)*
glycosyl ceramide (d18:1/20:0, d16:1/22:0)*
lactosyl-N-behenoyl-sphingosine (d18:1/22:0)*
sphingomyelin (d18:1/14:0, d16:1/16:0)*
sphingomyelin (d18:1/21:0, d17:1/22:0, d16:1/23:0)*
glycosyl-N-tricosanoyl-sphingadienine (d18:2/23:0)*
1-linoleoyl-2-arachidonoyl-GPC (18:2/20:4n6)*
sphingomyelin (d17:1/14:0, d16:1/15:0)*
1-palmitoyl-2-linoleoyl-GPC (16:0/18:2)
1-stearoyl-2-linoleoyl-GPI (18:0/18:2)
1-linoleoyl-2-linolenoyl-GPC (18:2/18:3)*
carotene diol (2)
myristoyl dihydrosphingomyelin (d18:0/14:0)*
carotene diol (3)
1-stearoyl-2-linoleoyl-GPC (18:0/18:2)*
1-linoleoyl-GPC (18:2)
tricosanoyl sphingomyelin (d18:1/23:0)*
1-lignoceroyl-GPC (24:0)
palmitoyl dihydrosphingomyelin (d18:0/16:0)*
1-(1-enyl-palmitoyl)-2-linoleoyl-GPC (P-16:0/18:2)*
carotene diol (1)
1,2-dilinoleoyl-GPC (18:2/18:2)
-1.0
-0.5
0.0
0.5
1.0
ACS de-escalation features
tetrahydrocortisone glucuronide (5)
cortolone glucuronide (1)
behenoyl dihydrosphingomyelin (d18:0/22:0)*
3-methyl-2-oxobutanoate
sphingomyelin (d18:0/18:0, d19:0/17:0)*
sphingomyelin (d18:0/20:0, d16:0/22:0)*
ursodeoxycholate
X-18886
X-25936
linoleate
isoursodeoxycholate
prolylglycine
1-stearoyl-rac-glycerol
X-21736
6-phosphogluconate
glucuronide of piperine metabolite C17H21NO3 (5)*
1-palmitoyl-2-palmitoleoyl-GPC (16:0/16:1)*
7-ketodeoxycholate
3-hydroxy-2-ethylpropionate
3-hydroxyoctanoate
X-12101
myristate (14:0)
2,3-butanediol
1-palmitoyl-2-oleoyl-GPI (16:0/18:1)*
taurohyocholate*
bilirubin degradation product, C17H20N2O5 (2)**
etiocholanolone glucuronide
N-acetylaspartate (NAA)
N-acetyl-aspartyl-glutamate (NAAG)
2-methylcitrate/homocitrate
3beta,7alpha-dihydroxy-5-cholestenoate
cortisol
bilirubin degradation product, C16H18N2O5 (2)**
dimethylarginine (ADMA + SDMA)
bilirubin degradation product, C16H18N2O5 (4)**
N6-acetyllysine
bilirubin degradation product, C16H18N2O5 (3)**
isobutyrylglycine (C4)
bilirubin degradation product, C16H18N2O5 (1)**
tauro-beta-muricholate
succinate
N-acetyl-isoputreanine
5alpha-pregnan-3beta,20alpha-diol monosulfate (2)
N,N-dimethylalanine
5-oxoproline
taurocholenate sulfate*
taurolithocholate 3-sulfate
taurodeoxycholic acid 3-sulfate
pregnanediol-3-glucuronide
X-25790
X-25420
taurochenodeoxycholic acid 3-sulfate
orotate
3-methoxytyrosine
salicylate
O-acetylsalicylate
-1.0
-0.5
0.0
0.5
1.0
Effect size (Cliff's Delta)


CIHD specific features
salicyluric glucuronide*
3-hydroxy-3-methylglutarate
X-25433
atorvastatin (lipitor)
1-oleoyl-2-arachidonoyl-GPE (18:1/20:4)*
glucuronate
2-hydroxy-3-methylvalerate
X-24812
X-24408
arachidonoylcarnitine (C20:4)
3-(4-hydroxyphenyl)lactate (HPLA)
p-hydroxyatorvastatin
1-methylhistidine
o-hydroxyatorvastatin
N-carbamoylaspartate
linoleylcarnitine
X-11381
betaine-aldehyde
gamma-glutamylmethionine
4-methyl-2-oxopentanoate
dihomo-linolenoylcarnitine (C20:3n3 or 6)*
phenylacetylcarnitine
2-hydroxy-4-(methylthio)butanoic acid
7-methylguanine
X-13658
4-hydroxyhippurate
ornithine
phenylacetylglutamate
X-23666
N-(2-furoyl)glycine
beta-hydroxyisovaleroylcarnitine
N-acetyl-beta-alanine
gamma-glutamyltryptophan
methionine
dihydroorotate
picolinate
beta-citrylglutamate
ectoine
sulfate*
N6,N6,N6-trimethyllysine
X-11378
methyl indole-3-acetate
acisoga
X-11795
vanillactate
taurochenodeoxycholate
N-acetylmethionine sulfoxide
X-24456
stearoyl-arachidonoyl-glycerol (18:0/20:4) [1]*
trimethylamine
oleoylcarnitine
X-16580
X-12100
2-hydroxyheptanoate*
choline
X-21796
2-hydroxyphenylacetate
N-acetylputrescine
glucuronide of C10H18O2 (7)*
arabinose
nisinate (24:6n3)
levulinoylcarnitine
X-17348
X-25468
N(1)-acetylspermidine
glucuronide of C10H18O2 (8)*
5,6-dihydrouracil
N-acetylalliin
suberoylcarnitine (C8-DC)
Taxon: Firmicutes bacterium CAG:94 (CAG00324)
decanoylcarnitine
succinimide
1,3,7-trimethylurate
X-12007
sulfate of piperine metabolite C16H19NO3 (2)*
N-acetyl-1-methylhistidine*
4-acetamidophenol
androstenediol (3alpha, 17alpha) monosulfate (3)
Taxon: Lachnoclostridium sp. (CAG00333)
Taxon: Bacteroides clarus (CAG00175)
octanoylcarnitine (C8)
1-oleoyl-GPG (18:1)*
Taxon: unclassified Oscillibacter (CAG01551)
Taxon: Firmicutes sp. (CAG01001)
Taxon: unclassified Burkholderiales (CAG01007)
epiandrosterone sulfate
1-(1-enyl-palmitoyl)-2-arachidonoyl-GPE (P-16:0/20:4)*
X-12112
pantoprazole
Taxon: unclassified (CAG00754)
docosahexaenoate (DHA; 22:6n3)
X-24952
1-myristoylglycerol (14:0)
Taxon: Bacteroides intestinalis (CAG00298)
4-methylbenzenesulfonate
1-margaroylglycerol (17:0)
X-17969
2-myristoylglycerol (14:0)
1-palmitoylglycerol (16:0)
Taxon: Clostridium sp. (CAG00493)
Taxon: unclassified (CAG00064)
Taxon: C. secundus / G. massiliensis (CAG00756)
theobromine
1-linolenoylglycerol (18:3)
Taxon: unclassified Butyricicoccus (CAG00893)
1-docosahexaenoylglycerol (22:6)
5alpha-pregnan-3beta,20beta-diol monosulfate (1)
Taxon: unclassified Lachnoclostridium (CAG00764)
1-palmitoyl-2-docosahexaenoyl-GPC (16:0/22:6)
sphingadienine
sphingomyelin (d18:1/20:0, d16:1/22:0)*
sphingomyelin (d18:1/19:0, d19:1/18:0)*
palmitoyl ethanolamide
glucoheptonate
sphingomyelin (d18:2/21:0, d16:2/23:0)*
12-HHTrE
behenoyl sphingomyelin (d18:1/22:0)*
1-linoleoyl-GPI* (18:2)*
sphingomyelin (d17:2/16:0, d18:2/15:0)*
cholesterol
Group comparison
HC vs CIHD
HC vs MMC
MMC vs CIHD
Feature type
Serum metabolites
Metagenomic features
Microbiome density features
-1.0
-0.5
0.0
0.5
1.0
Effect size (Cliff's Delta)
CIHD escalation features
X-21471
N-acetylglucosamine/N-acetylgalactosamine
2-hydroxyhippurate (salicylurate)
cystathionine
dimethylglycine
X-12104
X-19438
cysteine s-sulfate
X-26119
hexanoylcarnitine (C6)
OH-isovalerylcarnitine
cysteinylglycine disulfide*
xanthosine
perfluorohexanesulfonate (PFHxS)
X-24241
sucrose
argininate*
X-23739
1-oleoyl-2-docosahexaenoyl-GPE (18:1/22:6)*
cys-gly, oxidized
5-hydroxymethyl-2-furoylcarnitine*
lanthionine
X-23659
3-decenoylcarnitine
2-aminobutyrate
4-cresol
7-ketodeoxycholate
N-carbamoylalanine
2-hydroxyglutarate
citraconate/glutaconate
X-21470
dodecenedioate (C12:1-DC)*
3-(3-hydroxyphenyl)propionate sulfate
X-24425
nonadecanoate (19:0)
1-pentadecanoylglycerol (15:0)
Taxon: Ruminococcus sp. (CAG00250)
1-palmitoyl-GPA (16:0)
2-hydroxystearate
2-docosahexaenoylglycerol (22:6)*
2-stearoyl-GPE (18:0)*
oxalate (ethanedioate)
3-indolelglyoxylic acid
2,4-di-tert-butylphenol
histidine betaine (hercynine)*
cholesterol sulfate
phosphocholine
sphingomyelin (d18:1/17:0, d17:1/18:0, d19:1/16:0)
2-palmitoyl-GPC* (16:0)*
sphingomyelin (d18:2/14:0, d18:1/14:1)*
1-stearoyl-GPI (18:0)
1-palmitoyl-GPE (16:0)
1,2-dipalmitoyl-GPC (16:0/16:0)
1-stearoyl-GPE (18:0)
1-palmitoyl-GPI* (16:0)
glycerophosphoethanolamine
lignoceroyl sphingomyelin (d18:1/24:0)
lactosyl-N-behenoyl-sphingosine (d18:1/22:0)*
1-palmitoyl-2-stearoyl-GPC (16:0/18:0)
1-palmitoyl-GPC (16:0)
1-stearoyl-GPC (18:0)
glycosyl-N-tricosanoyl-sphingadienine (d18:2/23:0)*
tricosanoyl sphingomyelin (d18:1/23:0)*
glycerophosphorylcholine (GPC)
-1.0
-0.5
0.0
0.5
1.0
CIHD de-escalation features
behenoyl dihydrosphingomyelin (d18:0/22:0)*
1-stearoyl-GPG (18:0)
X-24544
cortisol
methylnaphthyl sulfate (2)*
linolenoylcarnitine (C18:3)*
linoleoylcarnitine (C18:2)*
biliverdin
2-O-methyluridine
O-sulfo-L-tyrosine
bilirubin degradation product, C17H18N2O4 (2)**
X-25523
bilirubin degradation product, C17H18N2O4 (1)**
nonanoylcarnitine (C9)
octadecenedioylcarnitine (C18:1-DC)*
myristoleoylcarnitine (C14:1)*
Microbial load index
Microbial load
3beta,7alpha-dihydroxy-5-cholestenoate
decanoylcarnitine (C10)
tauro-beta-muricholate
bilirubin degradation product, C16H18N2O5 (2)**
bilirubin degradation product, C16H18N2O5 (4)**
2-O-methylcytidine
homostachydrine*
bilirubin degradation product, C16H18N2O5 (1)**
glutamine_degradant*
glutarylcarnitine (C5-DC)
X-25790
taurodeoxycholic acid 3-sulfate
bilirubin degradation product, C16H18N2O5 (3)**
X-12126
taurocholenate sulfate*
bilirubin
X-25420
3beta-hydroxy-5-cholestenoate
taurochenodeoxycholic acid 3-sulfate
gamma-glutamylcitrulline*
O-acetylsalicylate
salicylate
-1.0
-0.5
0.0
0.5
1.0
Effect size (Cliff's Delta)

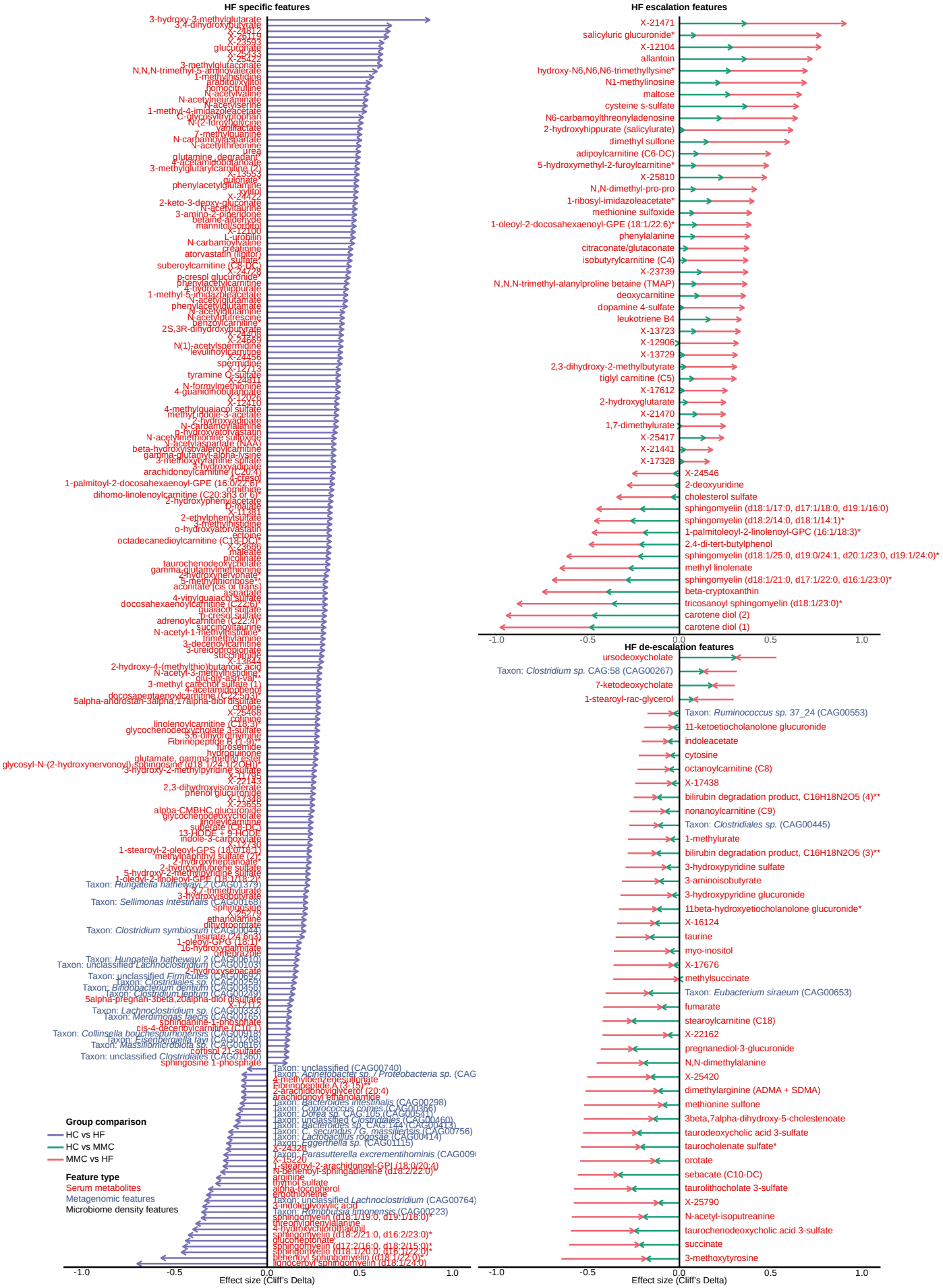
HF specific features
HF escalation features
HF de-escalation features
Group comparison
HC vs HF
HC vs MMC
MMC vs HF
Feature type
Serum metabolites
Metagenomic features
Microbiome density features
Effect size (Cliff's Delta)
-1.0
-0.5
0.0
0.5
1.0

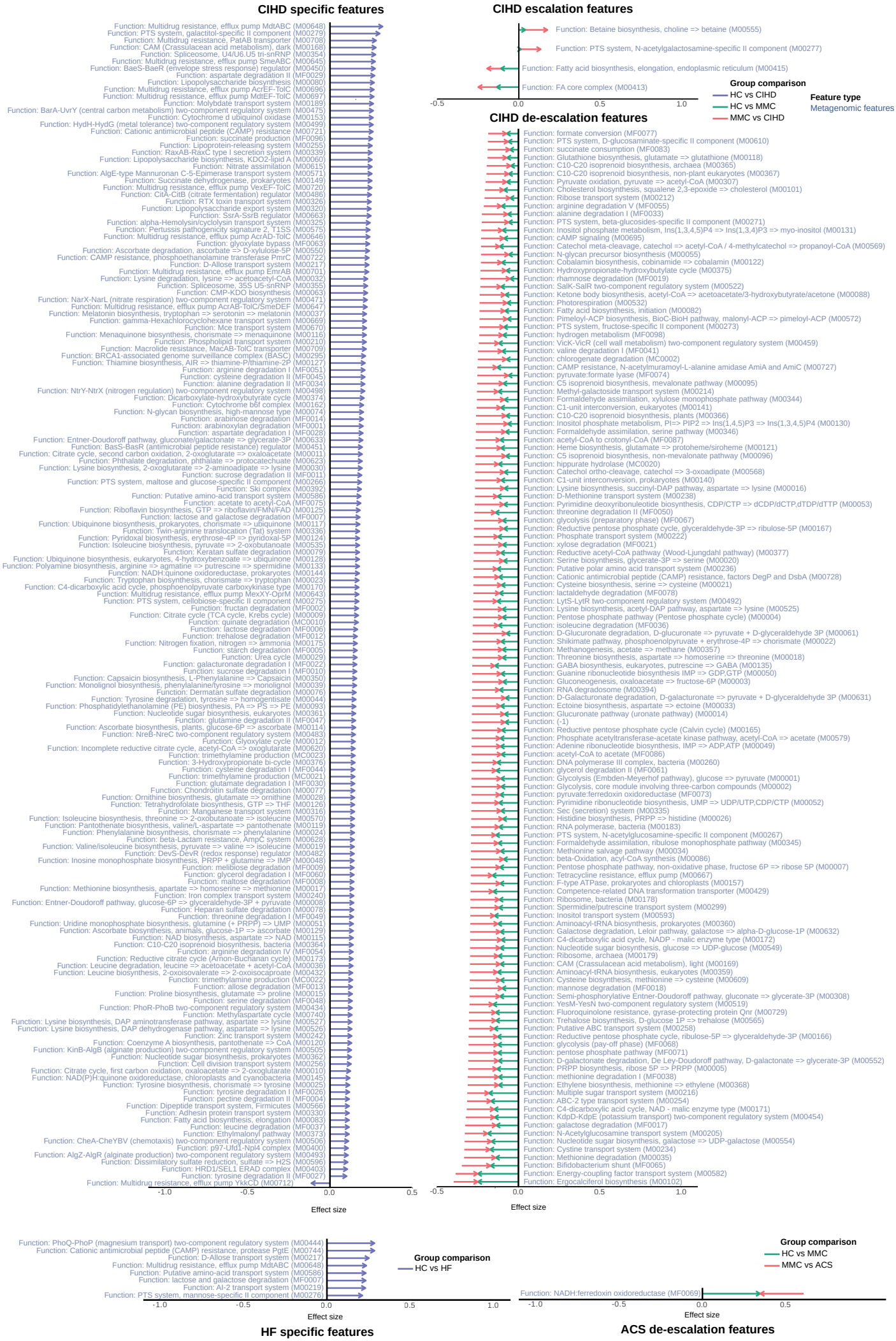
CIHD specific features
Function: Multidrug resistance, efflux pump MdtABC (M00648)
Function: PTS system, galactitol-specific II component (M00279)
Function: Multidrug resistance, PatAB transporter (M00708)
Function: CAM (Crassulacean acid metabolism), dark (M00168)
Function: Spliceosome, U4/U6.U5 tri-snRNP (M00354)
Function: Multidrug resistance, efflux pump SmeABC (M00645)
Function: BaeS-BaeR (envelope stress response) regulator (M00450)
Function: aspartate degradation II (MF0029)
Function: Lipopolysaccharide biosynthesis (M00080)
Function: Multidrug resistance, efflux pump AcrEF-TolC (M00696)
Function: Multidrug resistance, efflux pump MdtEF-TolC (M00697)
Function: Molybdate transport system (M00189)
Function: BarA-UvrY (central carbon metabolism) two-component regulatory system (M00475)
Function: Cytochrome d ubiquinol oxidase (M00153)
Function: HydH-HydG (metal tolerance) two-component regulatory system (M00499)
Function: Cationic antimicrobial peptide (CAMP) resistance (M00721)
Function: succinate production (MF0096)
Function: Lipoprotein-releasing system (M00255)
Function: RaxAB-RaxC type I secretion system (M00339)
Function: Lipopolysaccharide biosynthesis, KDO2-lipid A (M00060)
Function: Nitrate assimilation (M00615)
Function: AlgE-type Mannuronan C-5-Epimerase transport system (M00571)
Function: Succinate dehydrogenase, prokaryotes (M00149)
Function: Multidrug resistance, efflux pump VexEF-TolC (M00720)
Function: CitA-CitB (citrate fermentation) regulator (M00486)
Function: RTX toxin transport system (M00326)
Function: Lipopolysaccharide export system (M00320)
Function: SsrA-SsrB regulator (M00663)
Function: alpha-Hemolysin/cytolysin transport system (M00325)
Function: Pertussis pathogenicity signature 2, T1SS (M00575)
Function: Multidrug resistance, efflux pump AcrAD-TolC (M00646)
Function: glyoxylate bypass (MF0063)
Function: Ascorbate degradation, ascorbate => D-xylulose-5P (M00040)
Function: CAMP resistance, phosphoethanolamine transferase PmrC (M00722)
Function: D-Allose transport system (M00217)
Function: Multidrug resistance, efflux pump EmrAB (M00701)
Function: Lysine degradation, lysine => acetoacetyl-CoA (M00032)
Function: Spliceosome, 35S U5-snRNP (M00355)
Function: CMP-KDO biosynthesis (M00063)
Function: NarX-NarL (nitrate respiration) two-component regulatory system (M00471)
Function: Multidrug resistance, efflux pump AcrAB-TolC/SmeDEF (M00647)
Function: Melatonin biosynthesis, tryptophan => serotonin => melatonin (M00037)
Function: gamma-Hexachlorocyclohexane transport system (M00669)
Function: Mce transport system (M00670)
Function: Menaquinone biosynthesis, chorismate => menaquinone (M00116)
Function: Phospholipid transport system (M00210)
Function: Macrolide resistance, MacAB-TolC transporter (M00709)
Function: BRCA1-associated genome surveillance complex (BASC) (M00295)
Function: Thiamine biosynthesis, AIR => thiamine-P/thiamine-2P (M00127)
Function: arginine degradation I (MF0051)
Function: cysteine degradation II (MF0045)
Function: alanine degradation II (MF0034)
Function: NtrY-NtrX (nitrogen regulation) two-component regulatory system (M00498)
Function: Dicarboxylate-hydroxybutyrate cycle (M00374)
Function: Cytochrome b6f complex (M00162)
Function: N-glycan biosynthesis, high-mannose type (M00074)
Function: arabinose degradation (MF0014)
Function: arabinoxylan degradation (MF0001)
Function: aspartate degradation I (MF0028)
Function: Entner-Doudoroff pathway, gluconate/galactonate => glycerate-3P (M00633)
Function: BasS-BasR (antimicrobial peptide resistance) regulator (M00451)
Function: Citrate cycle, second carbon oxidation, 2-oxoglutarate => oxaloacetate (M00011)
Function: Phthalate degradation, phthalate => protocatechuate (M00623)
Function: Lysine biosynthesis, 2-oxoglutarate => 2-aminoadipate => lysine (M00030)
Function: sucrose degradation II (MF0011)
Function: PTS system, maltose and glucose-specific II component (M00269)
Function: Ski complex (M00392)
Function: Putative amino-acid transport system (M00586)
Function: acetate to acetyl-CoA (MF0075)
Function: Riboflavin biosynthesis, GTP => riboflavin/FMN/FAD (M00125)
Function: lactose and galactose degradation (MF0007)
Function: Ubiquinone biosynthesis, prokaryotes, chorismate => ubiquinone (M00117)
Function: Twin-arginine translocation (Tat) system (M00336)
Function: Pyridoxal biosynthesis, erythrose-4P => pyridoxal-5P (M00124)
Function: Isoleucine biosynthesis, pyruvate => 2-oxobutanoate (M00535)
Function: Keratan sulfate degradation (M00079)
Function: Ubiquinone biosynthesis, eukaryotes, 4-hydroxybenzoate => ubiquinone (M00128)
Function: Polyamine biosynthesis, arginine => agmatine => putrescine => spermidine (M00133)
Function: NADH:quinone oxidoreductase, prokaryotes (M00144)
Function: Tryptophan biosynthesis, chorismate => tryptophan (M00023)
Function: C4-dicarboxylic acid cycle, phosphoenolpyruvate carboxykinase type (M00170)
Function: Multidrug resistance, efflux pump MexXY-OprM (M00643)
Function: PTS system, cellobiose-specific II component (M00275)
Function: fructan degradation (MF0002)
Function: Citrate cycle (TCA cycle, Krebs cycle) (M00009)
Function: quinate degradation (MC0010)
Function: lactose degradation (MF0006)
Function: trehalose degradation (MF0012)
Function: Nitrogen fixation, nitrogen => ammonia (M00175)
Function: starch degradation (MF0005)
Function: Urea cycle (M00029)
Function: galacturonate degradation I (MF0022)
Function: sucrose degradation I (MF0010)
Function: Capsaicin biosynthesis, L-Phenylalanine => Capsaicin (M00359)
Function: Monolignol biosynthesis, phenylalanine/tyrosine => monolignol (M00039)
Function: Dermatan sulfate degradation (M00076)
Function: Tyrosine degradation, tyrosine => homogentisate (M00044)
Function: Phosphatidylethanolamine (PE) biosynthesis, PA => PE (M00093)
Function: Nucleotide sugar biosynthesis, eukaryotes (M00361)
Function: glutamine degradation II (MF0047)
Function: Ascorbate biosynthesis, plants, glucose-6P => ascorbate (M00114)
Function: NreB-NreC two-component regulatory system (M00483)
Function: Glyoxylate cycle (M00012)
Function: Incomplete reductive citrate cycle, acetyl-CoA => oxoglutarate (M00620)
Function: trimethylamine production (MC0023)
Function: 3-Hydroxypropionate bi-cycle (M00376)
Function: cysteine degradation I (MF0044)
Function: trimethylamine production (MC0021)
Function: glutamate degradation I (MF0030)
Function: Chondroitin sulfate degradation (M00077)
Function: Ornithine biosynthesis, glutamate => ornithine (M00028)
Function: Tetrahydrofolate biosynthesis, GTP => THF (M00126)
Function: Manganese transport system (M00316)
Function: Isoleucine biosynthesis, threonine => 2-oxobutanoate => isoleucine (M00570)
Function: Pantothenate biosynthesis, valine/L-aspartate => pantothenate (M00119)
Function: Phenylalanine biosynthesis, chorismate => phenylalanine (M00024)
Function: beta-Lactam resistance, AmpC system (M00628)
Function: Valine/isoleucine biosynthesis, pyruvate => valine => isoleucine (M00019)
Function: DevS-DevR (redox response) regulator (M00482)
Function: Inosine monophosphate biosynthesis, PRPP + glutamine => IMP (M00048)
Function: melibiose degradation (MF0009)
Function: glycerol degradation I (MF0060)
Function: maltose degradation (MF0008)
Function: Methionine biosynthesis, apartate => homoserine => methionine (M00017)
Function: Iron complex transport system (M00240)
Function: Entner-Doudoroff pathway, glucose-6P => glyceraldehyde-3P + pyruvate (M00008)
Function: Heparan sulfate degradation (M00078)
Function: threonine degradation I (MF0049)
Function: Uridine monophosphate biosynthesis, glutamine (+ PRPP) => UMP (M00051)
Function: Ascorbate biosynthesis, animals, glucose-1P => ascorbate (M00129)
Function: NAD biosynthesis, aspartate => NAD (M00115)
Function: C10-C20 isoprenoid biosynthesis, bacteria (M00364)
Function: arginine degradation IV (MF0054)
Function: Reductive citrate cycle (Arnon-Buchanan cycle) (M00173)
Function: Leucine degradation, leucine => acetoacetate + acetyl-CoA (M00036)
Function: Leucine biosynthesis, 2-oxoisovalerate => 2-oxoisocaproate (M00432)
Function: trimethylamine production (MC0022)
Function: allose degradation (MF0013)
Function: Proline biosynthesis, glutamate => proline (M00015)
Function: serine degradation (MF0048)
Function: PhoR-PhoB two-component regulatory system (M00434)
Function: Methylaspartate cycle (M00740)
Function: Lysine biosynthesis, DAP aminotransferase pathway, aspartate => lysine (M00527)
Function: Lysine biosynthesis, DAP dehydrogenase pathway, aspartate => lysine (M00526)
Function: Zinc transport system (M00242)
Function: Coenzyme A biosynthesis, pantothenate => CoA (M00120)
Function: KinB-AlgB (alginate production) two-component regulatory system (M00505)
Function: Nucleotide sugar biosynthesis, prokaryotes (M00362)
Function: Cell division transport system (M00256)
Function: Citrate cycle, first carbon oxidation, oxaloacetate => 2-oxoglutarate (M00010)
Function: NAD(P)H:quinone oxidoreductase, chloroplasts and cyanobacteria (M00145)
Function: Tyrosine biosynthesis, chorismate => tyrosine (M00025)
Function: tyrosine degradation I (MF0026)
Function: pectine degradation II (MF0004)
Function: Dipeptide transport system, Firmicutes (M00566)
Function: Adhesin protein transport system (M00330)
Function: Fatty acid biosynthesis, elongation (M00083)
Function: leucine degradation (MF0037)
Function: Ethylmalonyl pathway (M00373)
Function: CheA-CheYBV (chemotaxis) two-component regulatory system (M00506)
Function: p97-Ufd1-Npl4 complex (M00400)
Function: AlgZ-AlgR (alginate production) two-component regulatory system (M00493)
Function: Dissimilatory sulfate reduction, sulfate => H2S (M00596)
Function: HRD1/SEL1 ERAD complex (M00403)
Function: tyrosine degradation II (MF0027)
Function: Multidrug resistance, efflux pump YkkCD (M00712)
-1.0
-0.5
0.0
0.5
Effect size
CIHD escalation features
Function: Betaine biosynthesis, choline => betaine (M00555)
Function: PTS system, N-acetylgalactosamine-specific II component (M00277)
Function: Fatty acid biosynthesis, elongation, endoplasmic reticulum (M00415)
Function: FA core complex (M00413)
-0.5
0.0
0.5
1.0
Group comparison
HC vs CIHD
HC vs MMC
MMC vs CIHD
Feature type
Metagenomic features
CIHD de-escalation features
Function: formate conversion (MF0077)
Function: PTS system, D-glucosaminate-specific II component (M00610)
Function: succinate consumption (MF0083)
Function: Glutathione biosynthesis, glutamate => glutathione (M00118)
Function: C10-C20 isoprenoid biosynthesis, archaea (M00365)
Function: C10-C20 isoprenoid biosynthesis, non-plant eukaryotes (M00367)
Function: Pyruvate oxidation, pyruvate => acetyl-CoA (M00307)
Function: Cholesterol biosynthesis, squalene 2,3-epoxide => cholesterol (M00101)
Function: Ribose transport system (M00212)
Function: arginine degradation V (MF0055)
Function: alanine degradation I (MF0033)
Function: PTS system, beta-glucosides-specific II component (M00271)
Function: Inositol phosphate metabolism, Ins(1,3,4,5)P4 => Ins(1,3,4)P3 => myo-inositol (M00131)
Function: cAMP signaling (M00695)
Function: Catechol meta-cleavage, catechol => acetyl-CoA / 4-methylcatechol => propanoyl-CoA (M00569)
Function: N-glycan precursor biosynthesis (M00055)
Function: Cobalamin biosynthesis, cobinamide => cobalamin (M00122)
Function: Hydroxypropionate-hydroxybutylate cycle (M00375)
Function: rhamnose degradation (MF0019)
Function: SalK-SalR two-component regulatory system (M00522)
Function: Ketone body biosynthesis, acetyl-CoA => acetoacetate/3-hydroxybutyrate/acetone (M00088)
Function: Photorespiration (M00532)
Function: Fatty acid biosynthesis, initiation (M00082)
Function: Pimeloyl-ACP biosynthesis, BioC-BioH pathway, malonyl-ACP => pimeloyl-ACP (M00572)
Function: PTS system, fructose-specific II component (M00273)
Function: hydrogen metabolism (MF0098)
Function: VicK-VicR (cell wall metabolism) two-component regulatory system (M00459)
Function: valine degradation I (MF0041)
Function: chlorogenate degradation (MC0002)
Function: CAMP resistance, N-acetylmuramoyl-L-alanine amidase AmiA and AmiC (M00727)
Function: pyruvate:formate lyase (MF0074)
Function: C5 isoprenoid biosynthesis, mevalonate pathway (M00095)
Function: Methyl-galactoside transport system (M00214)
Function: Formaldehyde assimilation, xylulose monophosphate pathway (M00344)
Function: C1-unit interconversion, eukaryotes (M00141)
Function: C10-C20 isoprenoid biosynthesis, plants (M00366)
Function: Inositol phosphate metabolism, PI=> PIP2 => Ins(1,4,5)P3 => Ins(1,3,4,5)P4 (M00130)
Function: Formaldehyde assimilation, serine pathway (M00346)
Function: acetyl-CoA to crotonyl-CoA (MF0087)
Function: Heme biosynthesis, glutamate => protoheme/siroheme (M00121)
Function: C5 isoprenoid biosynthesis, non-mevalonate pathway (M00096)
Function: hippurate hydrolase (MC0020)
Function: Catechol ortho-cleavage, catechol => 3-oxoadipate (M00568)
Function: C1-unit interconversion, prokaryotes (M00140)
Function: Lysine biosynthesis, succinyl-DAP pathway, aspartate => lysine (M00016)
Function: D-Methionine transport system (M00238)
Function: Pyrimidine deoxyribonuleotide biosynthesis, CDP/CTP => dCDP/dCTP,dTDP/dTTP (M00053)
Function: threonine degradation II (MF0050)
Function: glycolysis (preparatory phase) (MF0067)
Function: Reductive pentose phosphate cycle, glyceraldehyde-3P => ribulose-5P (M00167)
Function: Phosphate transport system (M00222)
Function: xylose degradation (MF0021)
Function: Reductive acetyl-CoA pathway (Wood-Ljungdahl pathway) (M00377)
Function: Serine biosynthesis, glycerate-3P => serine (M00020)
Function: Putative polar amino acid transport system (M00236)
Function: Cationic antimicrobial peptide (CAMP) resistance, factors DegP and DsbA (M00728)
Function: Cysteine biosynthesis, serine => cysteine (M00021)
Function: lactaldehyde degradation (MF0078)
Function: LytS-LytR two-component regulatory system (M00492)
Function: Lysine biosynthesis, acetyl-DAP pathway, aspartate => lysine (M00525)
Function: Pentose phosphate pathway (Pentose phosphate cycle) (M00004)
Function: isoleucine degradation (MF0036)
Function: D-Glucuronate degradation, D-glucuronate => pyruvate + D-glyceraldehyde 3P (M00061)
Function: Shikimate pathway, phosphoenolpyruvate + erythrose-4P => chorismate (M00022)
Function: Methanogenesis, acetate => methane (M00357)
Function: Threonine biosynthesis, aspartate => homoserine => threonine (M00018)
Function: GABA biosynthesis, eukaryotes, putrescine => GABA (M00135)
Function: Guanine ribonucleotide biosynthesis IMP => GDP,GTP (M00050)
Function: Gluconeogenesis, oxaloacetate => fructose-6P (M00003)
Function: RNA degradosome (M00394)
Function: D-Galacturonate degradation, D-galacturonate => pyruvate + D-glyceraldehyde 3P (M00631)
Function: Ectoine biosynthesis, aspartate => ectoine (M00033)
Function: Glucuronate pathway (uronate pathway) (M00014)
Function: (-1)
Function: Reductive pentose phosphate cycle (Calvin cycle) (M00165)
Function: Phosphate acetyltransferase-acetate kinase pathway, acetyl-CoA => acetate (M00579)
Function: Adenine ribonucleotide biosynthesis, IMP => ADP,ATP (M00049)
Function: acetyl-CoA to acetate (MF0086)
Function: DNA polymerase III complex, bacteria (M00260)
Function: glycerol degradation II (MF0061)
Function: Glycolysis (Embden-Meyerhof pathway), glucose => pyruvate (M00001)
Function: Glycolysis, core module involving three-carbon compounds (M00002)
Function: pyruvate:ferredoxin oxidoreductase (MF0073)
Function: Pyrimidine ribonucleotide biosynthesis, UMP => UDP/UTP,CDP/CTP (M00052)
Function: Sec (secretion) system (M00335)
Function: Histidine biosynthesis, PRPP => histidine (M00026)
Function: RNA polymerase, bacteria (M00183)
Function: PTS system, N-acetylglucosamine-specific II component (M00267)
Function: Formaldehyde assimilation, ribulose monophosphate pathway (M00345)
Function: Methionine salvage pathway (M00034)
Function: beta-Oxidation, acyl-CoA synthesis (M00086)
Function: Pentose phosphate pathway, non-oxidative phase, fructose 6P => ribose 5P (M00007)
Function: Tetracycline resistance, efflux pump (M00667)
Function: F-type ATPase, prokaryotes and chloroplasts (M00157)
Function: Competence-related DNA transformation transporter (M00429)
Function: Ribosome, bacteria (M00178)
Function: Spermidine/putrescine transport system (M00299)
Function: Inositol transport system (M00593)
Function: Aminoacyl-tRNA biosynthesis, prokaryotes (M00360)
Function: Galactose degradation, Leloir pathway, galactose => alpha-D-glucose-1P (M00632)
Function: C4-dicarboxylic acid cycle, NADP - malic enzyme type (M00172)
Function: Nucleotide sugar biosynthesis, glucose => UDP-glucose (M00549)
Function: Ribosome, archaea (M00179)
Function: CAM (Crassulacean acid metabolism), light (M00169)
Function: Aminoacyl-tRNA biosynthesis, eukaryotes (M00359)
Function: Cysteine biosynthesis, methionine => cysteine (M00609)
Function: mannose degradation (MF0018)
Function: Semi-phosphorylative Entner-Doudoroff pathway, gluconate => glycerate-3P (M00308)
Function: YesM-YesN two-component regulatory system (M00519)
Function: Fluoroquinolone resistance, gyrase-protecting protein Qnr (M00729)
Function: Trehalose biosynthesis, D-glucose 1P => trehalose (M00565)
Function: Putative ABC transport system (M00258)
Function: Reductive pentose phosphate cycle, ribulose-5P => glyceraldehyde-3P (M00166)
Function: glycolysis (pay-off phase) (MF0068)
Function: pentose phosphate pathway (MF0071)
Function: D-galactonate degradation, De Ley-Doudoroff pathway, D-galactonate => glycerate-3P (M00552)
Function: PRPP biosynthesis, ribose 5P => PRPP (M00005)
Function: methionine degradation I (MF0038)
Function: Ethylene biosynthesis, methionine => ethylene (M00368)
Function: Multiple sugar transport system (M00216)
Function: ABC-2 type transport system (M00254)
Function: C4-dicarboxylic acid cycle, NAD - malic enzyme type (M00171)
Function: KdpD-KdpE (potassium transport) two-component regulatory system (M00454)
Function: galactose degradation (MF0017)
Function: N-Acetylglucosamine transport system (M00205)
Function: Nucleotide sugar biosynthesis, galactose => UDP-galactose (M00554)
Function: Cystine transport system (M00234)
Function: Methionine degradation (M00035)
Function: Bifidobacterium shunt (MF0065)
Function: Energy-coupling factor transport system (M00582)
Function: Ergocalciferol biosynthesis (M00102)
-0.5
0.0
0.5
1.0
Effect size
Function: PhoQ-PhoP (magnesium transport) two-component regulatory system (M00444)
Function: Cationic antimicrobial peptide (CAMP) resistance, protease PgtE (M00744)
Function: D-Allose transport system (M00217)
Function: Multidrug resistance, efflux pump MdtABC (M00648)
Function: Putative amino-acid transport system (M00586)
Function: lactose and galactose degradation (MF0007)
Function: AI-2 transport system (M00219)
Function: PTS system, mannose-specific II component (M00276)
Group comparison
HC vs HF
-1.0
-0.5
0.0
0.5
1.0
Effect size
HF specific features
Group comparison
HC vs MMC
MMC vs ACS
Function: NADH:ferredoxin oxidoreductase (MF0069)
-1.0
-0.5
0.0
0.5
Effect size
ACS de-escalation features

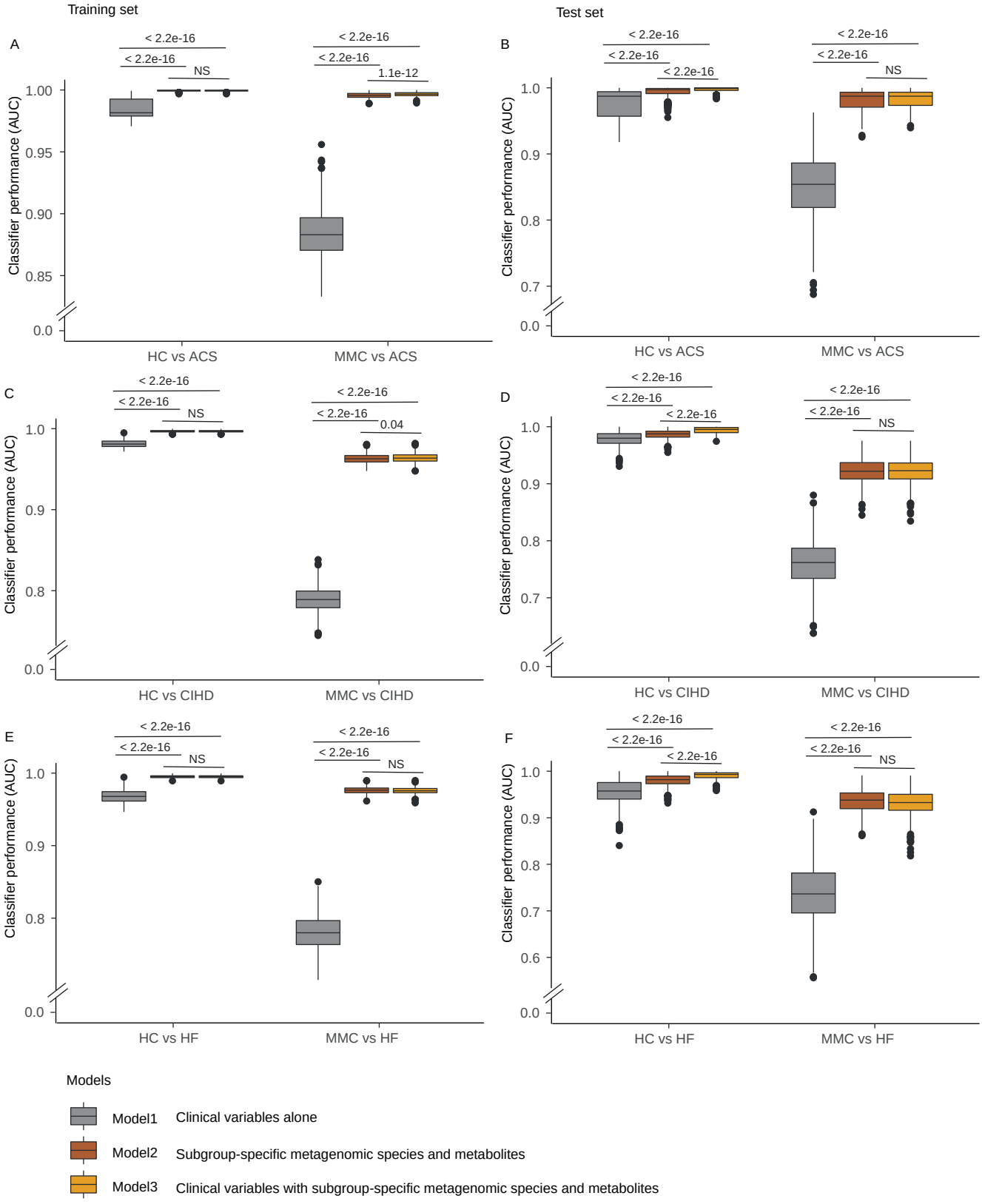
Training set
Test set
A
B
C
D
E
F
Classifier performance (AUC)
< 2.2e-16
NS
1.1e-12
0.04
HC vs ACS
MMC vs ACS
HC vs CIHD
MMC vs CIHD
HC vs HF
MMC vs HF
Models
Model1 Clinical variables alone
Model2 Subgroup-specific metagenomic species and metabolites
Model3 Clinical variables with subgroup-specific metagenomic species and metabolites